

The long non-coding RNA *HOTAIRM1* promotes tumor aggressiveness and radiotherapy resistance in glioblastoma

Inaugural dissertation

for the attainment of the title of doctor
in the Faculty of Mathematics and Natural Sciences
at the Heinrich Heine University Düsseldorf

presented by

Ulvi Ahmadov

from Nakhchivan, Azerbaijan

Düsseldorf, October 2019

from the institute for Department of Pediatric Oncology, Hematology and
Clinical Immunology, University Hospital Düsseldorf

Published by permission of the
Faculty of Mathematics and Natural Sciences at
Heinrich Heine University Düsseldorf

Supervisor: Prof. Dr. Guido Reifenberger

Co-supervisor: Prof. Dr. Andreas Reichert

Date of the oral examination:

Table of contents

Summary.....	6
Zusammenfassung.....	8
1 Introduction	10
1.1 Glioblastoma	10
1.1.1 Genetics of glioblastoma.....	10
1.1.2 Treatment	12
1.2 Long non-coding RNAs.....	13
1.2.1 Classification	13
1.2.2 Detection of long non-coding RNAs	14
1.2.3 Functional roles and actions of mechanism of long non-coding RNAs	16
1.2.4 Long non-coding RNAs in physiological conditions and diseases	18
1.2.5 <i>HOXA transcript antisense RNA myeloid-specific 1</i>	19
2 Aim of the study	22
3 Materials	23
3.1 Cell culture media and reagents	23
3.2 Cell lines.....	23
3.3 Kits, reagents and others materials.....	23
3.4 Antibodies.....	25
3.5 Buffers	25
3.6 Oligonucleotides	26
3.7 Software and hardware.....	26
4 Methods	28
4.1 Cell culture	28
4.2 RNA isolation and real-time quantitative PCR.....	28
4.3 SiRNA- and shRNA-mediated knockdown	28
4.4 RNA sequencing.....	29
4.5 Western blotting.....	29
4.6 Proteomics	30
4.7 CellTiter-Glo luminescent cell viability assay	31
4.8 <i>In vitro</i> invasion assay	31
4.9 Colony formation assay, N-acetyl cysteine treatment and <i>in vitro</i> radiation assay	32
4.10 Seahorse mito stress assay.....	32
4.11 Reactive oxygen staining.....	33

4.12	<i>In vivo</i> mouse experiments	33
4.13	Bionformatics and statistical analyses	34
5	Results	35
5.1	Functional consequences of knockdown of <i>HOXA transcript antisense RNA, myeloid-specific 1</i> in glioblastoma cell lines.....	35
5.1.1	Expression of <i>HOXA transcript antisense RNA, myeloid-specific 1</i> in glioblastoma cells.....	35
5.1.2	SiRNA-mediated knockdown of <i>HOXA transcript antisense RNA, myeloid-specific 1</i> decreases oncogenic potential of glioblastoma cells	36
5.1.3	Stable knockdown of <i>HOXA transcript antisense RNA, myeloid-specific 1</i> decreases oncogenic potential of glioblastoma cells	37
5.2	Proteogenomic analysis indicates mitochondrial dysfunction upon <i>HOXA transcript antisense RNA, myeloid-specific 1</i> knockdown in glioblastoma cells	39
5.2.1	Results of RNA sequencing following siRNA-mediated <i>HOXA transcript antisense RNA, myeloid-specific 1</i> knockdown.....	39
5.2.2	Results of proteomic analyses following siRNA-mediated <i>HOXA transcript antisense RNA, myeloid-specific 1</i> knockdown in glioblastoma cells	42
5.2.3	Integrated proteogenomic analysis of the <i>HOXA transcript antisense RNA, myeloid-specific 1</i> knockdown results indicate mitochondrial dysfunction	44
5.2.4	Proteomic analysis upon stable <i>HOXA transcript antisense RNA, myeloid-specific 1</i> knockdown in LN229 glioblastoma cells.....	46
5.3	Knockdown of <i>HOXA transcript antisense RNA, myeloid-specific 1</i> alters amino acid metabolism and leads to upregulation of <i>asparagine synthetase</i> in glioblastoma cells	49
5.4	Knockdown of <i>HOXA transcript antisense RNA, myeloid-specific 1</i> decreases maximal respiration in U251MG cells	51
5.5	<i>HOXA transcript antisense RNA, myeloid-specific 1</i> knockdown increased reactive oxygen species in glioblastoma cells.....	52
5.6	Antioxidant N-acetyl cysteine treatment rescues the phenotype induced by <i>HOXA transcript antisense RNA, myeloid-specific 1</i> knockdown in glioblastoma cells	53
5.7	<i>HOXA transcript antisense RNA, myeloid-specific 1</i> knockdown sensitizes LN229, SF126 and LN18 glioblastoma cells to radiation <i>in vitro</i>	54
5.8	<i>HOXA transcript antisense RNA, myeloid-specific 1</i> knockdown sensitizes LN229 glioblastoma cells to radiation <i>in vivo</i>	55
5.9	Glioblastoma cells with high levels of <i>HOXA transcript antisense RNA, myeloid-specific 1</i> are more sensitive to l-asparaginase treatment	56

5.10	<i>In silico</i> microRNA binding analysis shows a potential role of <i>HOXA</i> transcript antisense RNA, myeloid-specific 1 as a microRNA sponge for miRNAs targeting <i>transglutaminase 2</i>	57
5.11	<i>Transglutaminase 2</i> is downregulated upon <i>HOXA</i> transcript antisense RNA, myeloid-specific 1 knockdown in glioblastoma cells ...	60
5.12	SiRNA-mediated knockdown of <i>transglutaminase 2</i> decreases oncogenic potential in glioblastoma cells	60
6	Discussion.....	62
7	Conclusion and outlook	67
8	References.....	69
9	Acknowledgement.....	82
10	Appendix.....	83
10.1	Abbreviations.....	83
10.2	Nomenclature	85
10.3	Figure Directory	86
10.4	Table Directory	88

Summary

Glioblastomas without mutations in the *isocitrate dehydrogenase (IDH)* 1 or 2 gene, i.e., IDH-wildtype glioblastomas, are the most common and most malignant type of primary brain tumors in adults. Patients are treated with multimodal therapy consisting of surgical resection followed by radiotherapy and systemic chemotherapy with the DNA-alkylating drug temozolomide. Despite this aggressive therapy, IDH-wildtype glioblastoma remains a fatal disease and patient survival is poor as indicated by a median survival time of less than 2 years after diagnosis. Although there are growing insights into glioblastoma molecular genetics, only few molecular markers have been identified that may inform clinical decision making and guide therapy planning. Moreover, molecularly targeted therapies have failed in clinical trials to date and hence have not been implemented as a standard of care.

Previously depicted as ‘transcriptional noise’, it is now clear that long non-coding RNAs (lncRNA) play important roles in many aspects of cell biology and disease pathogenesis, including cancer growth. Previous studies by other authors as well as data from the own research group showed that elevated expression of the lncRNA *HOXA Transcript Antisense RNA, Myeloid-Specific 1 (HOTAIRM1)* is correlated with poor prognosis in glioblastoma patients. To investigate functional roles of *HOTAIRM1*, *HOTAIRM1*-knockdown glioblastoma cell line models were generated that uniformly showed reduced cell viability, less invasive growth and diminished colony formation capacity upon *HOTAIRM1* downregulation.

Integrated proteogenomic analyses revealed evidence for mitochondrial dysfunction upon *HOTAIRM1* depletion and impaired mitochondrial function could be experimentally validated *in vitro* by tricarboxylic acid cycle (TCA) metabolomics, Seahorse Mito Stress assays as well as H₂O₂ and MitoSOX reactive oxygen species (ROS) quantification. Moreover, antioxidant treatment using N-acetylcysteine (NAC) was able to rescue the phenotype caused by *HOTAIRM1* knockdown and hence further verified the ROS staining data. In addition, TCA metabolomics revealed that *HOTAIRM1* knockdown increased asparagine and decreases aspartate levels. *HOTAIRM1* knockdown protected glioblastoma cells against the effects of asparaginase treatment due to excess asparagine levels.

Most importantly, *HOTAIRM1* knockdown was found to increase radiosensitivity of glioblastoma cells *in vitro* and *in vivo*. Moreover, *in silico* microRNA binding analysis suggested a potential role of *HOTAIRM1* acting as a microRNA sponge for miR-17-5p targeting *TGM2*. In line, *HOTAIRM1* knockdown decreased expression of

transglutaminase 2 (TGM2) as a candidate protein implicated in mitochondrial function, and knockdown of *TGM2* mimicked the *in vitro* phenotype of *HOTAIRM1* downregulation in glioblastoma cells. In conclusion, the data summarized in this thesis support a role for *HOTAIRM1* as a driver of biological aggressiveness and radioresistance in glioblastoma.

Zusammenfassung

Glioblastome ohne Mutationen im *Isocitrat-Dehydrogenase (IDH)* - Gen 1 oder 2, sogenannte IDH-Wildtyp-Glioblastome, sind die häufigste und bösartigste Form von primären Hirntumoren bei Erwachsenen. Die Patienten werden mit einer multimodalen Therapie behandelt, die aus einer chirurgischen Resektion, gefolgt von Strahlentherapie und systemischer Chemotherapie mit dem DNA-alkylierenden Medikament Temozolomid besteht. Trotz dieser aggressiven Therapie bleibt das IDH-Wildtyp-Glioblastom eine tödliche Erkrankung und die Überlebenschancen sind schlecht, wie eine mittlere Überlebenszeit von weniger als 2 Jahren nach der Diagnose zeigt. Obwohl es immer mehr Erkenntnisse über die molekulare Genetik des Glioblastoms gibt, wurden nur wenige molekulare Marker identifiziert, die die klinische Entscheidungsfindung und die Therapieplanung unterstützen können. Darüber hinaus sind gezielte molekulare Therapien in klinischen Studien bisher gescheitert und wurden daher nicht als Behandlungsstandard eingesetzt.

Früher als "transkriptionelles Rauschen" bezeichnet, ist heute klar, dass lange nicht-kodierende RNAs (lncRNA) eine wichtige Rolle in vielen Aspekten der Zellbiologie und Krankheitspathogenese, einschließlich des Krebswachstums, spielen. Frühere Studien anderer Autoren sowie Daten aus der eigenen Forschungsgruppe zeigten, dass eine erhöhte Expression der lncRNA *Hoxa Transcript Antisense RNA, Myeloid-Specific 1 (HOTAIRM1)*, mit einer schlechten Prognose bei Glioblastompatienten verknüpft ist. Um die funktionellen Rollen von *HOTAIRM1* zu untersuchen, wurden *HOTAIRM1*-Knockdown-Glioblastom-Zelllinienmodelle generiert, die nach *HOTAIRM1*-Herrunterregulierung alle eine reduzierte Zellebensfähigkeit, ein weniger invasives Wachstum und eine verminderte Koloniebildungskapazität zeigten.

Integrierte proteogenomische Analysen ergaben Hinweise auf mitochondriale Funktionsstörungen bei *HOTAIRM1*-Abschaltung. Eine beeinträchtigte mitochondriale Funktionsfähigkeit konnte experimentell *in vitro* durch Tricarbonsäurezyklus-(TCA)-Metabolomik, Seahorse-Mito-Stress-Assays sowie HET- und MitoSOX-ROS-Quantifizierung validiert werden. Darüber hinaus konnte die antioxidative Behandlung mit N-Acetylcystein-Antioxidans (NAC) den durch den *HOTAIRM1*-Knockdown verursachten Phänotyp retten und damit die ROS-Färbedaten weiter verifizieren. Des Weiteren zeigten die TCA-Metabolomikdaten, dass der Knockdown von *HOTAIRM1* den Spiegel von Asparagin erhöht und den von Aspartat senkt. *HOTAIRM1*-Knockdown beschützte Glioblastom-Zellen vor der Wirkung einer Asparaginase-Behandlung.

Am wichtigsten ist, dass der Knockdown von *HOTAIRM1* die Strahlenempfindlichkeit der Glioblastomzellen *in vitro* und *in vivo* erhöht. Darüber hinaus deutete eine *in silico* microRNA-Bindungsanalyse eine potenzielle Rolle von *HOTAIRM1* als mikroRNA-Schwamm für miR-17-5p an, welche *TGM2* als Ziel hat. Folgerichtig verringerte ein *HOTAIRM1*-Knockdown die Expression von Transglutaminase 2 (*TGM2*), dessen Protein mutmaßlich eine Funktion in Mitochondrien ausübt. Ein Knockdown von *TGM2* spiegelte den *in vitro* - Phänotyp der *HOTAIRM1*-Herrunterregulierung in Glioblastomzellen. Zusammenfassend lässt sich sagen, dass die Daten dieser Arbeit die These unterstützen, dass *HOTAIRM1* als Treiber der biologischen Aggressivität und Strahlungsresistenz bei Glioblastomen fungiert.

1 Introduction

1.1 Glioblastoma

Primary central nervous system (CNS) tumors include a broad range of tumors of which gliomas encompass 80% of malignant CNS tumors in adulthood [175]. Glioblastoma is the most common malignant primary brain tumor and is supposed to arise from neural stem or progenitor cells [115, 131]. Histopathological features of glioblastoma include necrosis and/or microvascular proliferation, atypical nuclei (nuclear atypia), cellular pleomorphism (variation in the size and shape of the tumor cells) and mitotic activity [115]. Median overall survival of glioblastoma patients is 15-18 months, and the five-year survival rate is less than 10% [152, 154, 174].

In 2016, the World Health Organization (WHO) updated the classification system for CNS tumors with integrated histologic and molecular data [2]. Glioblastoma is a WHO grade IV tumor that is stratified according to the *isocitrate dehydrogenase (IDH)* gene 1 and 2 mutation status: IDH-wildtype (~90% of cases), IDH-mutant (~10% of cases) and NOS (not otherwise specified, <1% of cases) [116]. The most frequent group is IDH-wildtype glioblastoma which lacks IDH1-R132 or IDH2-R172 mutations. This group is preferentially found in patients over 55 years and typically develops as primary or *de novo* glioblastoma [130]. Unlike IDH-wildtype glioblastoma, IDH-mutant glioblastoma are less frequent. This group is more common in younger patients and includes so-called secondary glioblastomas that progress from preexisting lower grade diffuse gliomas [130]. Rarely, the IDH status of glioblastomas cannot be evaluated and these cases are classified as glioblastoma, NOS [116].

1.1.1 Genetics of glioblastoma

Over the past decade, molecular genetics and cell biology studies have greatly improved our understanding of glioblastoma biology. Several molecular profiling strategies highlighted important intertumoral heterogeneity of glioblastoma. Hallmark alterations in IDH-wildtype glioblastoma include large copy number alterations, focal amplifications and deletions, mutations and promoter methylation of various genes. Common alterations are trisomy 7 and chromosome 10 loss [165], *epidermal growth factor receptor (EGFR)* or *platelet-derived growth factor receptor alpha (PDGFRA)* gene amplification [126], loss of the *cyclin dependent kinase inhibitor 2A (CDKN2A)* gene [36], as well as mutations of the *RB transcriptional corepressor 1 (RB1)* gene [171], the *tumor protein p53 (TP53)* gene [114, 171], the *neurofibromin 1 (NF1)* gene

[62], the *phosphatase and tensin homolog (PTEN)* gene, the *telomerase reverse transcriptase (TERT)* promoter [10, 77, 127], the *B-Raf proto-oncogene, serine/threonine kinase (BRAF)*-V600E [76], and aberrant methylation of *O*-6-methylguanine-DNA methyltransferase (*MGMT*) gene promoter. Conversely, IDH-mutant glioblastomas have fewer hallmark alterations which include frequent *IDH1* or *IDH2*, *ATRX chromatin remodeler (ATRX)*, and *TP53* mutations [111, 130]. According to the Cancer Genome Atlas (TCGA) reports, mutations or gene copy number alterations in *p53* and *retinoblastoma (Rb)* pathways are profoundly dominant in glioblastoma patients, i.e., 87% and 78% of the cases, respectively. Crucial activators or upstream repressors of either the *p53* or *Rb* pathways are either homozygously deleted (*CDKN2A* locus) [21, 134, 135, 164] or up-regulated by gene amplifications (such as *cyclin dependent kinase 4 (CDK4)* and *MDM2 proto-oncogene (MDM2)*) [23]. Additionally, oncogenic pathways such as PI3K-AKT-mTOR and RAS-MAPK signaling pathways, and receptor tyrosine kinases (RTKs) are activated in glioblastoma. Moreover, constitutively activating deletion mutations in RTKs such as *EGFR* (~40 % of cases) [53, 100, 126, 134, 180] and in *PDGFRA* (~13 % of cases) are observed in glioblastomas [132].

Activating mutations in catalytic domain (*phosphatidylinositol-4,5-bisphosphate 3-kinase catalytic subunit alpha (PIK3CA)*) or regulatory domain (*phosphoinositide-3-kinase regulatory subunit 1 (PIK3R1)*) of *phosphatidylinositol 3-kinase (PI3K)* (~15 % of cases), and deletions or inactivating mutations in the primary negative regulator of the PI3K-AKT signaling pathway *PTEN* (~30 % of cases) are common alterations in this pathway [58, 74, 89, 121, 178]. Somatic gene mutations or deletions in *NF1*, a RAS antagonist, are detected in 15–18 % of IDH-wildtype glioblastomas [62].

Key clinicopathological characteristics of IDH-wildtype and IDH-mutant glioblastomas are summarized in Table 1.1. Furthermore, *IDH1/2* mutations are positively correlated with *TP53* and *ATRX* mutations and 1p/19q co-deletion. However, *IDH1/2* mutations are negatively correlated with *EGFR* gene amplification and monosomy of chromosome 10 that occur more often in IDH-wildtype glioblastomas. Thus, the development of IDH-mutant lower grade gliomas, as well as secondary glioblastomas derived therefrom, is clearly different compared to IDH-wildtype glioblastomas at the molecular level [2].

Table 1.1: Key characteristics of IDH-wildtype and IDH-mutant glioblastomas. The table is adapted from Ohgaki and Louis et al. [116, 130].

	IDH-wildtype glioblastoma	IDH-mutant glioblastoma
Synonym	Primary glioblastoma, IDH-wildtype	Secondary glioblastoma, IDH-mutant
Precursor lesion	Not identifiable; develops de novo	Diffuse astrocytoma Anaplastic astrocytoma
Proportion of glioblastoma	~90%	~10%
Median age at diagnosis	~62 years	~44 years
Male-to-female ratio	1.42:1	1.05:1
Mean length of clinical history	4 months	15 months
Median overall survival		
Surgery + radiotherapy	9.9 months	24 months
Surgery + radiotherapy + chemotherapy	15 months	31 months
Location	Supratentorial	Preferentially frontal
Necrosis	Extensive	Limited
<i>TERT</i> promoter mutations	72%	26%
<i>TP53</i> mutations	27%	81%
<i>ATRX</i> mutations	Rare	71%
<i>EGFR</i> amplification	35%	Rare
<i>PTEN</i> mutations	24%	Rare

1.1.2 Treatment

Current standard therapy for glioblastoma patients includes maximal surgical resection, followed by radiotherapy and treatment with the DNA alkylating agent temozolomide (TMZ) [157]. The vast majority of glioblastomas demonstrate remarkable resistance to radiation and chemotherapeutic agents, either upfront or during the course of treatment [2, 154, 174].

Still, only a few alterations have been established as robust predictive or prognostic biomarkers for clinical stratification of glioblastoma patients. Epigenetic silencing of the DNA repair gene *MGMT* predicts better response to TMZ and is associated with significantly prolonged survival in TMZ-treated patients due to its capacity to repair the alkylating lesions of the DNA caused by TMZ [69, 173, 177]. Furthermore, patients whose tumors are IDH-mutant have a better prognosis [176, 188]; however, the exact mechanism is still not fully understood.

1.2 Long non-coding RNAs

Increasing technology, specifically next-generation sequencing technologies, and better algorithms in bioinformatics made it possible to show that more than 75% of the human genome is actively transcribed into RNA, and while protein-coding transcripts (mRNAs) represent only a small portion (<2%), the remainder are non-coding RNAs (ncRNAs, Figure 1.1). [181]. Long non-coding RNAs (lncRNAs) are transcripts that do not code for proteins and are longer than 200 base pairs by definition. In the past, lncRNAs were assumed to be products of pervasive transcription, however, they have been shown to have different functions than classical (ribozymes, rRNAs) or small (microRNAs) non-coding RNAs [95]

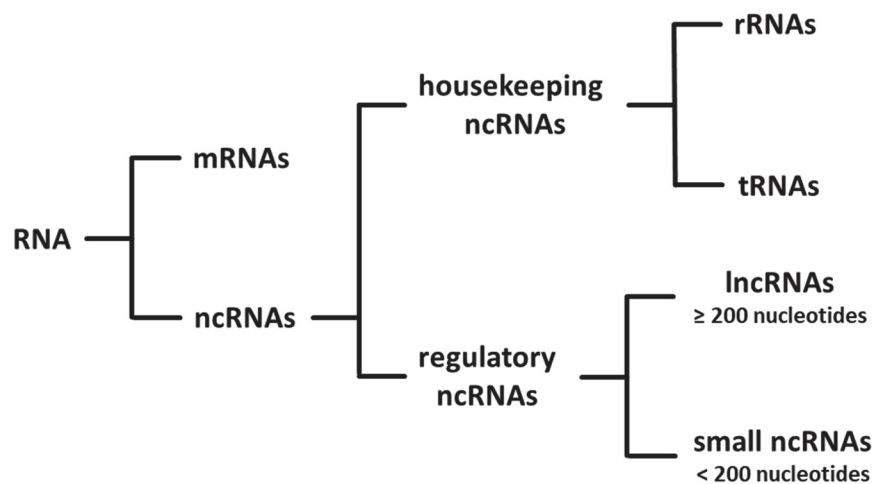


Figure 1.1: Classification of RNAs. RNAs are divided into protein coding RNAs (messenger RNAs = mRNAs) and non-coding RNAs (ncRNAs), which are separated into two classes: housekeeping (ribosomal and transfer RNAs, rRNAs and tRNAs, respectively) and regulatory (small and long ncRNAs). This figure is adapted from Inamura et al. [78].

1.2.1 Classification

Long non-coding RNAs are classified according to their genomic location and positional relationship to mRNAs. There are seven classes of lncRNAs: intergenic, intronic, bidirectional, enhancer, promoter-associated, sense and antisense lncRNAs [40] (Figure 1.2). The largest group of lncRNAs, long intergenic ncRNAs (lincRNAs), is located in the intergenic region of genome and do not overlap with any coding or non-coding genes. The lncRNAs that are transcribed from sense strand or antisense strand of the coding genes are referred to as sense lncRNAs or antisense lncRNAs, respectively. Both sense and antisense lncRNAs can overlap with intron(s) and/or

exon(s) of the coding genes. The lncRNAs located within introns of coding genes are referred to as intronic lncRNAs. lncRNAs transcribed from promoter and enhancer regions of the genome are called promoter-associated and enhancer lncRNAs (e-lncRNAs), respectively. Bidirectional lncRNAs are transcribed on the opposite site of coding genes within 1 kb of promoters and quite often sharing a promoter [40, 181].

Just like mRNAs, the majority of lncRNAs have classical 5' cap (m^7G) and 3' poly(A) tail, multiple exons, spliced variants (alternative isoforms) and they are mostly transcribed by RNA polymerase (Pol) II [46]. Despite the similarities with their mRNA counterparts, lncRNAs are less abundant than mRNAs. They are less conserved between species and often have tissue specific expression [133]. Finally, subcellular localization of lncRNAs is highly associated with their function [51, 95, 181].

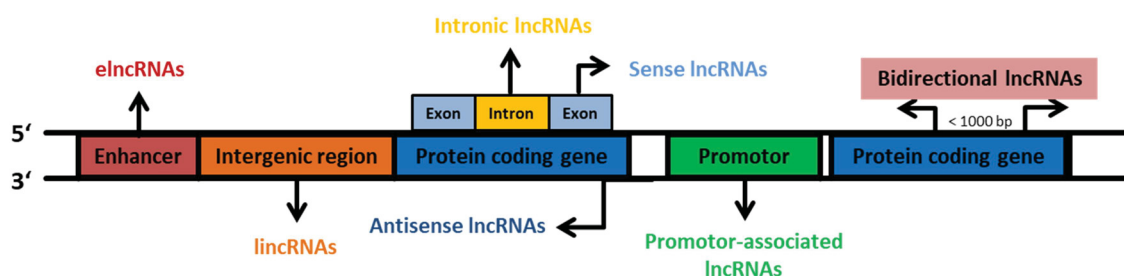


Figure 1.2: The diversity of long non-coding RNAs (lncRNAs) in the mammalian genome. Different compartments of the genome can produce various lncRNAs, such as enhancer lncRNAs (e-lncRNAs), long intergenic non-coding RNAs (lincRNAs), intronic lncRNAs, sense lncRNAs, antisense lncRNAs, promoter-associated lncRNAs and bidirectional lncRNAs. This figure is adapted from Hauptman and Glavac [66].

Circular RNAs (circRNAs) are another type of ncRNAs which have a closed loop structure, have no poly(A) tail and are more stable compared to other ncRNAs. They are produced from RNA Pol II-mediated transcripts and by the spliceosome machinery [28, 98, 190].

1.2.2 Detection of long non-coding RNAs

The identification of lncRNAs depends on the detection of transcripts that are larger than 200 bases but not translated into a protein. Moreover, transcripts lacking protein coding potential are differentiated from transcriptionally active chromatin byproducts by considering specific histone marks like histone 3-(H3)-K4–K36 domains in the promoter region [123]. lncRNAs can be directly detected and identified by microarrays, tiling

arrays and RNA sequencing. These methods are not mutually exclusive, rather often combined to identify lncRNAs in a single study.

Microarray-based approaches have been most commonly used as large-scale screening method within the past decade. Since there are microarrays designed to detect mRNAs which include certain lncRNAs, many researchers revealed that arrays like Affymetrix (MG_430 2.0, HG_U133plus2, U133A and B) could be used to study lncRNAs [110, 122, 144]. Therefore, publicly available published data in repositories like European Genome-phenome Archive (<https://www.ebi.ac.uk/ega/>), National Center for Biotechnology Information (NCBI) Gene Expression Omnibus (GEO) repository (<https://www.ncbi.nlm.nih.gov/gds>) and The Cancer Genome Atlas (TCGA) Genomic Data Commons (GDC) Data Portal (<https://portal.gdc.cancer.gov/>), and analysis platforms such as the R2 platform (R2: Genomics analysis and visualization platform (<http://r2.amc.nl>)) are an important resource for the study of lncRNAs.

1.2.2.1 RNA sequencing

RNA sequencing (RNA-seq) is based on next-generation sequencing principles that can detect and quantify both known and novel transcripts including lncRNAs at single nucleotide resolution. RNA-seq can be performed using ribosome depleted total RNA [99] or polyadenylated RNA. However, since not all lncRNA contain a poly-A tail, the latter starting material would not provide a complete picture of the lncRNAs expressed in a sample, thus ribosome depleted total RNA is advantageous [45].

Sequencing reads are aligned to reference genomes by using specific software programs like STAR and Bowtie2, and the output is then used to assemble the data at gene or transcript level. In addition, the unannotated transcripts which were not present in databases such as RefSeq, NONCODE or ENSEMBL, can be potential novel lncRNAs [85]. The potential novel lncRNA should then be verified for 1) whether or not the reads are transcriptional noise, 2) if those transcripts do not have coding potential and 3) if the transcript is greater than 200 bases before being considered as lncRNA. The candidates that have RNA Pol II binding sites and located within K4-K36 region are likely products of active transcription and are not considered as transcriptional noise [20, 52, 91]. The Coding Potential Calculator (CPC) algorithm, as an example, can be used to estimate the protein-coding potential of the new detected RNA species and can clarify, if it is a lncRNA or not [35, 90].

1.2.3 Functional roles and actions of mechanism of long non-coding RNAs

Long non-coding RNAs play important roles in gene expression regulation, physiological conditions and disease conditions [51]. The regulation of eukaryotic gene expression occurs on multiple levels, like on chromosome and chromatin, transcriptional, and post-transcriptional levels (Figure 1.3). At each level, lncRNA regulation is taking place. For example, the regulation of gene expression at chromosome and chromatin levels by lncRNAs is mediated through the regulation of genomic structures and nuclear architecture organization (Figure 1.3 (1)) [86]. *H19 imprinted maternally expressed transcript (H19)* and *X inactivation-specific transcription (XIST)* are examples of lncRNAs which regulate chromosome and chromatin by interfering with chromatin structure and organization [142].

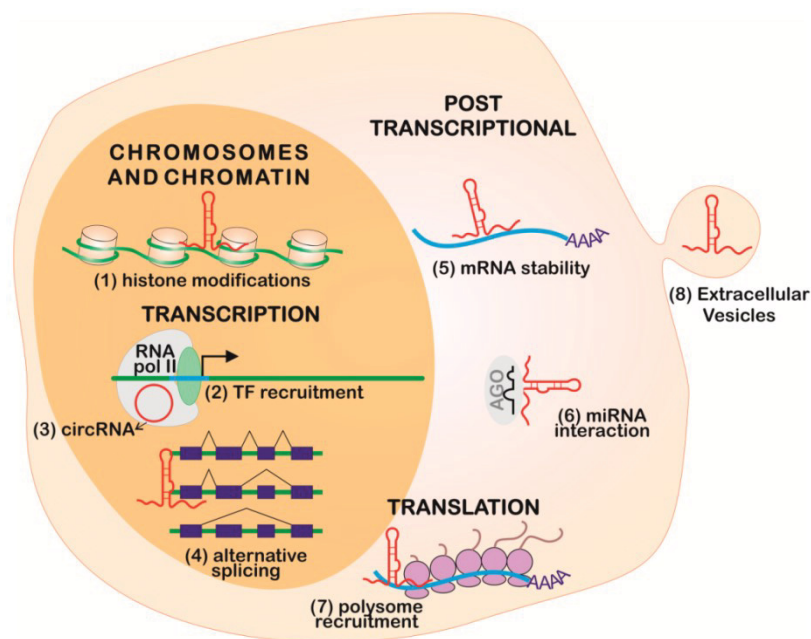


Figure 1.3: Long non-coding RNAs (lncRNAs) in gene expression regulation. Different lncRNA can regulate gene expression through histone modifications (chromatin and chromosome condensation (1), by direct recruitment of transcription factors (TF) (2), via binding to RNA Pol II (3), through mediating alternative splicing (4) and mRNA stability (5), by interacting with miRNA (6), by recruiting polysomes (7), and via secretion in vesicles may modulate gene expression in neighboring cells (8). This figure is obtained from Fernandes et al. [51].

Additionally, some lncRNAs can regulate gene expression at the transcriptional level by either indirectly or directly binding to RNA Pol II (Figure 1.3 (3)). Examples of lncRNAs acting at this regulatory level are *antisense organic cation/carnitine transporter 4* –

pseudogene 5 (asOct4-pg5), which can regulate epigenetic markers by acting *cis* and regulating its antisense mRNA counterpart, *Oct4* [67], and *circRNA eukaryotic translation initiation factor 3 subunit J (circEIF3J)* and *circRNA poly(A) binding protein interacting protein 2 (circPAIP2)* [31, 107], which bind directly to RNA Pol II. Other lncRNAs, such as *long non-coding RNA-regulator of reprogramming (lncRNA-ROR)* [49], can regulate transcription factor (TFs) recruitment (Figure 1.3 (2)) and lncRNAs like *extra coding CCAAT enhancer binding protein alpha (ecCEBPA)* [42] can control DNA methyltransferases recruitment [112]. It has also been shown that lncRNAs, such as *metastasis associated lung adenocarcinoma transcript 1 (MALAT1)* [56], can be secreted via extracellular vesicles (Figure 1.3 (8)), thereby acting as messengers in cell-to-cell communication to affect neighboring and distant cells [70].

Post-translational regulation by lncRNAs takes place at several points: interplay between lncRNAs and miRNAs (figure 1.4), alternative splicing (Figure 1.3 (4)), mRNA stability (Figure 1.3 (5)) and translation (Figure 1.3 (7)). Long non-coding RNAs can also act as “miRNA sponges”, which means as endogenous competitors RNAs (ceRNAs), by containing miRNA binding sequences that may result in less binding of miRNAs to the actual target mRNAs (Figure 1.4 A) [55, 65]. Both linear and circular RNAs can function as this kind of sponges [65], while this function is more common for circRNAs [13, 200]. In addition, lncRNAs can also act as miRNA precursors, primary miRNA (lnc-pri-miRNA), by using microprocessor Dicer and/or Drosha endoribonuclease cleavage to terminate transcription rather than the canonical cleavage-and-polyadenylation pathway (Figure 1.4 B) [41]. The lncRNA *LOC554202* is shown to be the precursor of miR-31 which was shown to play a role in preventing breast cancer metastasis [8]. Conversely, miRNAs can target lncRNAs to regulate their stability and half-lives (Figure 1.4 C) [194] which is the case for miR-152 that targets and decreases expression of lncRNA *XIST* in glioblastoma [191]. Finally, lncRNAs and miRNAs can compete in binding to the same target site of mRNAs (Figure 1.4 D) [48]. The lncRNA *beta-secretase-1-antisense (BACE1-AS)* is shown to compete with miR-485-5p to bind to its sense partner *BACE1* [48].

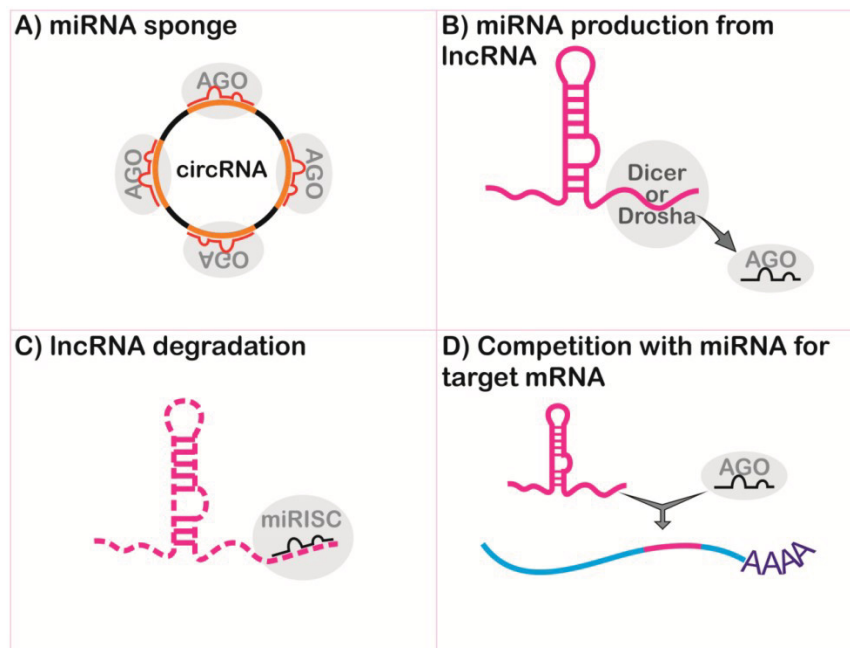


Figure 1.4: Interaction between microRNAs and long non-coding RNAs (lncRNAs). Both linear and circular forms of lncRNAs can act as miRNA sponges to reduce interaction between target mRNA-miRNA (A); lncRNAs can act as miRNA precursors to produce mature miRNAs after microprocessor (Dicer and/or Drosha) cleavage (B); lncRNAs can be degraded by miRNAs (C); lncRNAs can compete with miRNAs for the same mRNA binding site (D). circRNA: circular lncRNA; AGO: argonaute: proteins; miRISC: miRNA-induced silencing complex; Dicer: endoribonuclease; Drosha: endoribonuclease. This figure is obtained from Fernandes et. al. [51].

1.2.4 Long non-coding RNAs in physiological conditions and diseases

Due to their relevance and important roles in gene regulation, lncRNAs can be quite often linked to the development of several diseases such as cancer [73], cardiovascular disease [63], and fibrosis [82]. There are notable examples of potential oncogenic lncRNAs in the literature. One example is the lncRNA *nuclear paraspeckle assembly transcript 1 (NEAT1)* [75]. It is upregulated and associated with poor prognosis [50] in many cancers like hepatocellular carcinoma [170], non-small cell lung cancer (NSCLC) [79], cholangiocarcinoma [195] and breast cancer [105, 106]. *NEAT1* is associated with cell proliferation, invasion, tumorigenesis, and metastasis [79, 105, 106, 170, 195]. Another potent oncogenic lncRNA, which is associated with tumorigenesis in various tumor types [14], is *HOX transcript antisense RNA (HOTAIR)* [143]. *HOTAIR* promotes proliferation and migration in cervical cancer [80, 182], contributes to chemoresistance in colorectal cancer [22] and is associated with metastasis and poor survival in breast cancer [61]. Recently, a number of lncRNAs

were also studied in glioblastoma: *maternally expressed 3 (MEG3)* controls proliferation via interaction with p53 and *MDM2* proteins [11]; *colorectal neoplasia differentially expressed (CRNDE)* regulates glioma cell growth via mTOR signaling [169]; *HOXA11 antisense RNA (HOXA11-AS)* promotes glioma cell growth and metastasis by targeting the miR-130a-5p/high mobility group box 2 (HMGB2) axis. Although most of the studies describe the role of lncRNAs in cancer, there are also many lncRNAs dysregulated during chronic multifactorial diseases such as cardiovascular and neurological diseases [26, 34]. Certain lncRNAs are dysregulated in schizophrenia [37, 150], autism spectrum disorders [179, 203], and neurodegenerative diseases such as Alzheimer's [119], Parkinson's [83], and [128] Huntington's diseases. Dysregulation of lncRNAs has been detected in cardiovascular diseases [88, 94, 189, 201] and in diabetes mellitus [201]. Tissue-specific expression pattern and the correlation of their expression with certain disease promoting genes, which can modulate cancer progression, immune response or cell pluripotency [73], make lncRNAs attractive as potential prognostic or predictive biomarkers in various types of diseases [151].

1.2.5 ***HOXA transcript antisense RNA myeloid-specific 1***

The long non-coding RNA *HOXA transcript antisense RNA myeloid-specific 1 (HOTAIRM1)* gene locus maps between the *HOX1* and *HOXA2* genes on chromosome 7 and is transcribed in antisense orientation from the same CpG island where the *HOXA1* start site is embedded [196]. In this study, the authors originally described that up-regulation of *HOTAIRM1* is associated with retinoic acid (RA)–driven myelopoiesis of normal human hematopoietic and NB4 promyelocytic leukemia cells via modulating gene expression in the *HOXA* cluster.

HOTAIRM1 was shown to be transcribed in a number of tissues and dysregulated in certain diseases and various cancers [43, 117, 118, 167, 183, 198, 199]. Previous studies have reported that *HOTAIRM1* expression is increased in high-grade gliomas and in recurrent compared to primary glioblastomas [30, 197]. More recently, *HOTAIRM1* has been shown to promote glioma growth and invasion through up-regulation of *HOXA1* expression [104]. Despite the fact that *HOTAIRM1* was shown to be upregulated in higher grade of gliomas in that study, its relevance in patient survival and its contribution to therapy resistance remained unanswered to date.

In our laboratory, Daniel Picard performed bioinformatic analyses by using published expression datasets of glioblastomas from patients with long-term survival of more than

3 years as well as patients with short-term survival of less than 1 year after diagnosis [139]. A Volcano plot of lncRNAs associated with short-term versus long-term survival was generated (Figure 1.5 A). Only three lncRNAs were found to be upregulated and associated with short-term survival. Based on fold-change and statistical significance, *HOTAIRM1* was one of the strongest candidates. Two independent, non-overlapping studies (Gravendeel et al., (2009) [59], TCGA (2009) [23] (<https://www.cancer.gov/tcga>) were used to validate that higher *HOTAIRM1* expression was associated with poorer overall survival (Figure 1.5 B-C).

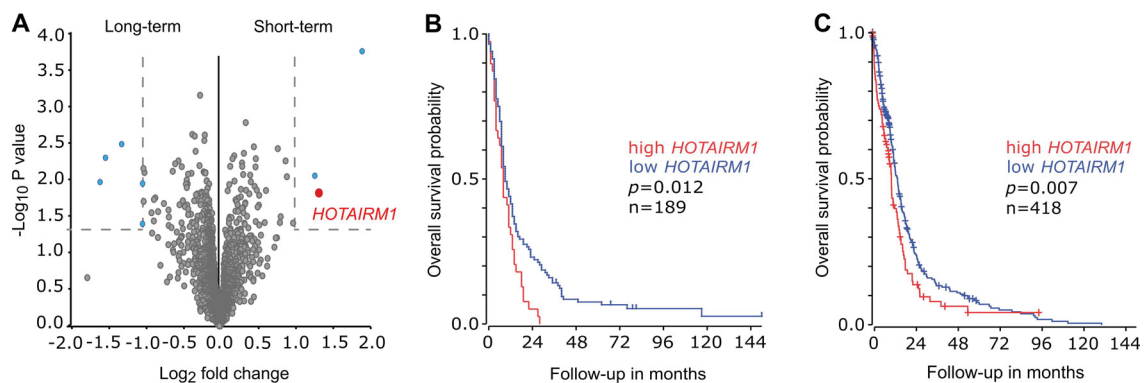


Figure 1.5: High *HOTAIRM1* expression is associated with poorer prognosis in glioblastoma. The Volcano plot shows differential expression of tumors from patients with long-term versus short-term survival. Blue circles represent significant genes (± 2 fold change and $p < 0.05$), the red circle highlights *HOTAIRM1* as gene of interest and grey circles are not significant (A). Kaplan-Meier survival plot for *HOTAIRM1* expression based on a publicly available glioblastoma data set [59] (B) and the TCGA data set [23] (C). Cut-off was determined by third quartile and log rank statistics were calculated.

Interestingly, using the Gravendeel et al. dataset [59], the prognostic value of *HOTAIRM1* was found to be independent of the *IDH1* mutation status (Figure 1.6 A-B). Additionally, *HOTAIRM1* was observed to be the only lncRNA upregulated when comparing samples with trisomy 7 against typical two copy number samples (Figure 1.6 C-D). This analysis was achieved using samples with both expression data and copy number information. Only by combining samples from 3 datasets (Murat et al., (2008); Sturm et al., (2012); Vital et al., (2010) [124, 158, 166] enough samples from the U133 P2 array (29 samples) were accumulated for the analysis, whereas the TCGA data set (<https://www.cancer.gov/tcga>), which was processed using the human exon 1.0 ST array, had 413 samples.

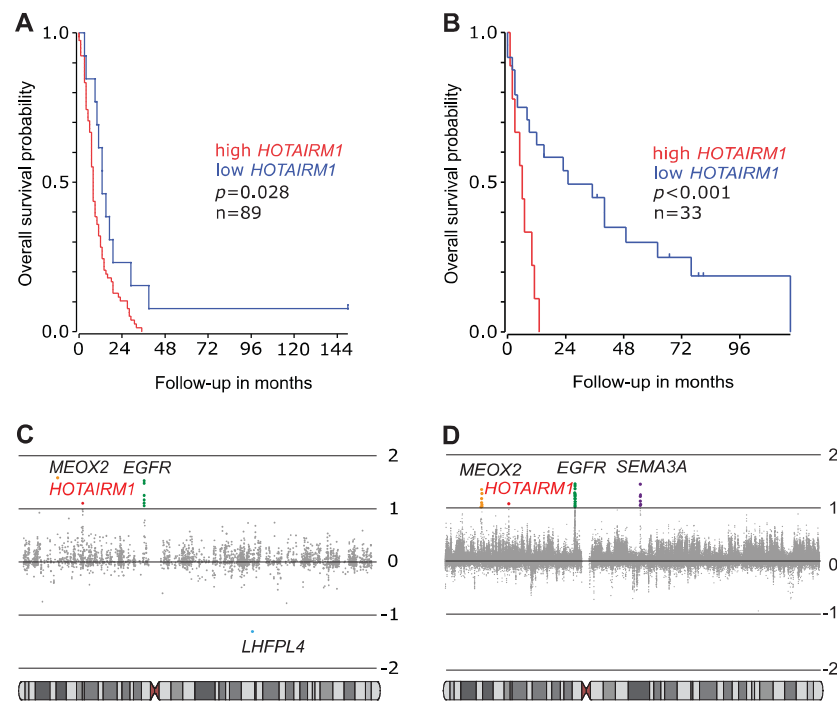


Figure 1.6: High *HOXA* transcript antisense RNA myeloid-specific 1 (*HOTAIRM1*) expression is independent of *IDH* status and is associated with trisomy 7 in glioblastoma. Subdivided Kaplan-Meier survival plot of Gravendell et al. based on *IDH1* status; *IDH1* wildtype (A) and mutant (B). Red and blue lines indicate high and low *HOTAIRM1* expression, respectively. Expressional analysis of combined (Murat et al., (2008); Sturm et al., (2012); Vital et al., (2010) [129, 164, 172] (C) and TCGA (2009) [23] (<https://www.cancer.gov/tcga>) (D). Cut-off was determined by third quartile and log rank statistics were calculated.

2 Aim of the study

Recent molecular genetic and cell biological studies have markedly improved our understanding of glioblastoma biology [2, 140]. However, only few alterations have been established as clinically relevant biomarkers to date, therefore, clinically relevant molecularly targeted therapy approaches are still missing. Since long non-coding RNAs (lncRNAs) have largely been ignored in previous studies and are found to have functional roles in tumorigenesis, cancer progression and therapy resistance [9, 68, 149], they might serve as potential biomarkers. Previous studies have reported that the long non-coding RNA *HOXA transcript antisense RNA myeloid-specific 1 (HOTAIRM1)* expression is increased in high-grade gliomas and in recurrent compared to primary glioblastomas [30, 197]. Moreover, our laboratory has also observed that high *HOTAIRM1* expression is associated with poor outcome glioblastoma patients.

Accordingly, the aim of this study is to elucidate the role of the long non-coding RNA *HOTAIRM1* in glioblastoma pathogenesis. If *HOTAIRM1* is a marker for aggressive biology in glioblastoma, a reduction in oncogenic potential of glioblastoma cells should be observed using siRNA- or shRNA-mediated knockdown, in line with other studies [104, 109]. To determine how *HOTAIRM1* can promote glioblastoma growth, a proteogenomic approach was performed. The final part of this thesis aimed to study *HOTAIRM1* in the context of glioblastoma therapy. To accomplish this, radiosensitivity of glioblastoma cells was assessed following *HOTAIRM1* downregulation and bioinformatic as well as experimental *in vitro* studies were performed to uncover underlying molecular pathomechanisms.

3 Materials

3.1 Cell culture media and reagents

The cell culture media and reagents used in this study are listed below in Table 3.1.

Table 3.1: List of media and cell culture reagents.

Name	Company	Catalog/Order number
Dulbecco's Modified Eagle Medium (DMEM) (1x) + GlutaMAX™	Thermo Fisher Scientific, Waltham, MA, USA	31966021
Penicillin/Streptomycin	Merck Millipore, Burlington, MA, USA	P4333-100ML
FBS (Fetal Bovine Serum), heat inactivated	Sigma-Aldrich, Taufkirchen, Germany	F9665
Phosphate Buffered Saline (PBS)	Sigma-Aldrich, St. Louis, MO, USA	D8537
Penicillin/Streptomycin	Merck Millipore, Burlington, MA, USA	P4333-100ML
Dimethylsulfoxide (DMSO)	AppliChem, Darmstadt, Germany	A3672
Puromycin	InvivoGen, San Diego, CA, USA	ant-pr-5
Blasticidin	InvivoGen, San Diego, CA, USA	ant-bl-1
Cell-Tak™	Corning, New York, USA	354240

3.2 Cell lines

The human glioblastoma cell lines T98G [156], U251MG [137], and U87MG [137] were obtained from American Type Culture Collection (ATCC, Manassas, VA). LN229 and LN18 [44] cell lines were provided by Dr. M. Hegi, Lausanne, while the SF126 [147] cell line was obtained from Japanese Collection of Research Bioresources Cell Bank (JCRB, Osaka, Japan).

3.3 Kits, reagents and others materials

The kits, chemicals, stains, and reagents used in this study are listed in Table 3.2.

Table 3.2: List of kits, chemicals, reagents and others.

Name	Company	Reference
TRIzol	Thermo Fisher Scientific, Waltham, MA, USA	15596026
RSC simplyRNA Tissue	Thermo Fisher Scientific, Waltham, MA, USA	AS1340
MMLV-RT	Thermo Fisher Scientific, Waltham, MA, USA	M3683
Lipofectamine RNAiMAX	Thermo Fisher Scientific,	13778150

Transfection Reagent Opti-MEM™	Waltham, MA, USA Thermo Fisher Scientific, Waltham, MA, USA	31985062
Polyethylenimine (PEI)	Merck Millipore, Burlington, MA, USA	408727
Polybrene (hexadimethrine bromide)	Merck Millipore, Burlington, MA, USA	107689
TruSeq RNA Sample Preparation v2 Kit	Illumina, San Diego, USA	RS-122-2001/2002
4',6-Diamidin-2- phenylindol (DAPI)	Thermo Fisher Scientific, Waltham, MA, USA	62248
Protein Assay Dye Reagent Concentrate	Bio-Rad, Hercules, USA	500-0006
Precision Blue Real-Time PCR Dye	Merck Millipore, Burlington, MA, USA	1722-5555
Protease Inhibitor Cocktail	Roche, Basel, Switzerland	4693132001
White bottom 96-well plate	Thermo Fisher Scientific, Waltham, MA, USA	136101
CellTiter-Glo	Promega, Madison, USA	G7570
BioCoat™ Matrigel Invasion Chamber	Corning, New York, USA	354480
Toluidine Blue	Sigma-Aldrich, St. Louis, MO, USA	89640
Vectashield Mounting Medium for Fluorescence	Vector Laboratories, Eching, Germany	H-1000
SuperSignal™ West Femto Maximum Sensitivity	Thermo Fisher Scientific, Waltham, MA, USA	C118A
Crystal violet	Sigma-Aldrich, St. Louis, MO, USA	32675
Eukitt Quick-Hardening Mounting Medium	Sigma-Aldrich, St. Louis, MO, USA	3989
Dihydroethidium (HET)	Thermo Fisher Scientific, Waltham, MA, USA	D11347
MitoSOX™ Red	Thermo Fisher Scientific, Waltham, MA, USA	M36008
Random Primer	Promega, Mannheim, Germany	34095
TaqMan® Gene Expression Master Mix	Applied Biosystems, Foster City, USA	4369016
Whatman™ Gel Blot Paper	GE Healthcare, Chicago, USA	GB003
Protein Standard	Sigma-Aldrich, St. Louis, MO, USA	P0914
Novex™ WedgeWell™ 4-12% Tris-Glycine Gel	Thermo Fisher Scientific, Waltham, MA, USA	XP04122BOX
Oligo(dT) Primer	Promega, Madison, USA	C110A
PageRuler™ Prestained Protein Ladder	Thermo Fisher Scientific, Waltham, MA, USA	26616
Ethanol absolute	VWR, Radnor, PA, USA	20.821.330
Formalin 10% Neutral Buffered	ScyTek Laboratories, Utah, USA	FRN999
2-Propanol	VWR, Radnor, PA, USA	20.842.330
Chloroform	Merck Millipore, Burlington, MA, USA	102.445
Albumin Fraction V	Roth, Karlsruhe, Germany	8076.4
GoTaq® qPCR Master Mix (2x)	Promega, Madison, USA	A600A

M-MLV Reverse Transcriptase	Promega, Madison, USA	M3681
RNase A (DNase-free)	AppliChem, Darmstadt, Germany	A3832
Amersham TM Protran TM 0.45 µm nitrocellulose membrane	Sigma-Aldrich, St. Louis, MO, USA	10600002
Seahorse XF96 Cell Culture Microplates	Agilent, Santa Clara, CA, USA	101085-004
Seahorse Mito Stress Test Kit	Agilent, Santa Clara, CA, USA	103015-100
Seahorse XF base assay medium	Agilent, Santa Clara, CA, USA	103334-100

3.4 Antibodies

The antibodies used in this study are listed below in Table 3.3.

Table 3.3: List of antibodies.

Name	Company	Reference
anti-Actin B (C4)	Merck Millipore, Burlington, MA, USA	MAB1501
anti-TGM2	Cell Signaling, Danvers, MA, USA	3557S
anti-ASNS	Cell Signaling, Danvers, MA, USA	20843
anti-ASPG	Cell Signaling, Danvers, MA, USA	65552
Anti-Mouse IgG, HRP-linked	Santa Cruz Biotechnology, Dallas, TX, USA	H2014
Anti-Rabbit IgG, HRP-linked	Cell Signaling, Danvers, MA, USA	7074S

3.5 Buffers

The buffers used for western blotting analysis in this study are listed below in Table 3.4.

Table 3.4: List of buffers.

Name	Composition
TBS-T	20 mM Tris (pH 7,5); 150 mM NaCl; 0,1% Tween 20
RIPA Lysis Buffer (10x)	Sigma-Aldrich, St. Louis, MO, USA (Reference #20-188)
Sample Buffer (5x)	1 M Tris/HCL (pH 6,8); 62,5% (v/v) Glycerin; 10% (w/v) sodium dodecyl sulfate (SDS)
Tris-Glycine SDS Running Buffer	Thermo Fisher Scientific, Waltham, MA, USA (Reference #LC2675)
Transfer Buffer (10x)	25 mM Tris; 190 mM Glycine

3.6 Oligonucleotides

The TagMan probes and siTOOLS, and the shRNA sequence, plasmids and primers used in this study are listed below in Table 3.5 and Table 3.6, respectively.

Table 3.5: List of TagMan and siTOOLS probes.

Name	Company	Reference
HOTAIRM1 (exon 1-3) specific TagMan probes	Integrated DNA Technologies (IDT), Coralville, IA, USA	Hs.PT.58.45434173
PGK1 specific TagMan probes	IDT, Coralville, IA, USA	Hs.PT.58v.606641
TGM2 specific TagMan probes	IDT, Coralville, IA, USA	Hs.PT.58.23141755
HOTAIRM1-siPOOLS (5 nmol)	siTOOLS Technology, Munich, Germany	100506311
neg control siPOOLS (5 nmol)	siTOOLS Technology, Munich, Germany	
TGM2 siPOOLS (5 nmol)	siTOOLS Technology, Munich, Germany	7052-TGM2

Table 3.6: List of shRNA sequence, plasmids and primers for GoTaq® real-time PCR.

Name	Sequences [5'-3']	Company/Reference
HOTAIRM1 siRNA	GGAGACTGGTAGCTTATTA	IDT, Leuven, Belgium
pLK0.1-TRC cloning vector		AddGene, Watertown, USA (#10878)
pMDL/pRRE		AddGene, Watertown, USA (#12251)
pRSV-Rev		AddGene, Watertown, USA (#12253)
pMD2.G		AddGene, Watertown, USA (#12259)
ASNS-forward	CTGCACGCCCTCTATGACAA	IDT, Leuven, Belgium
ASNS-reverse	GGCAGCCAATCCTTCTGTCT	IDT, Leuven, Belgium

3.7 Software and hardware

The software and hardware used in this study are listed below in Table 3.7 and Table 3.8, respectively.

Table 3.7: List of software.

Software	Company
Partek Flow	Partek Incorporated, Missouri, USA
STAR v2.4.1d aligner	https://github.com/alexdobin/STAR
Bowtie 2 v2.2.5 aligner	http://bowtie-bio.sourceforge.net/bowtie2/index.shtml
ENSEMBL Genome browser	https://www.ensembl.org
AxioVision Version 4.8	https://www.zeiss.com/microscopy/int/products/microscope-software/axiovision.html

Wave Version 2.4.0.60	Agilent, Santa Clara, CA, USA
ImageJ	Wayne Rasband at the National Institutes of Health; http://rsbweb.nih.gov/ij/
R2 platform	R2: Genomics Analysis and Visualization Platform (http://r2.amc.nl)
Proteome Discoverer (version 1.4.1.14)	Thermo Fisher Scientific, Waltham, MA, USA
Mascot (version 2.4)	Matrix Science, London, UK
TCGA	https://www.cancer.gov/tcga

Table 3.8: List of hardware.

Hardware	Product	Company
Maxwell RSC instrument	RNA Isolation System	Promega, Madison, USA
CFX384 Touch™	Real-Time PCR Detection System	Bio-Rad, Hercules, USA
Bioanalyzer	RNA quality analyzer	Agilent, Santa Clara, CA, USA
HiSeq 2500	Sequencer	Illumina, San Diego, USA
TissueLyser	Homogenizer	Qiagen, Hilden, Germany
RSLCnano U3000 HPLC	Mass spectrometer	Thermo Fisher Scientific, Waltham, MA, USA
QExactive plus	Mass spectrometer	Thermo Fisher Scientific, Waltham, MA, USA
Spark 10M	Microplate reader	Tecan, Maennedorf, Switzerland
Axiovert 200	Microscope	Zeiss, Oberkochen, Germany
Vi-CELL XR	Cell counter	Beckman Coulter, Brea, CA, USA
Gulmay RS225	Irradiation machine	Gulmay Medical, Surrey, UK
Axio Observer Z1	Microscope	Zeiss, Oberkochen, Germany
stereotactic device		Stoelting, IL, USA
cBot		Illumina, San Diego, USA
Acclaim PepMap RSLC C18, 2 cm x 100 µm x 3 µm, 100 Å	Trapping column	Thermo Fisher Scientific, Waltham, MA, USA
Acclaim PepMap RSLC C18, 25 cm x 75 µm x 2 µm, 100 Å	Analytical column	Thermo Fisher Scientific, Waltham, MA, USA
LAS-3000	Imaging System	Fujifilm, Tokyo, Japan
Axio Observer Z1	Microscope	Zeiss, Oberkochen, Germany
Progenesis QI (version 2.0)	Proteomics	Nonlinear Dynamics, Newcastle, UK

4 Methods

4.1 Cell culture

Established human glioblastoma cell lines T98G [156], LN229 [44], U251MG [137], LN18 [44], SF126 [147] and U87MG [137] were used in this study. All cell lines were grown in Dulbecco's modified Eagle's medium (DMEM, Thermo Fischer Scientific) supplemented with 10% heat-inactivated fetal bovine serum (FBS, Sigma-Aldrich) and with 1% Penicillin-Streptomycin (Merck). The cells were grown in a humidified atmosphere with 5% CO₂ atmosphere at 37 °C. Stable cells were grown and/or selected with the culture media containing either Blasticidin [T98G, LN18, SF126 and U87MG] (20 µg/ml, InvivoGen) or Puromycin [LN229 and U251MG] (2 µg/ml, InvivoGen).

4.2 RNA isolation and real-time quantitative PCR

Total RNA extraction was performed by using TRIzol (Thermo Fischer Scientific) or by using the Maxwell RSC instrument (RSC simplyRNA Tissue, Promega) according to the manufacturers' protocol. Reverse transcription for total RNA (1 µg) was performed using a MMLV-RT kit (Promega) with random hexamers according to the manufacturer's instructions. Real-time q-PCR (RT-qPCR) was subsequently performed with a 1:10 dilution of reverse-transcribed cDNA by using a CFX384 Touch™ Real-Time PCR Detection System (Bio-Rad). RT-qPCR TagMan Universal Master Mix II (Applied Biosystems) was employed, with *HOTAIRM1* specific TagMan probes (exon 1-3; Integrated DNA Technologies (IDT)), *TGM2* (IDT), *ASNS* (IDT) or *PGK1* (IDT) as an internal control.

4.3 SiRNA- and shRNA-mediated knockdown

T98G, LN229, LN18 and SF126 were seeded (100.000 cells per well) into 6 well-plates the day before either transient or stable knockdown. *HOTAIRM1* and *TGM2* transient knockdown and their negative controls were achieved by *HOTAIRM1* specific siPOOLS (siTOOLS Technology), *TGM2* specific siPOOLS (siTOOLS Technology) and non-target siPOOLS (Neg. control; siTOOLS Technology), respectively. Transfection of siPOOLS was performed by using Lipofectamine RNAiMAX Transfection Reagent (Gibco). Briefly, 7.5 µl RNAiMAX Transfection Reagent in 125 µl Opti-MEM (Gibco) pipetted well with 0.5 µl (5 pM) siPOOL in 125 µl Opti-MEM.

Lentivirus containing *HOTAIRM1* siRNA segments (sequence is 5'-GGAGACTGGTAGCTTATTTAA-3') was obtained from IDT. *HOTAIRM1*-pLK0.1-TRC plasmid with third generation lentiviral packaging plasmids (pMDL/pRRE, pRSV-Rev and pMD2.G) were transfected into HEK-293T cells using polyethylenimine (PEI, Merck) by following the manufacturer's protocols. Fresh culture media was added (without antibiotics) after 24 and 48 hours post transfection. The virus containing medium (48 hours and 72 days after transfection) was stored at -80°C. Cells were seeded at 6 well plates the day before transduction and were infected with 1.5 ml the viral suspension containing DMEM, 10% FBS and 2 µg/ml polybrene (Merck) for stable cell line generation. The virus medium was removed 24 hours post transduction and selected in medium supplemented with puromycin or blasticidin for at least a week.

4.4 RNA sequencing

Total RNA was isolated from *HOTAIRM1* knockdown and control cells of T98G, LN229 and LN18 72 hours post transfection using TRIzol reagent according to the manufacturer's protocol. Samples were then processed using the TruSeq RNA Sample Preparation v2 Kit (low-throughput protocol; Illumina) to prepare the barcoded libraries from 500ng total RNA. Libraries were validated and quantified using either DNA 1000 or high-sensitivity chips on a Bioanalyzer (Agilent). 7.5 pM denatured libraries were used as input into cBot (Illumina), followed by deep sequencing using HiSeq 2500 (Illumina) for 101 cycles, with an additional seven cycles for index reading. Fastq files were imported into Partek Flow (Partek Incorporated). Quality analysis and quality control were performed on all reads to assess read quality and to determine the amount of trimming required (both ends: 13 bases 5' and 1 base 3'). Trimmed reads were aligned against the hg38 genome using the STAR v2.4.1d aligner. Unaligned reads were further processed using Bowtie 2 v2.2.5 aligner. Finally, aligned reads were combined before quantifying the expression against the ENSEMBL (release 84) database by the Partek Expectation-Maximization algorithm. Partek flow default settings were used in all analyses.

4.5 Western blotting

Cells were lysed and protein was extracted using RIPA Lysis Buffer (Sigma-Aldrich) supplemented with protease and phosphatase inhibitor cocktail. Protein was quantified with the Bradford method using the Protein Assay Dye Reagent Concentrate (BioRad). Samples were separated by SDS polyacrylamide gel electrophoresis (SDS-PAGE, 30

min at 65 V, followed by 90 min at 130 V) using Novex™ WedgeWell™ 4-12% Tris-Glycine Gels (Invitrogen) and transferred to Amersham™ Protran™ 0.45 µm nitrocellulose membranes (Sigma-Aldrich) by wet blot (1h at 10 V) using the Mini Gel Tank and Blot Module (Thermo Fisher Scientific). In order to block unspecific binding sites, membranes were incubated with 5% BSA in TBS-T for 1 h at RT. Subsequently, membranes were incubated with primary antibodies diluted in blocking solution overnight at 4 °C. The next day, membranes were washed three times with TBS-T for 5 min at RT and incubated with secondary antibodies diluted in blocking solution for 1 h at RT. Following three washing steps with TBS-T for 5 min at RT, proteins were visualized using the SuperSignal® West Femto Maximum Sensitivity Substrate (Thermo Fisher Scientific) and detected using the LAS-3000 Imaging System (Fujifilm).

4.6 Proteomics

Proteins were extracted from frozen tissue sections as described elsewhere [138]. Briefly, cells were homogenized in urea buffer with a TissueLyser (Qiagen) and subsequent sonication. After centrifugation for 15 min at 14,000 xg and 4°C, supernatants were collected. Protein concentration was determined via Pierce 660 nm Protein Assay Dye Reagent Concentrate (BioRad) and 10 µg protein per sample were desalted through electrophoretic migration at 50 V for 10 min on a 4 -12 % Bis-Tris polyacrylamide gel (Thermo Fischer Scientific). After silver staining, protein bands were cut out, reduced, alkylated and digested with trypsin before peptide extraction via sonication. Peptides were dissolved and diluted with 0.1 % TFA (v/v).

For mass spectrometric analysis, 15 µL peptide solution per sample were analyzed on a nano-high-performance liquid chromatography electrospray ionization mass spectrometer. The analytical system was composed of a RSLCnano U3000 HPLC coupled to a QExactive plus mass spectrometer via a nano-electrospray ion source (Thermo Fischer Scientific). Injected peptides were concentrated and desalted at a flow rate of 6 µL/min on a trapping column (Acclaim PepMao C18, 2 cm x 100 µm x 3 µm particle size, 100 Å pore size; Thermo Fischer Scientific) with 0.1 % TFA (v/v) for 10 min. Subsequently, peptides were separated at a constant flowrate of 300 nL/min over a 120 min gradient on an analytical column (Acclaim PepMap RSLC C18, 25 cm x 75 µm x 2 µm particle size, 100 Å pore size; Thermo Fischer Scientific) at 60°C. Separation was achieved through a gradient from 4 to 40% solvent B (solvent A: 0.1% (v/v) formic acid in water, solvent B: 0.1% (v/v) formic acid, 84% (v/v) acetonitrile in water). Afterwards, peptides were ionized at a voltage of 1,400 V and introduced into the mass spectrometer operated in positive mode. MS scans were recorded in profile

mode in a range from 350-2000 m/z at a resolution of 70,000 while tandem mass spectra were recorded at a resolution of 17,500. Tandem mass spectra were recorded with a data dependent Top10 method and 30% normalized collision energy. Dynamic exclusion was activated with a repeat count of 1 for 100 s.

Proteome Discoverer (version 1.4.1.14, Thermo Fisher Scientific) was applied for peptide/protein identification with Mascot (version 2.4, Matrix Science) as search engine employing the UniProt database (human; including isoforms; date 2016-03-01). A false discovery rate of 1% ($p \leq 0.01$) on peptide level was set as identification threshold. Proteins were quantified with Progenesis Q1 for Proteomics (Version 2.0, Nonlinear Dynamics).

4.7 CellTiter-Glo luminescent cell viability assay

Cells were seeded (1000-4000 cells per well) into white bottom 96-well plates (Thermo Fischer Scientific) and incubated for 72 hours. Afterwards, cells were incubated with sterile 100 μ l of 1:1 diluted (with PBS) CellTiter-Glo (Promega) for 10 min at RT, shaken for 2 min and the absorbance was measured with a Spark 10M microplate reader (Tecan). All experiments were performed in a minimum of triplicates.

4.8 *In vitro* invasion assay

BioCoat™ Matrigel Invasion (Boyden) Chambers (Corning) were used for the invasion assay. Boyden membranes were activated by adding 500 μ l serum free medium for 2 hours at RT. Afterwards, 750 μ l medium containing 10 % FBS was added into the lower chamber. 2.5×10^5 cells in 500 μ l were resuspended in a serum free medium and were added to the upper chamber. The chambers were removed after 48 h incubation (at 37 °C) and the medium was removed and the membrane was washed once with PBS. Next, the cells that migrated across the polycarbonate membrane were fixed with methanol for 2 min and stained with 1 % toluidine blue for 2 min. The membrane was washed 4 times with distilled water and cells remaining in the upper chamber were removed using a cotton swap. Membranes were allowed to air dry for a minimum of one hour before being mounted on a glass slide with oil. Finally, six random fields were selected and imaged (20X) using an Axiovert 200 microscope (Zeiss) and the AxioVision (Version 4.8) software. Invading cells from a single membrane were counted and summed. The experiments were done a minimum of three times.

4.9 Colony formation assay, N-acetyl cysteine treatment and *in vitro* radiation assay

Cells were harvested by trypsin and counted with Vi-CELL XR (Beckman Coulter), plated on culture treated 100 mm dishes (500 - 1000 cells per plate) and cultured for 21 days. At the end of the incubation period, medium was removed from dishes and cells were washed once in PBS and fixed with 10% formalin for 45 min. Cells were then stained with 0.1% crystal violet for 1h, washed in H₂O to remove excess dye and were allowed to air dry overnight. The following day, colonies that are visible with naked eye were counted. All experiments were performed a minimum of three biological replicates.

For the N-acetyl cysteine (NAC) treatment, colony formation assay was performed as described above with NAC (1 mM) or with PBS (control) to evaluate the effect of the treatment.

For the *in vitro* radiation assay, cells were harvested and counted as previously, suspended in 50 ml Falcon (10,000 cells per ml) and irradiated at 2 and 4 Gy by using Gulmay RS225 irradiation machine (Gulmay Medical). Afterwards, colony formation assay was performed as described above to evaluate the effect of the irradiation.

4.10 Seahorse mito stress assay

LN229 and U251 *HOTAIRM1* knockdown and control cells were seeded into Cell-Tak™ (Corning) coated Seahorse XF96 Cell Culture Microplates (Agilent Technologies) one day prior to the assay at densities of 7500 and 15000 cells per well. Optimal cell numbers for Seahorse experiments (ECAR 10-90, OCAR 40-200) were determined prior to final experiments. Mitochondrial flux was assessed using the Seahorse Mito Stress Test Kit (Agilent Technologies). This assay consists of three subsequent injections of oligomycin (1 µM), carbonyl cyanide-4-phenylhydrazone (FCCP) (0.75 µM) and rotenone/antimycin A (0.5 µM). The assay is done according to the manufacturer instructions. Before the assay, culture medium was exchanged for Seahorse XF base assay medium (Agilent Technologies), supplemented with 2 mM glutamine and 10 mM glucose and the cell culture microplate placed in a non-CO₂ incubator at 37°C for one hour. Preparation of compounds, loading of the sensor cartridge and the assay run were performed according to manufacturer's protocol – standard assay. 4',6-Diamidin-2-phenylindol (DAPI; Thermo Fisher Scientific) staining was performed after the assay and measured parameters were normalized to DNA content (relative fluorescence). The analysis of Seahorse data was conducted using

the Seahorse XF Mito Stress Test Report Generator and Wave Software (version 2.4.0.60, Agilent Technologies).

4.11 Reactive oxygen staining

The measurements of cellular and mitochondrial ROS production were performed with some modifications as described previously [44]. Briefly, cells were incubated with dihydroethidium (HET, 10 μ M, 10 min, and 37°C; Thermo Fisher Scientific) or the mitochondria-targeted variant MitoSOX TM Red (5 μ M, 10 min, 37°C; Thermo Fisher Scientific). Reaction was stopped by washing the cells three times with PBS. The red fluorescence was documented using an Axio Observer Z1 microscope (Zeiss) with the dihydroethidium filter set (F39-500, F48-515, F47-895; AHF Analysetechnik). Images were analysed and fluorescence intensity was quantified using ImageJ software (Wayne Rasband at the National Institutes of Health; <http://rsbweb.nih.gov/ij/>).

4.12 *In vivo* mouse experiments

The *in vivo* mouse experiments were performed by Dr. M. Silginer and Dr. P. Roth in the laboratory of Prof. Dr. M. Weller, Department of Neurology, University Hospital Zurich, Switzerland. All procedures were performed in accordance with the guidelines of Swiss federal law on animal protection. Crl: CD1 Foxn1 nude mice were purchased from Charles River Laboratories (Sulzfeld, Germany). 6-10 week old mice were used in all experiments. Mice were anaesthetized using an intraperitoneal 3 component injection consisting of fentanyl, midazolam and medetomidin, fixed under a stereotactic device (Stoelting) and a burr hole was drilled in the skull 2 mm lateral and 1 mm posterior to the bregma. A Hamilton syringe needle was introduced to a depth of 3 mm and LN229 human glioma cells (75,000) in a volume of 2 μ l PBS were injected into the right striatum. Local cranial radiotherapy with a single dose of 12 Gy was performed at day 15 after tumor implantation using a Gulmay 200 kV X-ray unit (Gulmay Medical) at 1 Gy/min at room temperature. The mice were observed daily and euthanized when neurological symptoms developed or at defined time points for histological analysis. Tumor incidences and sizes were determined on 8 μ m thick cryosections stained with hematoxylin and eosin.

4.13 Bionformatics and statistical analyses

Protein coding genes were filtered out from the Affymetrix U133 Plus 2 array for a final set of 2858 lncRNAs. Initial identification of lncRNAs in long-term versus short-term survivors of glioblastoma was carried out based on the GSE53733 data set (139), excluding the patients with intermediate-term survival.

Kaplan-Meier survival curves for GSE16011 were generated using the R2 platform (R2: Genomics Analysis and Visualization Platform (<http://r2.amc.nl>)) filtered for glioblastoma samples only and IBM SPSS statistics (version 21 IBM corporation) for the TCGA data (Affymetrix Human Exon 1.0 ST array, <https://www.cancer.gov/tcga>) using the last quartile to categorize samples as high *HOTAIRM1* for both datasets.

Trisomy analysis was performed by plotting expression fold change based on trisomy status versus wildtype. U133 Plus 2 glioblastoma datasets with copy number information (n = 29) were taken from GSE7696, GSE36245 and GSE43289, and TCGA samples from the Affymetrix Human Exon 1.0 ST array were plotted separately (samples with undetermined copy number status were removed).

GeneSet Enrichment Analysis was performed using the t value from the paired T-test for both transient transfected RNA Sequencing and proteomics data. Gene sets were comprised of curated pathways from several databases including GO, Reactome, KEGG (March 24 2016 version; http://download.baderlab.org/EM_Genesets/current_release/Human/symbol/) and visualized by using Cytoscape (www.cytoscape.org; $p \leq 0.001$, $q \leq 0.05$, similarity cutoff 0.5).

Micro-RNAs were predicted using the miRanda tool (<https://omictools.com/miranda-tool>) for *HOTAIRM1* and the 12 downregulated proteins (stable LN229 knockdown proteomics). miRNAs were filtered for overlap *HOTAIRM1* and the 12 downregulated proteins, miRNAs present and negatively correlated with *HOTAIRM1* expression in gliomas in the TCGA data set.

Statistical analyses were performed with GraphPad Prism (version 5.0). The mean \pm SEM of at least three independent experiments was used to express obtained data. Two-way ANOVA was used for statistical analyses. Paired T-test and Mann-Whitney test (non-parametric t-test) were used for comparison between two groups. The differences were considered statistically significant at $p < 0.05$.

5 Results

5.1 Functional consequences of knockdown of *HOXA transcript antisense RNA, myeloid-specific 1* in glioblastoma cell lines

5.1.1 Expression of *HOXA transcript antisense RNA, myeloid-specific 1* in glioblastoma cells

Our laboratory previously identified *HOTAIRM1* as a marker of worse prognosis in glioblastoma patients and, therefore, the cellular and molecular effects of modulating *HOTAIRM1* in glioblastoma cell lines were determined. Using previously published data, *HOTAIRM1* was detected to have lower expression in non-neoplastic (“healthy”) brain tissues relative to various glioma cell lines whose *HOTAIRM1* expression levels were in the range of those detected in primary glioblastoma tissues (Figure 5.1).

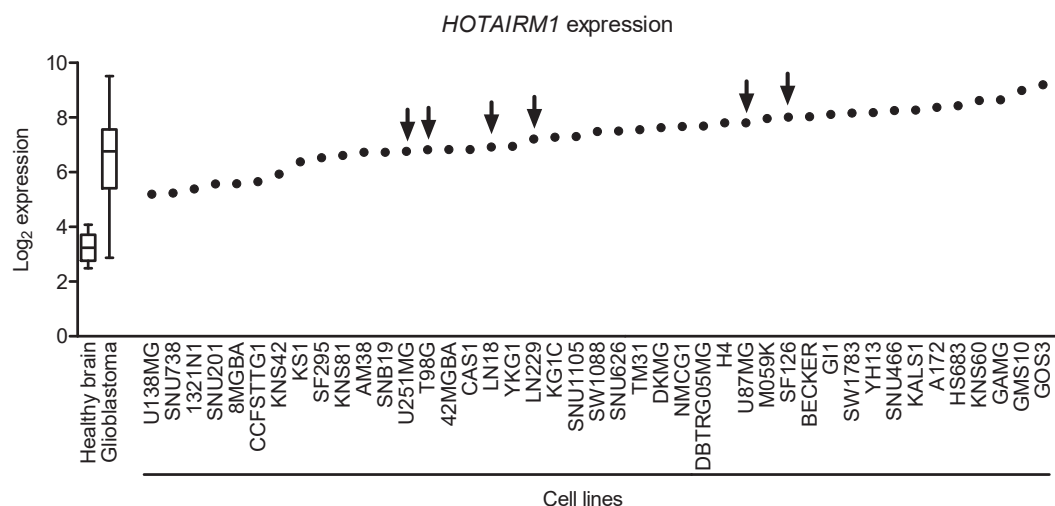


Figure 5.1: Expression of *HOXA transcript antisense RNA, myeloid-specific 1* (*HOTAIRM1*) in non-neoplastic (“healthy”) brain tissues, primary glioblastoma tissues and various cell lines. *HOTAIRM1* expression levels were derived from Affymetrix U133 Plus 2 array data as obtained via the R2 platform (R2: Genomics Analysis and Visualization Platform (<http://r2.amc.nl>)). Arrows indicate glioma cell lines available in the own working group.

To validate the expression of *HOTAIRM1* levels in the glioma cell lines available in our group, qRT-PCR experiments were performed, the results of which are shown in Figure 5.2. The cell lines with relatively high *HOTAIRM1* expression levels were used for the *HOTAIRM1* knockdown experiments, while LN308 cell line was excluded.

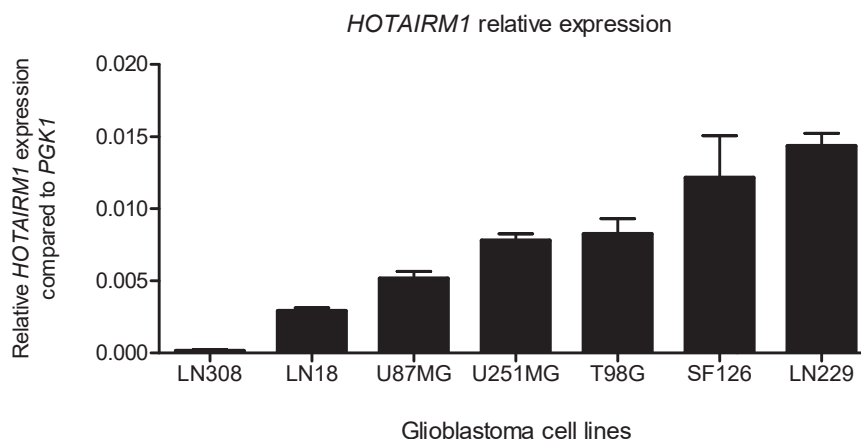


Figure 5.2: Relative expression of *HOXA transcript antisense RNA, myeloid-specific 1* (*HOTAIRM1*) in glioblastoma cell lines. qRT-PCR was performed using TaqMan probes against *HOTAIRM1* or *phosphoglycerate kinase 1* (*PGK1*) (housekeeping gene). Mean \pm SEM is shown. $n = 3$.

5.1.2 SiRNA-mediated knockdown of *HOXA transcript antisense RNA, myeloid-specific 1* decreases oncogenic potential of glioblastoma cells

To functionally investigate the role of *HOTAIRM1* in glioblastoma cells, siRNA-mediated knockdown experiments were performed using siPOOLS (purchased from siTOOLS) against *HOTAIRM1* or non-targeting siRNA controls. A *HOTAIRM1* knockdown efficiency greater than 80% was achieved in all cell lines after 72 hours post-transfection as measured by qRT-PCR (Figure 5.3 B). After successful transient knockdown in all used cell lines, *in vitro* characterization of cell viability via CellTiter-Glo (72 hours, Figure 5.3 B), invasiveness using a Boyden chamber assay (48 hours, Figure 5.3 C), and stemness using a colony formation assay by low density seeding (21 days, Figure 5.3 D) were performed. These experiments revealed that *HOTAIRM1* knockdown significantly reduced cell viability by 20-30%, invasiveness by 35-50%, and colony formation by 25-40% in various glioblastoma cell lines relative to control transfected cells.

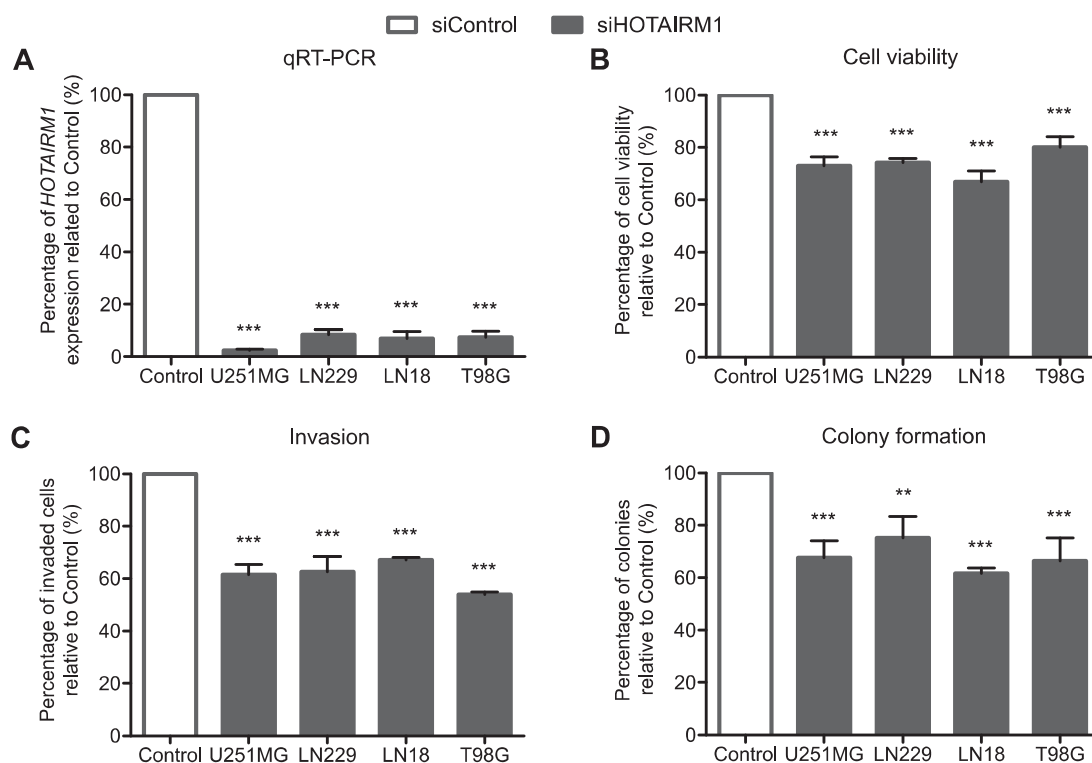


Figure 5.3: SiRNA-mediated *HOXA* transcript antisense RNA, myeloid-specific 1 (*HOTAIRM1*) knockdown decreases oncogenic potential in established glioblastoma cell lines. SiRNA-mediated knockdown was achieved using siPOOLS (siTOOLS). qRT-PCR was performed using TaqMan probes against *HOTAIRM1* or *phosphoglycerate kinase 1* (*PGK1*) (housekeeping gene) (A). Cell viability was measured using CellTiter-Glo assays (B). Invasive propensity was measured using Boyden chamber assays (C). Colony formation assays were done by seeding cells at a density of 500 (U251MG and LN18) to 1000 (LN229 and T98G) cells into 10 cm dishes (D). Histogram bars are as follows, outline bars are indicating the results of the respective control-transfected cells set to 100%. Filled bars are results obtained with *HOTAIRM1* knockdown cells. siControl: non-target siRNA; siHOTAIRM1: siRNA against *HOTAIRM1*. Two-way ANOVA was used for statistical analyses; mean \pm SEM, *** $p < 0.001$, ** $p < 0.01$. $n = 3$.

5.1.3 Stable knockdown of *HOXA* transcript antisense RNA, myeloid-specific 1 decreases oncogenic potential of glioblastoma cells

To further validate the findings obtained by transient *HOTAIRM1* knockdown, a stable knockdown system using a lentiviral shRNA was established. Twenty-four hours post infection, cell lines were selected initially using puromycin (LN229 and U251MG) and subsequently using blasticidin (LN18, SF126 and U87MG). Once the LN229 and U251MG cell lines were transduced and selected using puromycin, a knockdown of 65% was achieved (Figure 5.4 B). However, the relative expression of *HOTAIRM1* for the LN229 shControl in the stably transfected cell line was observed to be much higher than the parental samples (Figure 5.4 A). Therefore, clones were established for both LN229 and U251MG. Avoiding this unintentional overexpression of *HOTAIRM1*,

another selection marker (Figure 5.4 B) was tested. Blasticidin did not significantly alter the expression of *HOTAIRM1* and, therefore, new stable *HOTAIRM1* knockdown cell lines were generated with a plasmid carrying blasticidin as selection marker.

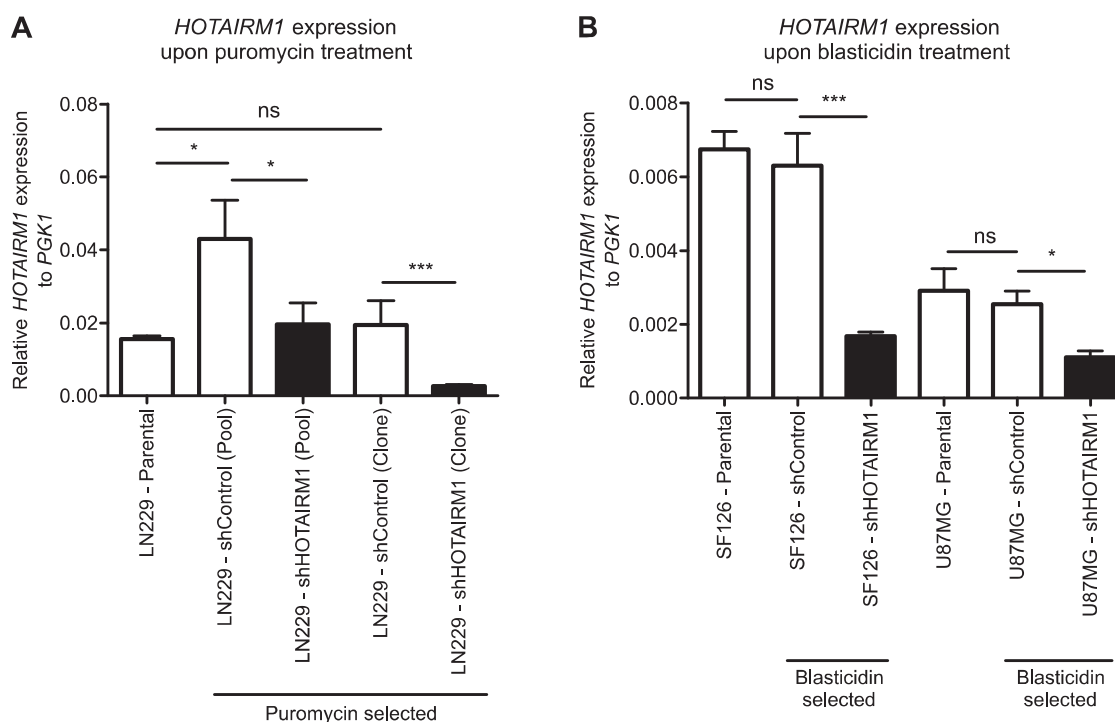


Figure 5.4: *HOXA* transcript antisense RNA, myeloid-specific 1 (*HOTAIRM1*) expression is affected by selection antibiotic. Comparison of relative *HOTAIRM1* expression after puromycin selection (parental, shControl and shHOTAIRM1) in stably transfected LN229 cells (**A**). *HOTAIRM1* expression after blasticidin (2 μ g/ml) treatment in SF126 and U87MG (parental, shControl and shHOTAIRM1) cells (**B**). qRT-PCR was performed using TaqMan probes against *HOTAIRM1* or *phosphoglycerate kinase 1* (*PGK1*) (housekeeping gene). Calculations were based on relative *HOTAIRM1* expression normalized to *PGK1* expression. Parental: non-treated cells; shControl: non-target shRNA; shHOTAIRM1: shRNA against *HOTAIRM1*. Two-way ANOVA was used for statistical analyses; mean \pm SEM, *** $p < 0.001$, * $p < 0.05$. $n = 3$.

Stable knockdown efficiency of 65-85% was achieved in all cell lines (Figure 5.5 A) and the functional characterization of knockdown and control cells was performed like it was shown in the siRNA-mediated *HOTAIRM1* knockdown models (Figure 5.5 B-D). Cell viability was decreased by 20-40% (Figure 5.5 B) and invasiveness by 10-70% (Figure 5.5 C) similar to the results obtained by siRNA-mediated knockdown. Additionally, colony formation potential was reduced in most cell lines by 25-70% (Figure 5.5 D).

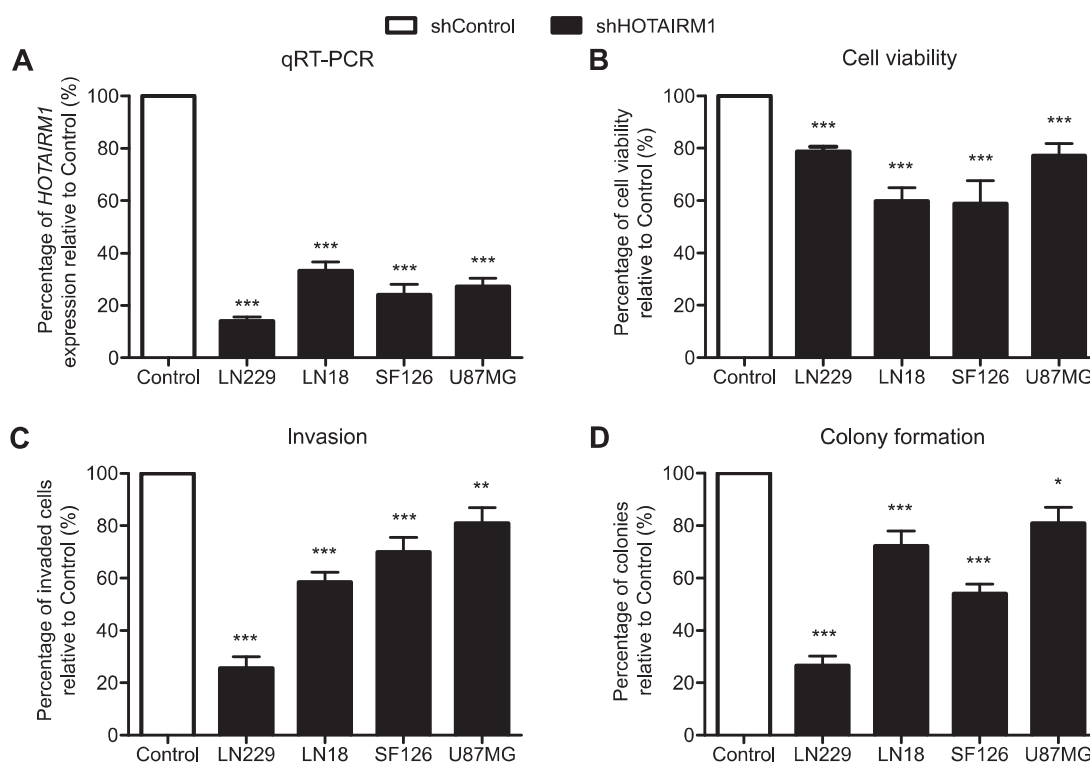


Figure 5.5: Stable *HOXA* transcript antisense RNA, myeloid-specific 1 (*HOTAIRM1*) knockdown decreases oncogenic potential in established glioblastoma cell lines. Stable knockdown was achieved using shRNA against *HOTAIRM1*. qRT-PCR was performed using TaqMan probes against *HOTAIRM1* or *phosphoglycerate kinase 1* (*PGK1*) (housekeeping gene) (A). Cell viability was measured using CellTiter-Glo assays (B). Invasive propensity was measured using Boyden chamber assays (C). Colony formation assays were done by seeding cells at a density of 500 (U251MG and LN18) to 1000 (LN229, U87MG and SF126) cells into 10 cm dishes (D). Histogram bars are as follows: outline bars represent results obtained for control-transfected cells set to 100% and filled bars are results obtained for the respective glioma cells after *HOTAIRM1* knockdown. shControl: non-target shRNA; shHOTAIRM1: shRNA against *HOTAIRM1*. Two-way ANOVA was used for statistical analyses; mean \pm SEM, *** $p < 0.001$, ** $p < 0.01$. $n = 3$.

5.2 Proteogenomic analysis indicates mitochondrial dysfunction upon *HOXA* transcript antisense RNA, myeloid-specific 1 knockdown in glioblastoma cells

5.2.1 Results of RNA sequencing following siRNA-mediated *HOXA* transcript antisense RNA, myeloid-specific 1 knockdown

To gain a better understanding of the molecular consequences of *HOTAIRM1* knockdown in glioblastoma cells RNA sequencing was performed for U251MG, LN229 and T98G cells 72 hours post-transfection with either the *HOTAIRM1* siPOOL or with control siRNA. Raw reads were trimmed for quality, aligned using STAR (<https://research.csc.fi/-/star-aligner>) against the whole genome and annotated against

ENSEMBL (<https://www.ensembl.org>), both hg19, and finally normalized using counts per million. T-tests were performed comparing *HOTAIRM1* knockdown glioblastoma cells against controls. Data were analysed using GeneSet Enrichment Analysis (GSEA) and the output was visualized using cytoscape ($p < 0.05$, $q < 0.05$). The GSEA input uses all available gene information without filtering for significance. Therefore, as seen in our previous experiments, if a false discovery rate (FDR) q value > 0.05 is used, the results can only rarely be validated. As shown in Figure 5.6, all of the significant genesets were negatively enriched for the *HOTAIRM1* knockdown glioblastoma cells, with overall descriptive terms including DNA damage, transcription, mitochondrial respiration and mitosis.

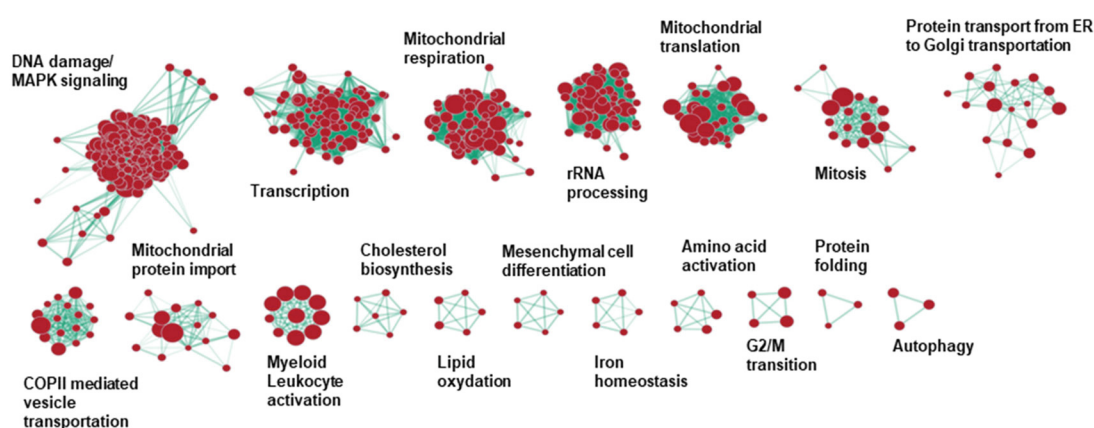


Figure 5.6: RNA sequencing results upon siRNA-mediated *HOXA transcript antisense RNA, myeloid-specific 1 (HOTAIRM1)* knockdown in U251MG, LN229 and T98G glioblastoma cell lines. The analysis was based on comparison between control cells vs *HOTAIRM1* knockdown cells. The genesets with significant p - and q -value ($p < 0.05$, $q < 0.05$) were used in Cytoscape molecular interaction visualization. Red circles: negatively enriched genesets in *HOTAIRM1* knockdown cells.

Table 5.1 and Table 5.2 show the positively and negatively enriched genesets in the *HOTAIRM1* knockdown cells, respectively. None of the positively enriched genesets for *HOTAIRM1* knockdown cells showed a significant false discovery rate ($q < 0.05$). The top 10 hits of the negatively enriched genesets include transcription, cell cycle and ATP production, as it was demonstrated in Figure 5.6.

Table 5.1: GeneSet Enrichment Analysis (GSEA) based on RNA sequencing upon *HOXA transcript antisense RNA, myeloid-specific 1 (HOTAIRM1)* siRNA-mediated knockdown in glioblastoma cells. Positively enriched genesets in the *HOTAIRM1* knockdown cells are listed according to their normalized expression score values. NES: normalized expression score; NOM: nominal; FDR: false discovery rate.

GeneSet details	NES	NOM <i>p</i> -value	FDR <i>q</i> -value
CADHERIN SIGNALING PATHWAY_PANTHER PATHWAY_P00012	2.11899	<0.001	0.16766
LIMB DEVELOPMENT_GOBP_GO:0060173	2.01167	0.00238	0.30982
APPENDAGE DEVELOPMENT_GOBP_GO:0048736	1.99275	<0.001	0.25373
APPENDAGE MORPHOGENESIS_GOBP_GO:0035107	1.93417	<0.001	0.34565
HISTONE-LYSINE N-METHYLTRANSFERASE ACTIVITY_GOMF_GO:0018024	1.92291	<0.001	0.30706

Table 5.2: GeneSet Enrichment Analysis (GSEA) based on RNA sequencing upon *HOXA transcript antisense RNA, myeloid-specific 1 (HOTAIRM1)* siRNA-mediated knockdown in glioblastoma cells. Top 10 negatively enriched genesets in the *HOTAIRM1* knockdown cells are listed according to their normalized expression score values. NES: normalized expression score; NOM: nominal; FDR: false discovery rate

GeneSet details	NES	NOM <i>p</i> -value	FDR <i>q</i> -value
RUNX1 REGULATES TRANSCRIPTION OF GENES INVOLVED IN DIFFERENTIATION OF HSCS_REACTOME DATABASE ID RELEASE 61_8939236	-2.22344	<0.001	<0.001
REGULATION OF MITOTIC CELL CYCLE_REACTOME DATABASE ID RELEASE 61_453276	-2.17473	<0.001	<0.001
ACTIVATED PKN1 STIMULATES TRANSCRIPTION OF AR (ANDROGEN RECEPTOR) REGULATED GENES KLK2 AND KLK3_REACTOME_R-HSA- 5625886.1	-2.16665	<0.001	3.36E-04
DEPOSITION OF NEW CENPA-CONTAINING NUCLEOSOMES AT THE CENTROMERE_REACTOME_R-HSA-606279.1	-2.16189	<0.001	2.52E-04
RESPIRATORY ELECTRON TRANSPORT, ATP SYNTHESIS BY CHEMIOSMOTIC COUPLING, AND HEAT PRODUCTION BY UNCOUPLING PROTEINS_REACTOME_R-HSA-163200.1	-2.15902	<0.001	2.01E-04
APC C-MEDIATED DEGRADATION OF CELL CYCLE PROTEINS_REACTOME DATABASE ID RELEASE 61_174143	-2.15268	<0.001	4.19E-04
APC C:CDC20 MEDIATED DEGRADATION OF MITOTIC PROTEINS_REACTOME_R-HSA-176409.2	-2.15107	<0.001	3.59E-04
ACTIVATION OF APC C AND APC C:CDC20 MEDIATED DEGRADATION OF MITOTIC PROTEINS_REACTOME DATABASE ID RELEASE 61_176814	-2.15100	<0.001	3.14E-04

NUCLEOSOME ASSEMBLY_REACTOME_R-HSA-774815.1	-2.15021	<0.001	2.79E-04
RNA POLYMERASE I PROMOTER OPENING_REACTOME_R-HSA-73728.2	-2.14531	<0.001	2.51E-04

5.2.2 Results of proteomic analyses following siRNA-mediated *HOXA transcript antisense RNA, myeloid-specific 1* knockdown in glioblastoma cells

In addition to RNA sequencing, proteomics analyses of the same cell lines with or without *HOTAIRM1* knockdown were performed. Peptides were detected and proteins with two or more peptides were considered. Protein abundance data were processed using GSEA and visualized as for RNA sequencing. As shown in Figure 5.7, upon siRNA-mediated *HOTAIRM1* knockdown, genesets were differentially enriched both positively and negatively, unlike the RNA sequencing. Positively enriched genesets upon *HOTAIRM1* knockdown include terms related to cytoskeleton, vesicle transport and post-translational modifications. As for the negatively enriched genesets, these terms include mRNA processing and mitochondrial translation.

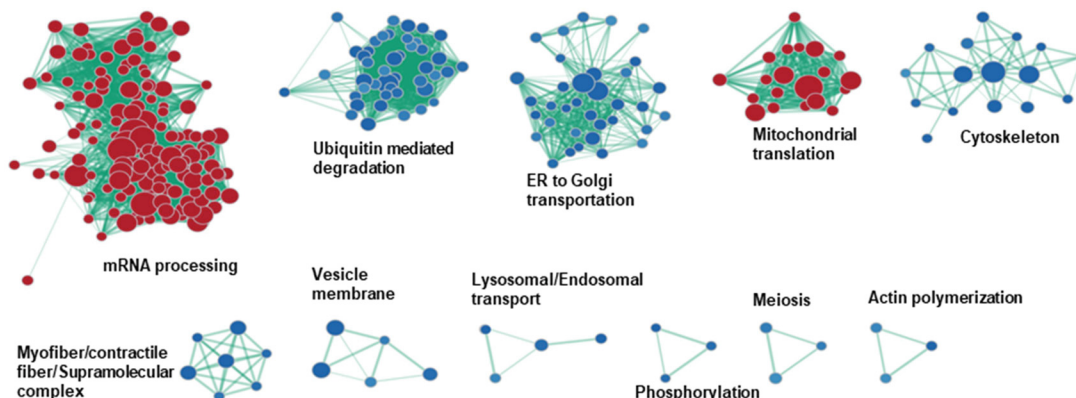


Figure 5.7: Proteomics results obtained upon siRNA-mediated *HOXA transcript antisense RNA, myeloid-specific 1 (HOTAIRM1)* knockdown in U251MG, LN229 and T98G cell lines. The analysis was based on comparison between control cells vs knockdown cells. The genesets with significant p - and q -value ($p < 0.05$, $q < 0.05$) were used in Cytoscape interaction visualization. Red circles: negatively enriched genesets in *HOTAIRM1* knockdown cells; blue circles: positively enriched genesets in *HOTAIRM1* knockdown cells.

Table 5.3 demonstrates that the top 10 positively enriched geneset terms are related to the golgi vesicle transportation, as well as antigen processing and phosphorylation. In Table 5.4, the majority of the top 10 negatively enriched genesets upon *HOTAIRM1* knockdown involve ribosome RNA processing.

Table 5.3: GeneSet Enrichment Analysis (GSEA) results using proteomic data upon *HOXA* transcript antisense RNA, myeloid-specific 1 (*HOTAIRM1*) siRNA-mediated knockdown. Top 10 positively enriched genesets in the *HOTAIRM1* knockdown cells are listed according to their normalized expression score values. NES: normalized expression score; NOM: nominal; FDR: false discovery rate.

GeneSet details	NES	NOM <i>p</i> -value	FDR <i>q</i> -value
CLASS I MHC MEDIATED ANTIGEN PROCESSING & PRESENTATION_REACTOME_R-HSA-983169.3	2.30708	<0.001	5.23E-04
GOLGI VESICLE TRANSPORT_GOBP_GO:0048193	2.21344	<0.001	0.005067
REGULATION OF PHOSPHATASE ACTIVITY_GOBP_GO:0010921	2.19807	<0.001	0.005149
ANTIGEN PRESENTATION: FOLDING, ASSEMBLY AND PEPTIDE LOADING OF CLASS I MHC_REACTOME DATABASE ID RELEASE 61_983170	2.1921	<0.001	0.004262
PROTEIN UBIQUITINATION INVOLVED IN UBIQUITIN-DEPENDENT PROTEIN CATABOLIC PROCESS_GOBP_GO:0042787	2.12129	<0.001	0.010577
ER TO GOLGI ANTEROGRADE TRANSPORT_REACTOME_R-HSA-199977.3	2.12091	<0.001	0.008901
ANTIGEN PROCESSING: UBIQUITINATION & PROTEASOME DEGRADATION_REACTOME DATABASE ID RELEASE 61_983168	2.11776	<0.001	0.007933
TRANSPORT TO THE GOLGI AND SUBSEQUENT MODIFICATION_REACTOME_R-HSA-948021.2	2.10455	<0.001	0.008475
GOLGI-TO-ER RETROGRADE TRANSPORT_REACTOME DATABASE ID RELEASE 61_8856688	2.07161	<0.001	0.01416
REGULATION OF DEPHOSPHORYLATION_GOBP_GO:0035303	2.05964	9.29E-04	0.015143

Table 5.4: GeneSet Enrichment Analysis (GSEA) using proteomic data upon *HOXA* transcript antisense RNA, myeloid-specific 1 (*HOTAIRM1*) siRNA-mediated knockdown. Top 10 negatively enriched genesets in the *HOTAIRM1* knockdown cells are listed according to their normalized expression score values. NES: normalized expression score; NOM: nominal; FDR: false discovery rate.

GeneSet details	NES	NOM <i>p</i> -value	FDR <i>q</i> -value
RIBOSOME BIOGENESIS_GOBP_GO:0042254	-3.206222	<0.001	<0.001
RNA PROCESSING_GOBP_GO:0006396	-3.094729	<0.001	<0.001
RRNA PROCESSING_GOBP_GO:0006364	-3.088324	<0.001	<0.001
RRNA PROCESSING_REACTOME_R-HSA-72312.3	-3.081031	<0.001	<0.001
MAJOR PATHWAY OF RRNA PROCESSING IN THE NUCLEOLUS AND CYTOSOL_REACTOME_R-HSA-6791226.3	-3.06467	<0.001	<0.001
RRNA PROCESSING IN THE NUCLEUS AND CYTOSOL_REACTOME_R-HSA-8868773.2	-3.03982	<0.001	<0.001
RRNA METABOLIC PROCESS_GOBP_GO:0016072	-3.029373	<0.001	<0.001

RIBONUCLEOPROTEIN COMPLEX BIOGENESIS_GOBP_GO:0022613	-2.961836	<0.001	<0.001
NCRNA PROCESSING_GOBP_GO:0034470	-2.935496	<0.001	<0.001
STRUCTURAL CONSTITUENT OF RIBOSOME_GOMF_GO:0003735	-2.858148	<0.001	<0.001

5.2.3 Integrated proteogenomic analysis of the *HOXA transcript antisense RNA, myeloid-specific 1* knockdown results indicate mitochondrial dysfunction

Integrative proteogenomics is a powerful approach that combines multiple data types. In this instance, RNA sequencing and proteomic data were used. First, data from the siRNA-mediated *HOTAIRM1* knockdown of both data types were visualized in Cytoscape as before. Data were then merged and only genesets present in both RNA sequencing and proteomics analyses were retained. Genesets were further manually curated so that enriched terms without consistent activation or inhibition between RNA sequencing and proteomics were removed.

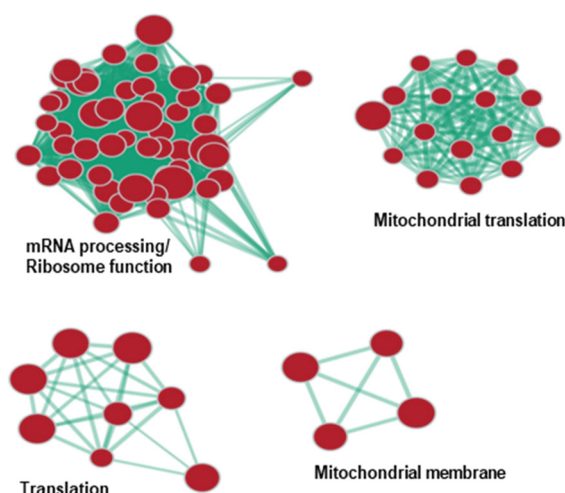


Figure 5.8: Integrative proteogenomics analysis results. GeneSet Enrichment Analysis (GSEA) was done for merged RNA sequencing and proteomics data. The integrative analysis shows genesets that are enriched in both data types. Red circles: negatively enriched genesets in *HOXA transcript antisense RNA, myeloid-specific 1 (HOTAIRM1)* knockdown cells.

As can be seen in Figure 5.8, overlapping nodes contain genesets for mRNA processing and translation, as well as, mitochondrial translation and membrane. According to Table 5.5, five out of the top 10 genesets are involved in mitochondria regulation, specifically translation, three are for ribosome and the other two are for

general translation. In summary, mitochondrial dysregulation after *HOTAIRM1* knockdown was revealed using a proteogenomic approach.

Table 5.5: GeneSet Enrichment Analysis (GSEA) of integrated proteogenomic datasets obtained upon *HOXA* transcript antisense RNA, myeloid-specific 1 (*HOTAIRM1*) siRNA-mediated knockdown in glioma cells. The genesets printed in red color are mitochondria-related genesets. The genesets are listed according to the RNA sequencing *q*-values. RNA-seq: RNA sequencing; NES: normalized expression score; NOM: nominal; FDR: false discovery rate.

GeneSet details	RNA-seq NES	RNA-seq NOM <i>p</i> -value	RNA-seq FDR <i>q</i> -value	Proteomics NES	Proteomics NOM <i>p</i> -value	Proteomics FDR <i>q</i> -value
MITOCHONDRIAL INNER MEMBRANE_GOCC_GO:005743	-2.108	<0.001	0.00014	-2.072	<0.001	0.01962
STRUCTURAL CONSTITUENT OF RIBOSOME_GOMF_GO:003735	-2.100	<0.001	0.00017	-2.858	<0.001	<0.001
MITOCHONDRIAL TRANSLATION ELONGATION_REACTOME_R-HSA-5389840.1	-2.092	<0.001	0.00019	-2.306	<0.001	0.00112
RIBOSOMAL SUBUNIT_GOCC_GO:0044391	-2.141	<0.001	0.00021	-2.715	<0.001	<0.001
MITOCHONDRIAL TRANSLATION INITIATION_REACTOME DATABASE ID RELEASE 61_5368286	-2.082	<0.001	0.00022	-2.345	<0.001	0.00061
MITOCHONDRIAL TRANSLATION_REACTOME DATABASE ID RELEASE 61_5368287	-2.074	<0.001	0.00023	-2.330	<0.001	0.00074
RIBOSOME_GOCC_GO:0005840	-2.073	<0.001	0.00023	-2.707	<0.001	<0.001
MITOCHONDRIAL TRANSLATIONAL ELONGATION_GOBP_GO:0070125	-2.075	<0.001	0.00023	-2.307	<0.001	0.00109
TRANSLATION_REACTOME_R-HSA-72766.3	-2.073	<0.001	0.00024	-2.206	<0.001	0.00472
TRANSLATION_GOBP_GO:0006412	-2.068	<0.001	0.00024	-2.084	<0.001	0.01834
MITOCHONDRIAL TRANSLATION TERMINATION_REACTOME_R-HSA-5419276.1	-2.063	<0.001	0.00028	-2.337	<0.001	0.00065
ORGANELLE INNER	-2.058	<0.001	0.00033	-2.066	<0.001	0.02018

MEMBRANE_GOCC_GO:0 019866						
MITOCHONDRIAL TRANSLATION_GOBP_GO: :0032543	-2.043	<0.001	0.00038	-2.225	<0.001	0.00370
PEPTIDE BIOSYNTHETIC PROCESS_GOBP_GO:004 3043	-2.050	<0.001	0.00039	-1.994	<0.001	0.03187
LARGE RIBOSOMAL SUBUNIT_GOCC_GO:0015 934	-2.045	<0.001	0.00039	-2.524	<0.001	<0.001
TRANSLATIONAL ELONGATION_GOBP_GO: 0006414	-2.046	<0.001	0.00040	-2.289	<0.001	0.00142
MITOCHONDRIAL TRANSLATIONAL TERMINATION_GOBP_GO: :0070126	-2.039	<0.001	0.00042	-2.3571	<0.001	0.00048
AMIDE BIOSYNTHETIC PROCESS_GOBP_GO:004 3604	-2.030	<0.001	0.00046	-1.935	<0.001	0.04255
ORGANELLAR RIBOSOME_GOCC_GO:00 00313	-2.025	<0.001	0.00051	-2.288	0.0021	0.00142
MITOCHONDRIAL GENE EXPRESSION_GOBP_GO: 0140053	-2.011	<0.001	0.00062	-2.278	<0.001	0.00158
MITOCHONDRIAL RIBOSOME_GOCC_GO:00 05761	-2.002	<0.001	0.00070	-2.263	<0.001	0.00199

5.2.4 Proteomic analysis upon stable *HoxA* transcript antisense RNA, myeloid-specific 1 knockdown in LN229 glioblastoma cells

Finally, a proteomic analysis using LN229 stable *HOTAIRM1* knockdown and control cells was performed to further characterize proteins showing differential expression in relation to *HOTAIRM1* expression. The data were analyzed as indicated above. Genesets that were upregulated upon *HOTAIRM1* knockdown that passed the significance thresholds ($p < 0.05$, $q < 0.05$) included geneset clusters related to tricarboxylic acid cycle (TCA) cycle, glycolysis and nucleic acid synthesis, and carboxylic acid biosynthesis (Figure 5.9). As can be seen in Table 5.6, the majority of terms encompassed in the upregulated data all relate to the TCA cycle or to nucleic acid synthesis, whereas terms in the downregulated table (Table 5.7) did not pass the FDR threshold ($q < 0.05$) and are, therefore, non-significant. Considering that TCA cycle is associated with mitochondria, this data points out mitochondrial dysregulation in line with the integrated proteogenomics results. Therefore, these data obtained in

stably transfected glioblastoma cells support the observations described above for the siRNA-mediated *HOTAIRM1* knockdown models.

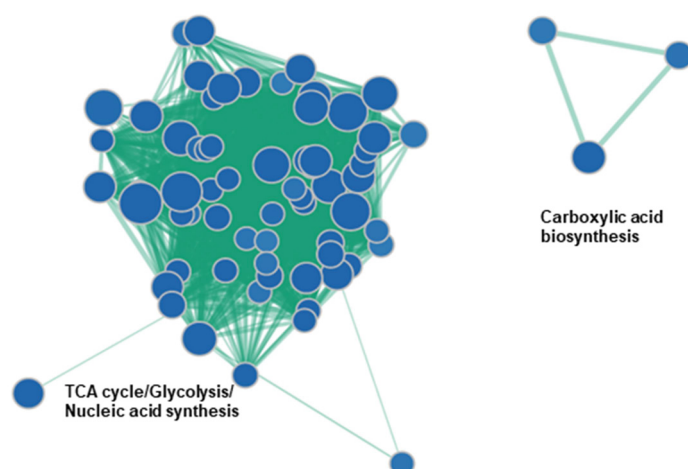


Figure 5.9: Proteomics result upon *HOXA* transcript antisense RNA, myeloid-specific 1 (*HOTAIRM1*) stable knockdown in LN229 glioblastoma cells. The analysis was based on comparison between control cells vs stable *HOTAIRM1* knockdown cells. The genesets with significant p - and q -value ($p < 0.05$, $q < 0.05$) were used in Cytoscape molecular interaction visualization. Blue circles: positively enriched genesets upregulated in *HOTAIRM1* knockdown cells.

Table 5.6: GeneSet Enrichment Analysis (GSEA) results after proteomics upon *HOXA* transcript antisense RNA, myeloid-specific 1 (*HOTAIRM1*) stable knockdown in LN229 glioblastoma cells. Positively enriched genesets in the *HOTAIRM1* knockdown cells are listed according to their normalized expression score values. NES: normalized expression score; NOM: nominal; FDR: false discovery rate.

GeneSet details	NES	NOM p -value	FDR q -value
MONOSACCHARIDE BIOSYNTHETIC	2.21157	<0.001	0.00264
PROCESS_GOBP_GO:0046364			
PYRIDINE-CONTAINING COMPOUND METABOLIC	2.18854	<0.001	0.00184
PROCESS_GOBP_GO:0072524			
MONOSACCHARIDE METABOLIC	2.18763	<0.001	0.00123
PROCESS_GOBP_GO:0005996			
HEXOSE BIOSYNTHETIC	2.09992	<0.001	0.00526
PROCESS_GOBP_GO:0019319			
GLUCONEOGENESIS_GOBP_GO:0006094	2.06175	<0.001	0.00918
PYRIDINE NUCLEOTIDE METABOLIC	2.06005	<0.001	0.00782
PROCESS_GOBP_GO:0019362			
NICOTINAMIDE NUCLEOTIDE METABOLIC	2.04710	<0.001	0.00941
PROCESS_GOBP_GO:0046496			
RIBONUCLEOSIDE TRIPHOSPHATE METABOLIC	2.03329	<0.001	0.01107
PROCESS_GOBP_GO:0009199			
SMALL MOLECULE BIOSYNTHETIC	2.03168	<0.001	0.01007

PROCESS_GOBP_GO:0044283			
OXIDOREDUCTION COENZYME METABOLIC	2.03167	<0.001	0.00906
PROCESS_GOBP_GO:0006733			
HEXOSE METABOLIC PROCESS_GOBP_GO:0019318	2.02777	<0.001	0.00862
PURINE NUCLEOSIDE TRIPHOSPHATE METABOLIC	2.01712	<0.001	0.00996
PROCESS_GOBP_GO:0009144			
GLYCOLYTIC PROCESS_GOBP_GO:0006096	2.00377	<0.001	0.01110
RIBONUCLEOSIDE DIPHOSPHATE METABOLIC	2.00351	<0.001	0.01042
PROCESS_GOBP_GO:0009185			
GLUCONEOGENESIS_REACTOME_R-HSA-70263.2	2.00138	<0.001	0.01008
PURINE RIBONUCLEOSIDE DIPHOSPHATE METABOLIC	1.98683	<0.001	0.01228
PROCESS_GOBP_GO:0009179			
PURINE RIBONUCLEOSIDE TRIPHOSPHATE	1.98352	<0.001	0.01228
METABOLIC PROCESS_GOBP_GO:0009205			
ADP METABOLIC PROCESS_GOBP_GO:0046031	1.98242	<0.001	0.01177
ATP METABOLIC PROCESS_GOBP_GO:0046034	1.98136	<0.001	0.01126
CARBOHYDRATE BIOSYNTHETIC	1.98003	<0.001	0.01089
PROCESS_GOBP_GO:0016051			

Table 5.7: GeneSet Enrichment Analysis (GSEA) results after proteomics upon *HOXA transcript antisense RNA, myeloid-specific 1 (HOTAIRM1)* stable knockdown in LN229 glioblastoma cells. Negatively enriched genesets in the *HOTAIRM1* knockdown cells are listed according to their normalized expression score values. NES: normalized expression score; NOM: nominal; FDR: false discovery rate.

GeneSet details	NES	NOM p-value	FDR q-value
REGULATION OF	-1.79480	0.01218	1
CYTOKINESIS_GOBP_GO:0032465			
REGULATION OF CELL	-1.75311	0.01475	1
DIVISION_GOBP_GO:0051302			
ACTIVATION OF THE PRE-REPLICATIVE	-1.72488	0.01389	1
COMPLEX_REACTOME DATABASE ID RELEASE			
61_68962			
PID_TCR_PATHWAY_MSIGDB_C2_PID_TCR_PATH	-1.62282	0.04110	1
WAY			
TRANSFERASE ACTIVITY, TRANSFERRING ACYL	-1.60273	0.00812	1
GROUPS_GOMF_GO:0016746			
TCR SIGNALING IN NAIVE CD4+ T	-1.58560	0.04342	1
CELLS_PATHWAY INTERACTION DATABASE NCI-			
NATURE CURATED DATA_TCR SIGNALING IN			
NAIVE CD4+ T CELLS			
PID_INSULIN_PATHWAY_MSIGDB_C2_PID_INSULI	-1.55641	0.04670	1
N_PATHWAY			
ACETYLTRANSFERASE	-1.55101	0.02500	1
ACTIVITY_GOMF_GO:0016407			
TETHERING COMPLEX_GOCC_GO:0099023	-1.54698	0.03819	1
REGULATION OF DNA	-1.53722	0.03276	1
REPLICATION_GOBP_GO:0006275			
INSULIN PATHWAY_PATHWAY INTERACTION	-1.52728	0.04095	1

DATABASE NCI-NATURE CURATED			
DATA_INSULIN PATHWAY			
CLATHRIN-COATED VESICLE_GOCC_GO:0030136	-1.51654	0.02121	1
FAS_IJB_FAS	-1.51594	0.02222	1
N-ACYLTRANSFERASE	-1.51451	0.04178	1
ACTIVITY_GOMF_GO:0016410			
PROTEIN SERINE/THREONINE KINASE	-1.49782	0.02091	1
ACTIVITY_GOMF_GO:0004674			
POSTSYNAPSE_GOCC_GO:0098794	-1.48981	0.04894	1
PEPTIDYL-SERINE	-1.48416	0.04587	1
MODIFICATION_GOBP_GO:0018209			
SYNAPSE PART_GOCC_GO:0044456	-1.46143	0.04596	1
UBIQUITIN LIGASE COMPLEX_GOCC_GO:0000151	-1.45312	0.04200	1
DNA-DIRECTED RNA POLYMERASE	-1.41953	0.04298	1
COMPLEX_GOCC_GO:0000428			
RNA POLYMERASE	-1.40500	0.04255	1
COMPLEX_GOCC_GO:0030880			
COVALENT CHROMATIN	-1.40356	0.04233	1
MODIFICATION_GOBP_GO:0016569			
PROTEIN KINASE ACTIVITY_GOMF_GO:0004672	-1.32465	0.04268	1
TRANSFERASE COMPLEX_GOCC_GO:1990234	-1.30101	0.02339	1

5.3 Knockdown of *HoxA* transcript antisense RNA, myeloid-specific 1 alters amino acid metabolism and leads to upregulation of asparagine synthetase in glioblastoma cells

Since the proteogenomic analysis revealed an influence of *HOTAIRM1* on mitochondrial function as a major effect, this finding was further pursued and validated. The initial experiment evaluating mitochondrial function was to assess the metabolite levels in the TCA cycle. Metabolomics assays measuring 15 metabolites involved or related to the TCA cycle were performed to detect effects upon *HOTAIRM1* modulation. Figure 5.10 panel A shows that the abundance of aspartate significantly decreased and the abundance of asparagine significantly increased (1.5 fold, $p < 0.05$), while the other metabolites were not significantly deregulated after *HOTAIRM1* knockdown. Increased asparagine and decreased aspartate levels indicate dysregulation of ETC function and TCA cycle, and hence altered mitochondrial function [32]. In a next step, the enzymes asparagine synthetase (ASNS), which converts aspartate to asparagine, and asparaginase (ASPG), which degrades asparagine to aspartate were investigated further. First, the RNA and protein levels of ASNS and ASPG were measured by qRT-PCR (Figure 5.10 B) or western blotting (Figure 5.10 C-

D). As a result, it was observed that *HOTAIRM1* knockdown leads to significant upregulation of ASNS in stably transfected LN229 cells (Figure 5.10 B-C) and therefore increased asparagine and decreased aspartate levels.

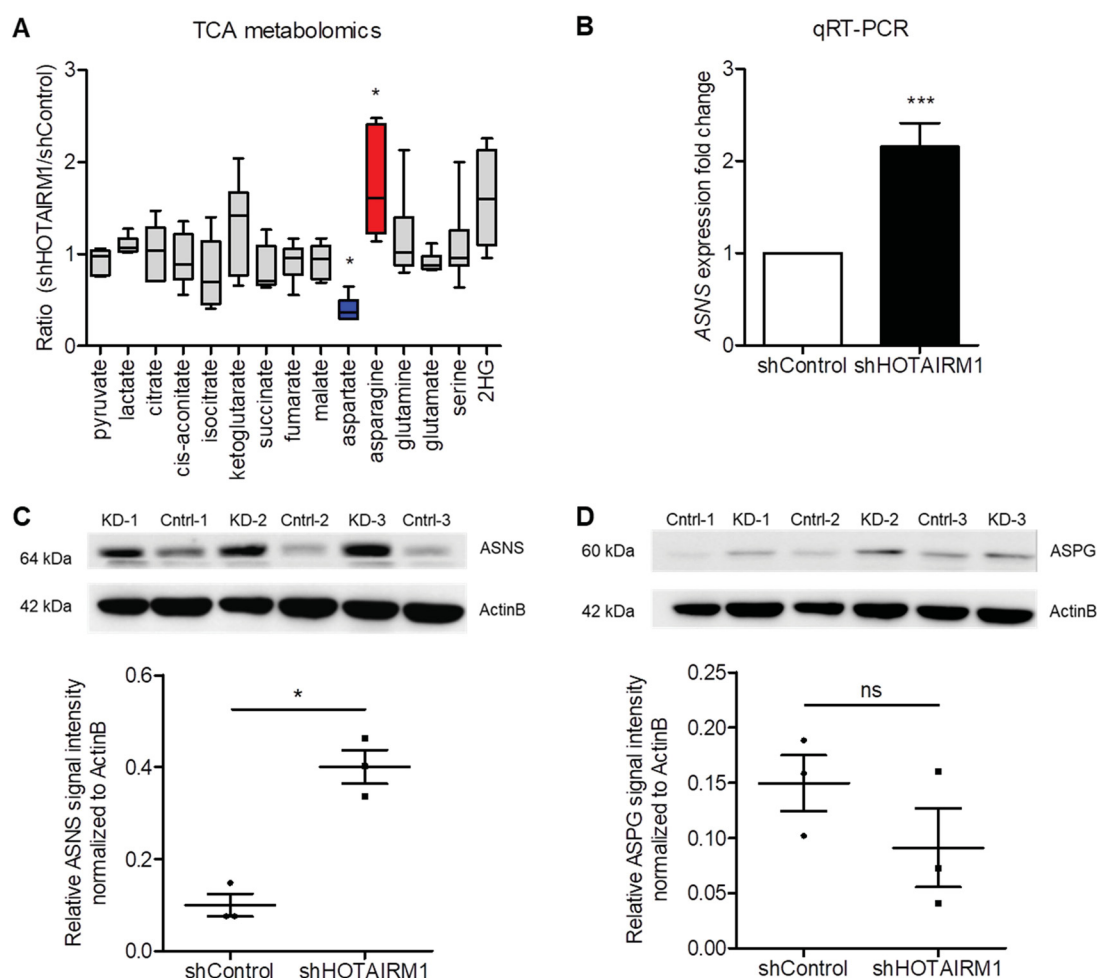


Figure 5.10: Tricarboxylic acid cycle (TCA) metabolomics assay. Knockdown of *HOXA transcript antisense RNA, myeloid-specific 1 (HOTAIRM1)* in stable U251MG and LN229 glioblastoma cells result in decreased aspartate and increased asparagine levels (**A**). *Asparagine synthetase (ASNS)* expression in stably transfected *HOTAIRM1* knockdown and control LN229 cells (**B**). qRT-PCR was performed using TaqMan probes against *ASNS* or *phosphoglycerate kinase 1 (PGK1)* (housekeeping gene). Western blotting analysis of *ASNS* (**C**) and *asparaginase (ASPG)* (**D**) protein expression in stable *HOTAIRM1* knockdown and corresponding control-transfected LN229 cells with the quantifications below the blots. TCA metabolomics: blue color: downregulation (1.5 fold, * $p < 0.05$); red color: upregulation (1.5 fold, * $p < 0.05$). shControl: non-target shRNA; shHOTAIRM1: shRNA against *HOTAIRM1*; KD: *HOTAIRM1* knockdown cells; Cntrl: control cells; replicate 1-3; 2HG = 2-hydroxyglutarate. Two-way ANOVA was used for statistical analyses for panel A. Student t-test was used for statistical analyses for panel B-D. Mean \pm SEM, *** $p < 0.001$, * $p < 0.05$. $n = 3$

5.4 Knockdown of *HOXA transcript antisense RNA, myeloid-specific 1* decreases maximal respiration in U251MG cells

To further investigate and validate the mitochondrial dysfunction phenotype upon *HOTAIRM1* knockdown, a “Seahorse Mito Stress” assay was performed to measure mitochondrial function. The Mito Stress assay involves four compounds that modulate cellular respiration to measure oxygen consumption rate (OCR): oligomycin (an ATP synthase complex V inhibitor), carbonyl cyanide-p-trifluoromethoxyphenylhydrazone (FCCP) (an uncoupling agent), rotenone (a complex I inhibitor) and antimycin A (a complex III inhibitor). First, the basal respiration is measured by the Seahorse instrument. Next, ATP production is measured by oligomycin (1 μ M) injection which causes a decrease in OCR level. Afterwards, FCCP (0.75 μ M) injection disrupts the mitochondrial membrane potential and OCR reaches the maximum that is used to calculate spare respiratory capacity by subtracting basal respiration from maximal respiration; spare respiratory capacity refers to the capacity of the cell upon increased energy demand or under stress as a response. The third injection is a rotenone (0.5 μ M)/antimycin A (0.5 μ M) combination to shut down the mitochondrial respiration which is used to calculate non-mitochondrial respiration.

The analysis was performed using stable *HOTAIRM1* knockdown U251MG cells and respective control-transfected cells (Figure 5.11 A) as well as LN229 *HOTAIRM1* knockdown and control cells (data not shown). In stably transfected U251MG cells, the basal OCR levels differ between the knockdown and the control cells, still, upon normalization to the U251MG control basal level, *HOTAIRM1* knockdown showed a consistent decrease in maximal respiration and spare respiration capacity, indicating that there is mitochondrial dysfunction after *HOTAIRM1* knockdown.

When stably transfected LN229 cells were used, these cells did not attach completely to the specific Seahorse microplates and measurements therefore could not be performed reliably. Thus, due to this technical problem, LN229 cells could not be evaluated with the Seahorse Mito Stress assay.

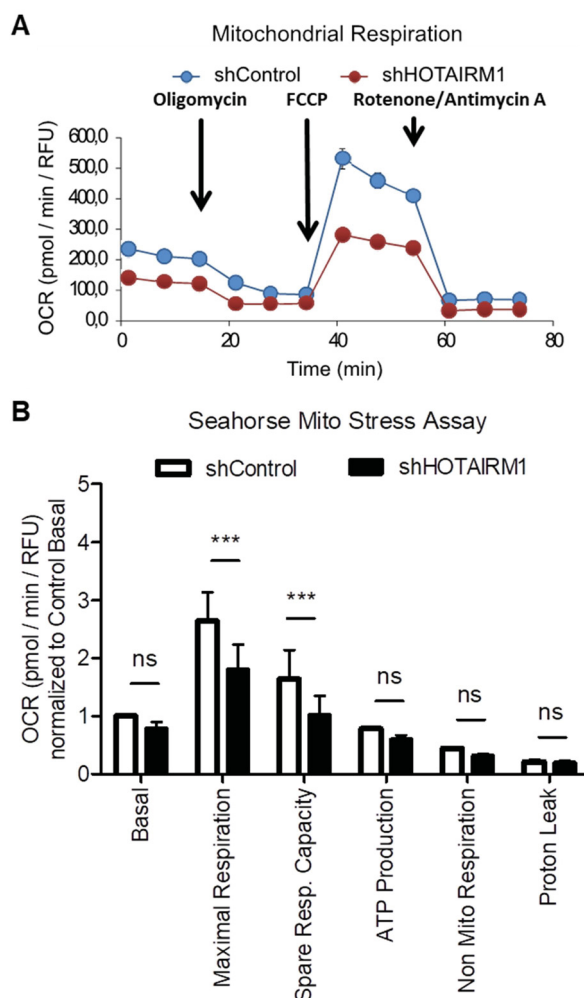


Figure 5.11: Seahorse Mito Stress assay for stably transfected *HOXA* transcript antisense RNA, myeloid-specific 1 (*HOTAIRM1*) knockdown and control U251MG cells. Representative assay output of one replicate (A). Oxygen consumption rate (OCR) measurements of biological triplicates of Mito Stress assay (B). OCR measurements were normalized to basal level of control cells. shControl: non-target shRNA; shHOTAIRM1: shRNA against *HOTAIRM1*. RFU: relative fluorescence units; Resp.: respiration. Two-way ANOVA were used for statistical analyses. Mean \pm SEM; *** $p < 0.001$. $n = 3$, replicas = 6.

5.5 *HOXA* transcript antisense RNA, myeloid-specific 1 knockdown increased reactive oxygen species in glioblastoma cells

Previous studies have shown that impaired electron transport leads to decreased ATP production and accumulation of free radicals, including reactive oxygen species (ROS) [15]. Therefore, ROS measurements were carried out using a dihydroethidium (HET) and MitoSOX staining which measures nuclear/cytoplasmic and mitochondrial ROS, respectively. LN229, SF126 and U87MG *HOTAIRM1* stable knockdown and their respective control-transfected cells were processed (Figure 5.12). *HOTAIRM1*

knockdown cells showed significantly increased ROS levels compared to control cells in almost all evaluated cellular compartments. These data further suggest that mitochondrial function in the *HOTAIRM1* stable knockdown glioblastoma cells is impaired.

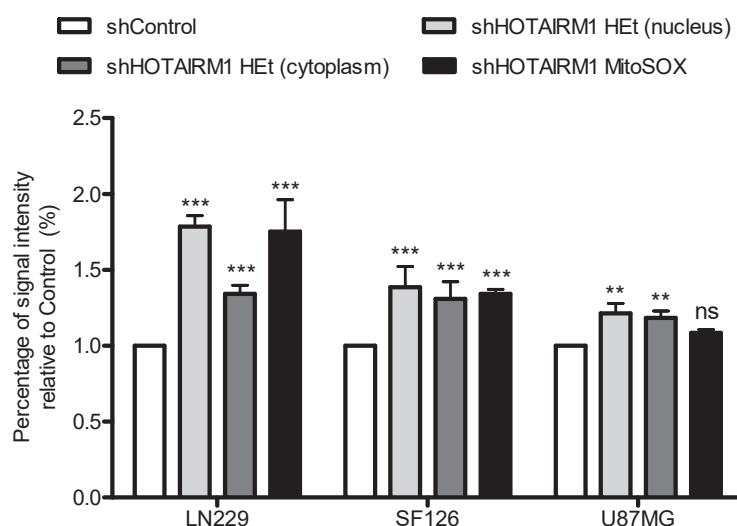


Figure 5.12: Reactive oxygen species (ROS) staining. HET (general superoxide indicator) and MitoSox (mitochondrial superoxide indicator) stainings were performed on LN229, SF126 and U87MG *HOXA transcript antisense RNA, myeloid-specific 1 (HOTAIRM1)* stable knockdown and control-transfected cells. Shown are the detected ROS levels normalized to the control cells. shControl: non-target shRNA; shHOTAIRM1: shRNA against *HOTAIRM1*; student t-test was used for statistical analyses; mean \pm SEM, *** $p < 0.001$, ** $p < 0.01$. $n = 3$.

5.6 Antioxidant N-acetyl cysteine treatment rescues the phenotype induced by *HOXA transcript antisense RNA, myeloid-specific 1* knockdown in glioblastoma cells

After using several methods to demonstrate that *HOTAIRM1* knockdown cells have a decreased mitochondrial function leading to increased ROS production, a ROS scavenger treatment was performed to rescue the phenotype. The antioxidant N-acetyl cysteine (NAC) was used to treat LN229 and LN18 *HOTAIRM1* knockdown and control cell lines with 1 mM final concentration of NAC or vehicle control. Afterwards, colony formation assays were performed for 21 days. Control cell lines showed the expected significant reduction of colonies after knockdown of *HOTAIRM1*; however, NAC treatment rescued the effect of *HOTAIRM1* knockdown on colony formation in both LN229 and LN18 cell lines (Figure 5.13).

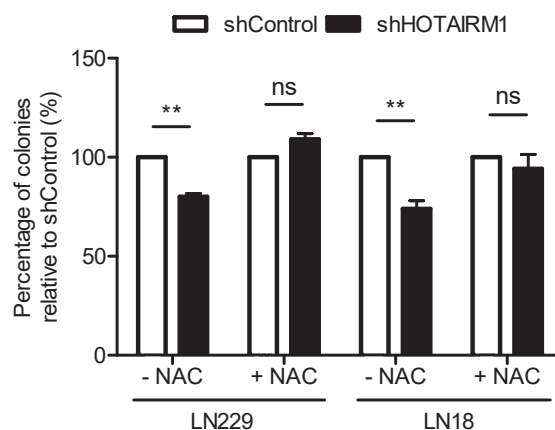


Figure 5.13: Antioxidant N-acetyl cysteine (NAC) treatment in stable LN229 and LN18 cells. NAC treatment performed for both shControl and shHOTAIRM1 cells in combination with colony formation assay by adding NAC to the culture media. The calculations were made to respective normalized shControl cells. shControl: non-target shRNA; shHOTAIRM1: shRNA against *HOXA transcript antisense RNA, myeloid-specific 1 (HOTAIRM1)*. Two-way ANOVA were used for statistical analyses; mean \pm SEM and, ** $p < 0.01$. $n = 3$.

5.7 *HOXA transcript antisense RNA, myeloid-specific 1* knockdown sensitizes LN229, SF126 and LN18 glioblastoma cells to radiation *in vitro*

In glioblastoma patients, radiation is part of the standard of care treatment and, importantly, there is a strong cellular survival correlation between the amount of ROS and radiation exposure *in vitro* [129, 192]. Therefore, altered levels of *HOTAIRM1* were tested for a potential effect on the survival of glioblastoma cells after exposure to radiation. Cells were irradiated with 0, 2 or 4 Gy (gray), and colony formation assays were performed as before. In figure 5.14, a significant decrease in colonies after irradiation at the 21 day endpoint was demonstrated. Although the self-renewal capacity of *HOTAIRM1* knockdown cells was already reduced, a significant decrease in colonies for LN229, SF126 and LN18 after irradiation was observed in a dose-dependent manner.

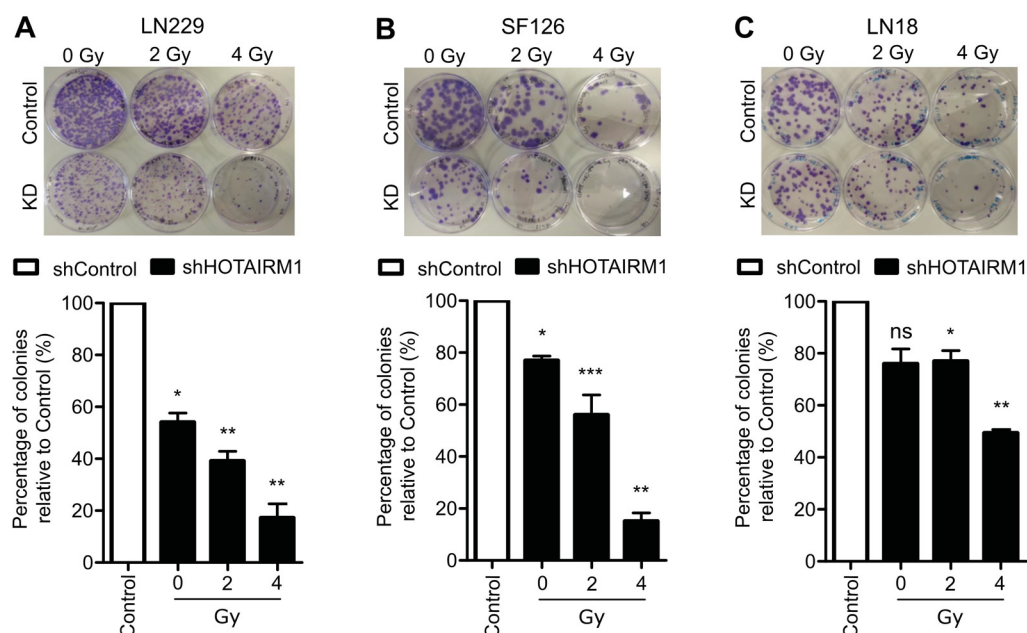


Figure 5.14: *HOXA* transcript antisense RNA, myeloid-specific 1 (*HOTAIRM1*) knockdown sensitizes glioblastoma cells to radiation *in vitro*. Representative images and triplicate quantification of colony formation assays at 21 days post irradiation at indicated doses for stably transfected LN229 (A), SF126 (B) and LN18 (C) cell lines. Colony counts normalized to the respective controls at 0, 2 and 4 Gy. Control/shControl: non-target shRNA; KD/shHOTAIRM1: shRNA against *HOTAIRM1*; Gy: gray. Student's t-test was used for statistical analysis. Mean \pm SEM, *** $p < 0.001$, ** $p < 0.01$, * $p < 0.05$. $n = 3$.

5.8 *HOXA* transcript antisense RNA, myeloid-specific 1 knockdown sensitizes LN229 glioblastoma cells to radiation *in vivo*

After showing a mitochondrial deficiency in several assays and increased ROS levels as well as increased radiosensitivity upon *HOTAIRM1* knockdown *in vitro*, orthotopic intracerebral implantations of LN229 knockdown and control cells were performed by our collaborators in Zurich and transplanted mice were subjected to radiation (12 Gy) or followed up without any treatment. There was no survival benefit in mice bearing *HOTAIRM1* knockdown cells (Figure 5.15 A). On the other hand, there was a strong significant increase in survival in mice bearing *HOTAIRM1* knockdown cells after exposure to radiation (Figure 5.15 B).

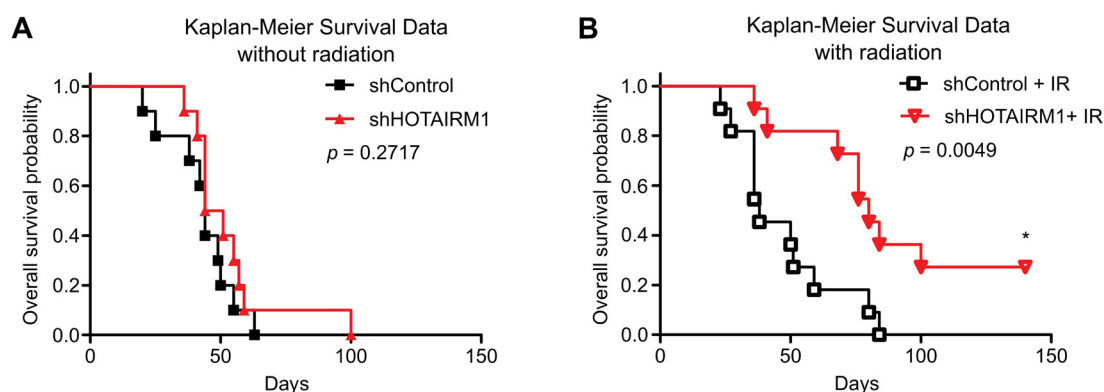


Figure 5.15: Survival curves and tumor growth in mice carrying orthotopic LN229 xenografts with and without radiation. Kaplan-Meier survival plot showing shHOTAIRM1 and shControl cells: plot shows mice which received no radiation (**A**) and mice treated with radiation (**B**). Red and black lines represent shHOTAIRM1 and shControl, respectively. shControl: non-target shRNA; shHOTAIRM1: shRNA against *HOTAIRM1*; IR: irradiation. 10 mice were used per group. Log-rank test was used for statistical analysis.

5.9 Glioblastoma cells with high levels of *HoxA* transcript antisense RNA, myeloid-specific 1 are more sensitive to l-asparaginase treatment

Having shown that glioblastoma cells and tumors with decreased expression of *HOTAIRM1* were more sensitive to radiation, cells with high *HOTAIRM1* expression levels were tested whether they were sensitive to specific pharmacological treatment. Considering the significant alteration in aspartate and asparagine levels between *HOTAIRM1* knockdown and control cells (Figure 5.16), treatment with l-asparaginase (ASPG), which is used as a treatment in a number of cancers [18, 87, 160], was performed to test whether it would influence the outcome in glioblastoma cells according to their expression levels of *HOTAIRM1*. Therefore, stable transfected LN229 cells were tested with different doses of ASPG using the CellTiter-Glo assay as a read out for cell viability. The ASPG treatment was significantly more effective in LN229 cells with high *HOTAIRM1* expression (Figure 5.16).

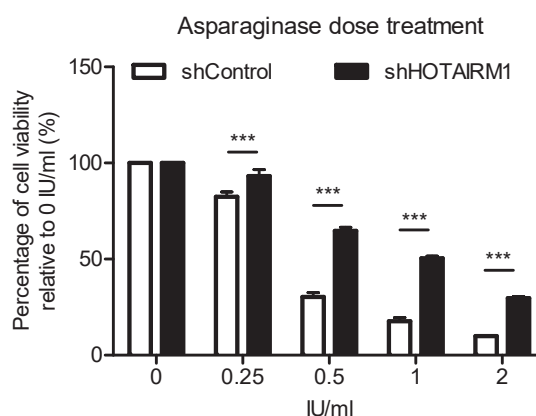


Figure 5.16: Asparaginase dose kinetics in stable transfected *HOXA* transcript antisense RNA, myeloid-specific 1 (*HOTAIRM1*) knockdown and control LN229 cells. Control-transfected cells with high levels of *HOTAIRM1* are more sensitive to asparaginase (ASPG) treatment. ASPG dose kinetics evaluated by CellTitre-Glo assay. Signals from both control cells and knockdown cells were normalized to the respective untreated (0 IU/ml) dose. UI: international unit; shControl: non-target shRNA; shHOTAIRM1: shRNA against *HOTAIRM1*. Two-way ANOVA was used for statistical calculation; mean \pm SEM, *** $p < 0.001$, * $p < 0.05$. $n = 3$.

5.10 *In silico* microRNA binding analysis shows a potential role of *HOXA* transcript antisense RNA, myeloid-specific 1 as a microRNA sponge for miRNAs targeting transglutaminase 2

To identify potential mechanisms underlying the observed phenotypes of *HOTAIRM1* knockdown in glioblastoma cells, differentially expressed proteins in the proteomic data set obtained from stably transfected LN229 glioblastoma cells were identified. As seen in Tables 5.8 and 5.9, there were 16 proteins that are upregulated and 12 proteins that were downregulated upon *HOTAIRM1* stable knockdown in the LN229 cells, respectively.

Table 5.8: List of top significantly upregulated proteins following *HOXA* transcript antisense RNA, myeloid-specific 1 (*HOTAIRM1*) stable knockdown in LN229 glioblastoma cells. The proteins are listed according to their q -values.

Protein ID	Description	Fold change	p -value	q -value
L1CAM	Neural cell adhesion molecule L1	1.74303	2.01E-06	0.00362
LCN2	Neutrophil gelatinase-associated lipocalin	12.0809	1.11E-05	0.00385
HSD17B10	3-hydroxyacyl-CoA dehydrogenase type-2	1.91749	6.58E-06	0.00385

AKR1C3	Aldo-keto reductase family 1 member C3	1.99863	2.18E-05	0.00522
CALB2	Calretinin	1.85151	5.60E-05	0.01011
KYNU	Kynureninase	1.91012	0.00011	0.01627
DYNLRB1	Dynein light chain roadblock-type 1	1.58320	0.00012	0.01642
ANKRD52	Serine/threonine-protein phosphatase 6 regulatory ankyrin repeat subunit C	3.11078	0.00021	0.02369
RAP1GAP2	Rap1 GTPase-activating protein 2	1.64261	0.00024	0.02369
PDLIM4	PDZ and LIM domain protein 4	1.64951	0.00048	0.03625
INF2	Inverted formin-2	1.62381	0.00047	0.03625
AKR1B1	Aldose reductase	1.75732	0.00059	0.04126
GAK	Cyclin-G-associated kinase	1.75092	0.00096	0.04641
SLC2A1	Solute carrier family 2, facilitated glucose transporter member 1	1.57233	0.00091	0.04641
L3HYPDH	Trans-L-3-hydroxyproline dehydratase	1.53126	0.00099	0.04641
DDT	D-dopachrome decarboxylase	1.64757	0.00109	0.04672

Table 5.9: List of top significantly downregulated proteins following *HOXA* transcript antisense RNA, myeloid-specific 1 (*HOTAIRM1*) stable knockdown in LN229 glioblastoma cells. The proteins are listed according to their *q*-values. Transglutaminase 2 (TGM2) is used for further assays and is highlighted.

Protein ID	Description	Fold change	<i>p</i> -value	<i>q</i> -value
TMEM87A	Transmembrane protein 87A	-6.44115	1.28E-05	0.00385
MYO6	Myosin-VI	-3.57295	1.00E-05	0.00385
RFTN1	Raftlin	-1.84698	4.56E-06	0.00385
NGFR	Nerve growth factor receptor	-15.5604	2.31E-05	0.00522
TGM2	Transglutaminase 2	-1.62376	3.20E-05	0.00641
HAT1	Histone acetyltransferase type B catalytic subunit	-1.61425	0.00011	0.01627
SLC4A7	Sodium bicarbonate cotransporter 3	-2.20409	0.00024	0.02369
PKN2	Serine/threonine-protein kinase N2	-1.69435	0.00032	0.02888
C16orf58	Chromosome 16 open reading frame 58	-2.21576	0.00037	0.03146
SORT1	Sortilin	-2.08654	0.00059	0.04126
UBR1	E3 ubiquitin-protein ligase UBR1	-1.57988	0.00070	0.04252
HSPA14	Heat shock 70 kDa protein 14	-2.13546	0.00091	0.04641

Since one function of lncRNAs is related to their ability of working as a microRNA (miRNA) sponge, an *in silico* analysis using the MiRanda tool (<https://omictools.com/miranda-tool>) was performed. miRNA binding analysis for *HOTAIRM1* and the 12 genes encoding the downregulated proteins identified from the stable LN229 proteomics data was performed to identify common miRNAs that may bind to one or more of the mRNAs for the downregulated proteins. The total miRNAs

predicted were filtered for miRNAs overlapping with miRNAs detected in *HOTAIRM1* and miRNAs which were negatively correlated with *HOTAIRM1* in TCGA data (<https://www.cancer.gov/tcga>). This *in silico* analysis revealed 15 miRNAs targeting *HOTAIRM1* and several mRNAs of the proteins of interest (Table 5.10). Surprisingly, 14 of 15 miRNAs were found to be targeting the mRNA of *transglutaminase 2* (*TGM2*), which has been shown to play a role in a broad range of cellular processes including mitochondrial function [97] and therapy resistance [12, 38, 93]. Additionally, *HOTAIRM1* has been shown to be a sponge for the most significant miRNA candidate: hsa-miR-17-5p [117, 141], which could be verified in this analysis.

Table 5.10: List of microRNAs predicted to bind to *HOXA transcript antisense RNA, myeloid-specific 1 (HOTAIRM1)* and the mRNAs of one or more of the 12 downregulated proteins identified upon *HOTAIRM1* knockdown in LN229 cells. microRNAs are ranked based on *p*-values. *Transglutaminase 2 (TGM2)* is highlighted in the table. miRNA: microRNA; mRNA: messenger RNA; TCGA: The Cancer Genome Atlas.

miRNA	mRNA	TCGA correlation	<i>p</i> -value
hsa-miR-17-5p	TGM2	-0.397026	3.29E-05
hsa-miR-93	TGM2	-0.395785	3.50E-05
hsa-miR-95	TGM2	-0.354698	0.0002368
hsa-miR-20b	TGM2	-0.343056	0.00038901
hsa-miR-328	TGM2	-0.342861	0.00039218
hsa-miR-106a	TGM2	-0.327445	0.00073486
hsa-miR-20a	TGM2	-0.321762	0.00091882
hsa-miR-20b	RFTN1	-0.317927	0.00106573
hsa-miR-130b	TGM2	-0.315417	0.00117314
hsa-miR-17-5p	RFTN1	-0.310938	0.00138963
hsa-miR-93	RFTN1	-0.305739	0.001686
hsa-miR-153	RFTN1	-0.296443	0.00236182
hsa-miR-153	TGM2	-0.295234	0.00246571
hsa-miR-95	RFTN1	-0.285786	0.0034302
hsa-miR-92	SORT1	-0.28524	0.00349507
hsa-miR-106b	TGM2	-0.281732	0.00393889
hsa-miR-106a	RFTN1	-0.253882	0.00966134
hsa-miR-95	SLC4A7	-0.25275	0.0100009
hsa-miR-25	NGFR	-0.252134	0.0101904
hsa-miR-101	TGM2	-0.24385	0.0130574
hsa-miR-598	TGM2	-0.239846	0.0146794
hsa-miR-92	TGM2	-0.234186	0.0172689
hsa-miR-328	SORT1	-0.232079	0.018329
hsa-miR-20a	RFTN1	-0.224141	0.0228423
hsa-miR-328	RFTN1	-0.223122	0.0234852
hsa-miR-25	TGM2	-0.219973	0.0255714
hsa-miR-17-5p	SORT1	-0.217921	0.0270137
hsa-miR-148b	SLC4A7	-0.205092	0.0376912
hsa-miR-130b	SORT1	-0.203905	0.0388369
hsa-miR-130b	RFTN1	-0.201252	0.0415039
hsa-miR-106b	RFTN1	-0.198482	0.0444489
hsa-miR-328	HAT1	-0.1969	0.046208

hsa-miR-20a	SORT1	-0.196052	0.0471739
hsa-miR-148b	RFTN1	-0.194955	0.0484485
hsa-miR-106a	SORT1	-0.194221	0.0493178

5.11 *Transglutaminase 2* is downregulated upon *HOXA transcript antisense RNA, myeloid-specific 1* knockdown in glioblastoma cells

The downregulation of *TGM2* in the stable cell line models was validated at both the RNA (Figure 5.17 A) and protein levels (Figure 5.17 B and C) and decreased *TGM2* expression upon *HOTAIRM1* stable knockdown was clearly detected.

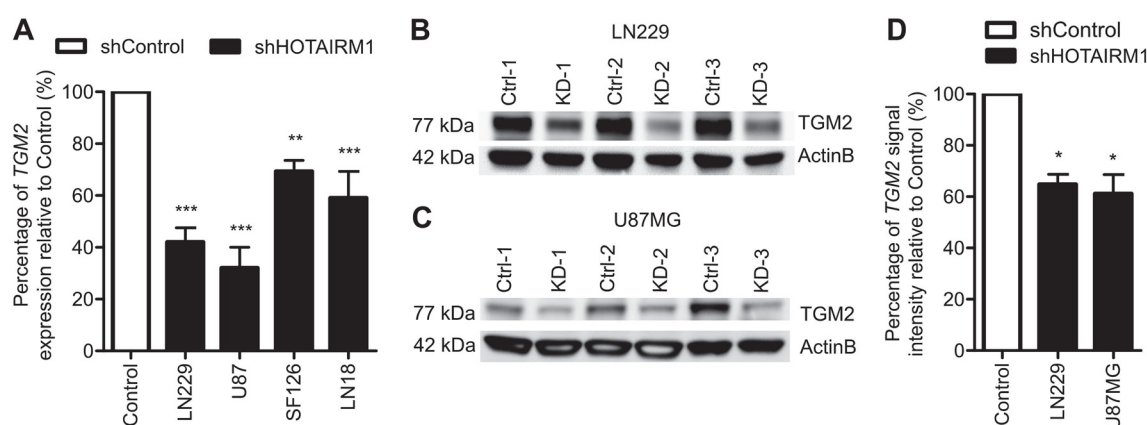


Figure 5.17: *Transglutaminase 2* (*TGM2*) is downregulated upon *HOXA transcript antisense RNA, myeloid-specific 1* (*HOTAIRM1*) knockdown in glioblastoma cells. qRT-PCR was performed using TaqMan probes against *TGM2* or *phosphoglycerate kinase 1* (*PGK1*) (housekeeping gene) to check the *TGM2* expression upon *HOXA transcript antisense RNA, myeloid-specific 1* (*HOTAIRM1*) stable knockdown in stable LN229, U87MG, SF126 and LN18 cell lines (A). Two-way ANOVA is used for statistical calculation. Western blotting analysis of *TGM2* upon *HOTAIRM1* knockdown was performed in stable LN229 (B) and U87MG (C) cell lines and the signal intensities on the blots were quantified (D). shControl: non-target shRNA; shHOTAIRM1: shRNA against *HOTAIRM1*; Ctrl: control; KD: *HOTAIRM1* knockdown; student's t-test was used for statistical analysis. Mean \pm SEM, *** $p < 0.001$, ** $p < 0.01$, * $p < 0.05$. $n = 3$.

5.12 SiRNA-mediated knockdown of *transglutaminase 2* decreases oncogenic potential in glioblastoma cells

Having verified decreased *TGM2* expression after *HOTAIRM1* knockdown in glioblastoma cells, the possibility that *TGM2* alone could have an oncogenic effect in

vitro was tested. siRNA-mediated *TGM2* knockdown in LN229 and SF126 cells achieved 75% efficacy in both cell lines using siPOOLS (siTOOLS) against *TGM2* (Figure 5.18 A). Interestingly, knockdown of *TGM2* also decreased *HOTAIRM1* expression by 40% and 20% for LN229 and SF126, respectively (Figure 5.18 B). The cell viability was decreased by 12-20% (Figure 5.18 C) and there were fewer colonies by 25-40% (Figure 5.18 D). These data suggest that knockdown of *TGM2* can mimic the effect of *HOTAIRM1* on the phenotype of glioblastoma cells.

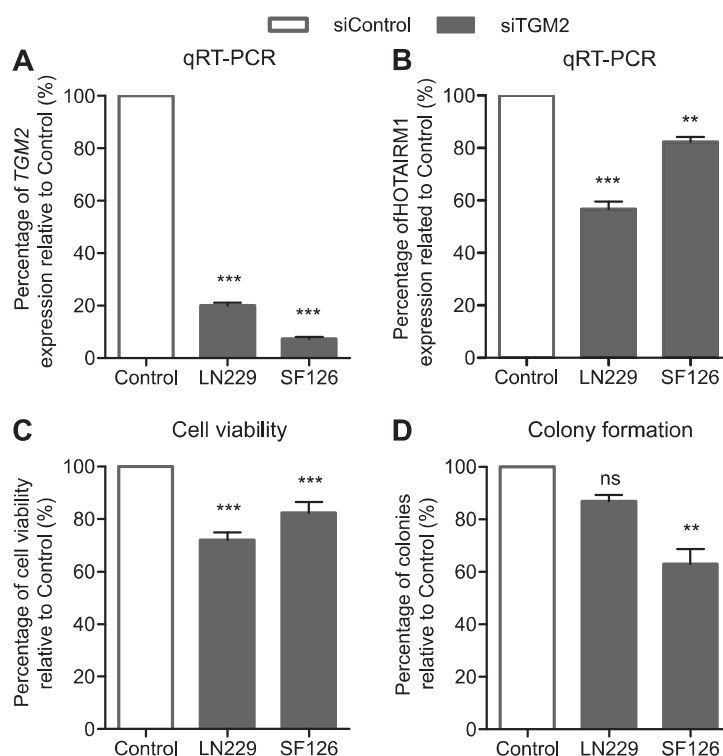


Figure 5.18: SiRNA-mediated *transglutaminase 2* (*TGM2*) knockdown decreases oncogenic potential in established glioblastoma cell lines. SiRNA-mediated *TGM2* knockdown was achieved using siPOOLS (siTOOLS). qRT-PCR was performed using TaqMan probes against *TGM2* (A), *HOXA* transcript antisense RNA, myeloid-specific 1 (*HOTAIRM1*) (B) or *phosphoglycerate kinase 1* (*PGK1*) (housekeeping gene). Cell viability was measured using CellTiter-Glo assays (C). Colony formation assays were done by seeding cells at a density of 1000 cells into 10 cm dishes (D). Histogram bars are as follows, outline bars are respective control and filled bars are *TGM2* knockdown. siControl: non-target siRNA; siTGM2: siRNA against *TGM2*. Two-way ANOVA was used for statistical analyses; mean \pm SEM, *** $p < 0.001$, ** $p < 0.01$. $n = 3$.

6 Discussion

Increasing evidence suggests that alterations in lncRNA expression contribute to the aggressive growth behavior and therapy resistance of different cancer entities [6, 17, 162], including malignant brain tumors such as glioblastoma [27, 64, 103, 120, 184, 186]. Previously generated data from our laboratory provided further evidence that higher expression levels of the long non-coding RNA *HOTAIRM1* are linked to shorter survival of glioblastoma patients. Consistent with our observations, *HOTAIRM1* was recently shown by other investigators to be aberrantly expressed in high-grade gliomas [104]. In addition, high *HOTAIRM1* expression has been associated with shorter survival in acute myeloid leukemia patients with the intermediate-risk cytogenetic category [43], in pancreatic ductal adenocarcinoma [202], the basal-like subgroup of in breast cancer [159], and in glioma [155]. Therefore, to elucidate the biological functions of *HOTAIRM1* in glioblastoma, well established glioblastoma cell lines with high expression of *HOTAIRM1* were used and siRNA- as well as shRNA-mediated knockdown approaches were performed. For the first stable knockdown of *HOTAIRM1* in glioblastoma cells, a lentivirus-based plasmid with puromycin as a selection marker was used. However, puromycin based antibiotic selection increased *HOTAIRM1* expression in the cells. Although the knockdown efficiency after puromycin selection was strong, the expression levels of *HOTAIRM1* in knockdown cells were as high as in the parental cell lines. In contrast, blasticidin based antibiotic selection didn't affect the *HOTAIRM1* expression as demonstrated in Figure 5.4. Therefore, a different plasmid was used, including blasticidin as a selection marker, for further stable transfection of cell lines.

In accordance with the studies by Li et al. (2018) [104] and Liang et al. (2019) [109], a consistent decrease in tumor promoting features was found upon *HOTAIRM1* knockdown across the investigated glioblastoma models. In particular, *HOTAIRM1* knockdown resulted in reduced viability, invasive growth and colony formation of various glioblastoma cell lines *in vitro*. To uncover potential mechanism underlying the effects of *HOTAIRM1* on aggressiveness of glioblastoma, a proteogenomic approach was used. Since there are multiple types of genetic, epigenetic, and genomic changes in cancer [24], an approach that integrates multiple “omics” data sets may be advantageous to studies based only on one type of “omic” measurement. Accordingly, an integrative analysis of RNA sequencing and proteomics, shortly proteogenomics was performed. Geneset enrichment analysis of RNA sequencing and proteomics data sets revealed nineteen and eleven significantly enriched geneset clusters upon *HOTAIRM1* knockdown in glioblastoma cells, which made it challenging to propose a

precise role of *HOTAIRM1* in glioblastoma, especially when using a single approach. On the other hand, proteogenomics identified only four genesets that had consistent activation or inhibition between RNA sequencing and proteomics. This approach revealed that *HOTAIRM1* plays a role in mRNA processing and translation, and mitochondrial translation and membrane function. Translation is one of the most energy-consuming cellular processes and thus linked to cellular energy production [19, 146, 163] in mitochondria [47]. Hence, the dysregulation of mRNA processing and translation might be linked directly to mitochondrial dysfunction itself. This hypothesis was further substantiated by the finding of increased ROS levels as an indicator for mitochondrial dysfunction [15] in *HOTAIRM1* knockdown compared to control glioblastoma cells. Mitochondria play a central role in energy metabolism [47], β -oxidation of fatty acids [168], amino acids metabolism [60], biogenesis of heme- and iron-sulfur (Fe-S) cluster [7, 136], programmed cell death [81, 92, 161], synthesis of steroids [148] and hormonal signaling [187]. To validate the proteogenomics findings, tricarboxylic acid cycle (TCA) metabolomics was performed since the citric acid/TCA cycle is associated with mitochondria and plays a central role in energy metabolism, macromolecule synthesis and redox balance in cells [4]. The TCA cycle includes a series of enzyme-catalyzed biochemical reactions that occur in the mitochondrial matrix [153]. Additionally, intermediate metabolites for fatty acids, glucose and nonessential amino acid production are synthesized in TCA cycle [4]. Therefore, changes in TCA metabolite levels would indicate mitochondrial dysfunction. Hence, as it is shown in Figure 5.10, increased asparagine and decreased aspartate levels might indicate impairment of the TCA cycle in *HOTAIRM1* knockdown glioblastoma cells, as well as electron transport chain (ETC). Interestingly, aspartate is part of the malate-aspartate shuttle, and is important for ATP production and normal physiological mitochondrial function [32].

Upon *HOTAIRM1* knockdown increased asparagine synthetase and decreased asparaginase levels was observed in glioblastoma cells. Although, this data cannot explain the link between *HOTAIRM1* knockdown and changes in metabolite levels, the finding itself is clinically relevant. Asparaginase is used in the treatment of various leukemias and several malignant solid cancers, and has been proposed as an alternative treatment option in glioblastoma [29, 84]. Additionally, the protective role of lower *HOTAIRM1* level against asparaginase treatment could be explained by having excess asparagine levels in these cells [54].

To further investigate mitochondrial dysfunction, Seahorse Mito Stress assays were performed using U251MG and LN229 stable *HOTAIRM1* knockdown and control-

transfected glioblastoma cell lines. The assay for U251MG cells showed a distinct decrease in maximal and spare respiration capacity upon *HOTAIRM1* knockdown. These results suggest that glioblastoma cells with lower *HOTAIRM1* expression cannot use their mitochondria as efficiently as control cells, which have higher *HOTAIRM1* expression. In view of the fact that, mitochondria are reprogrammed in cancer [39] and lower *HOTAIRM1* expression being associated with longer survival of glioblastoma patients [109], *HOTAIRM1*-associated mitochondrial reprogramming might contribute to more aggressive behavior in glioblastoma.

Unfortunately, the second used cell line, LN229, was unsuitable for the Seahorse Mito Stress assay (data is not shown). According to the assay, upon 50-90% cell confluency, the optimal oxygen consumption rate (OCR) should be between 50-400 pmol/min/relative fluorescence units (RFU), the OCR values for LN229 cells were less than 50 pmol/min/ RFU due to low cell attachment on the specific Seahorse plates. Therefore, additional assays were performed to support the U251MG observation. Under normal physiological conditions, a small portion (1-5%) of oxygen is converted to ROS and mitochondria generate the majority of ROS within a cell [172]. The loss of structural integrity of mitochondria, as well as malformations in the ETC and increased oxidative stress are associated with mitochondrial dysfunction [33]. Hence H₂O₂ and MitoSOX reactive oxygen species staining were performed and increased ROS levels were observed in all cellular compartments, which support a role of mitochondrial dysfunction in relation to phenotypic effects of modulating *HOTAIRM1* expression in glioblastoma cells. Accumulated superoxide radicals contribute to genomic instability, oxidative stress and cellular injury [72]. Moreover, persistent and acute ROS exposure causes oxidative damage and this leads to malfunctioning ETC complexes and inefficient (or compromised) TCA [57]. Therefore, antioxidant treatment was carried out using N-acetyl cysteine (NAC) to rescue the phenotype caused by *HOTAIRM1* knockdown and further verify the ROS staining data. NAC has been shown to reverse the cellular effects of ROS [16]. Rescuing the phenotype caused by *HOTAIRM1* knockdown through NAC treatment was successful, which further validated a role of this lncRNA in regulating mitochondrial function and ROS levels.

Since radiation sensitivity has been associated with intracellular ROS levels [3], a potential role of *HOTAIRM1* modulation in radioresistance of glioblastoma cell *in vitro* and *in vivo* was also investigated in this thesis. First, stable *HOTAIRM1* knockdown and control-transfected LN229, SF126 and LN18 cell lines were irradiated with 2 and 4 Gy, and the effects of irradiation were evaluated with colony formation assays [3, 129]. As is expected for cell lines with impaired mitochondria and increased ROS production,

HOTAIRM1 knockdown cells had proportionally fewer colonies after irradiation compared to controls. This observation might be explained by increased radiosensitivity upon increased intracellular ROS levels, in addition to excess ROS levels in *HOTAIRM1* knockdown cells, which results in more severe DNA damage and cellular injury [72]. Moreover, using an orthotopic xenograft model of LN229 glioma cells with and without *HOTAIRM1* knockdown, it was revealed that mice have longer survival when harboring *HOTAIRM1* knockdown LN229 gliomas that are treated with irradiation. In contrast to findings reported for orthotopic U87MG gliomas, which revealed reduced *in vivo* tumor growth of knockdown versus control cells [104], prolonged survival of untreated *HOTAIRM1* knockdown was not observed in LN229-transplanted mice.

Taking together, these findings indicate that expression of *HOTAIRM1* may increase radioresistance of glioblastoma and thereby contribute to shorter patient survival. However, based on the available *in vitro* findings from this study and others [104, 109] as well as the reported *in vivo* growth-promoting activity in the U87MG model [104], it cannot be ruled out that treatment-independent mechanisms may contribute to the poor prognostic role of high *HOTAIRM1* expression. Moreover, a recent study reported that *HOTAIRM1* may also modulate the response of glioma cells to TMZ [109].

To better understand the pathomechanisms underlying regulation of mitochondrial function, tumor growth and radiosensitivity by *HOTAIRM1*, candidate proteins were identified that showed significant differential expression following *HOTAIRM1* knockdown in LN229 glioblastoma cells. Thereby, the expression of *HOTAIRM1* and *transglutaminase 2* (*TGM2* or *TG2*) was found to be correlated in glioblastoma cells (Figure 5.17 and 5.18). *TGM2* belongs to a family of thiol enzymes called transglutaminases and encodes a multifunctional enzyme playing roles in gene regulation, cytoskeleton rearrangement, cell death, and signaling [1, 96, 125, 185]. It is also involved in the progression of various diseases [113], therapy resistance and tumorigenesis [101, 102, 193]. *TGM2* is localized in mitochondria, as well as the cytoplasm, ER and plasma membranes. The function of *TGM2* in mitochondria is an emerging field [97]. Importantly, *TGM2* plays a role in metabolism and mitochondrial respiration [145]. Hence, *TGM2* was a good candidate to further investigate and a decreased oncogenic potential upon *TGM2* knockdown was observed in line consistent with the recent literature [71, 108]. Moreover, this data supported the proteomic data and suggested that *HOTAIRM1* knockdown effects could partially be explained through decreased *TGM2* expression.

This type of co-regulation could be due to potential sponging of *TGM2*-regulating miRNAs by *HOTAIRM1*, in line with recent data implicating *HOTAIRM1* as a miRNA sponge [109, 117, 141]. Using *in silico* miRNA binding prediction, putative miRNA binding sites that are shared between *HOTAIRM1* and *TGM2* were identified, with the most promising candidate seed sequences being those of *miR-17-5p*. Recently published data described that *HOTAIRM1* can act as a sponge for *miR-17-5p* [117, 141], that *TGM2* can confer radioresistance [5, 193] and that *miR-17-5p* is upregulated upon radiation in glioblastoma [25]. Collectively, these data suggest that *HOTAIRM1* may contribute to glioma growth and therapy resistance by sponging *miR-17-5p* (and other miRNAs), and thereby increasing *TGM2* transcript and protein levels. However, this proposed molecular model of linking *HOTAIRM1*, *miR-17-5p* and *TGM2* in a tumor-promoting pathway requires further experimental validation.

7 Conclusion and outlook

The work summarized in this thesis demonstrates that elevated expression of *HOTAIRM1* is associated with a more aggressive phenotype of glioblastoma in patients and experimental model systems. SiRNA- or shRNA-mediated *HOTAIRM1* knockdown in glioblastoma cell models consistently showed reduced cell viability, less invasive growth and diminished colony formation capacity upon *HOTAIRM1* downregulation. Therefore, it can be postulated that *HOTAIRM1* knockdown decreases oncogenic potential in glioblastoma. Importantly, unique proteogenomic data were utilized and a novel role for *HOTAIRM1* in regulating mitochondrial function and ROS levels in glioblastoma cells was determined. Using NAC, the phenotype caused by *HOTAIRM1* knockdown could be rescued and the asparaginase dose kinetics revealed that *HOTAIRM1* knockdown protects cell from asparaginase treatment. Moreover, *HOTAIRM1* was shown to modulate radiosensitivity of glioblastoma cells *in vitro* and *in vivo*. *HOTAIRM1* knockdown decreased expression of *TGM2* as a candidate protein implicated in mitochondrial function, and knockdown of *TGM2* mimicked the *in vitro* phenotype of *HOTAIRM1* downregulation in glioblastoma cells. Furthermore, the *in silico* microRNA binding prediction suggests that *HOTAIRM1* might potentially sponge *miR-17-5p* that is also targeting *TGM2*. In conclusion, the results presented in this theses support a role for *HOTAIRM1* as a candidate lncRNA driving tumor growth, therapy sensitivity and poor prognosis in glioblastoma, the most common malignant brain tumor.

Further investigations should be done to strengthen the data generated to date. In particular, the role of *TGM2* as a promising candidate regulated by *HOTAIRM1* should be addressed in further studies. Since *TGM2* is involved in therapy resistance [12, 38, 93] and knockdown of *TGM2* mimicked the *in vitro* phenotype of *HOTAIRM1* downregulation, its role in radioresistance should be investigated both *in vitro* and *in vivo*. The potential role of *TGM2* in radioresistance might explain the mechanism of *HOTAIRM1* radiosensitizing glioblastoma cells. Therefore, the correlation between *HOTAIRM1* and *TGM2* should be investigated further, in particular focusing of the potential molecular link involving *miR-17-5p*. Therefore, the expression of *miR-17-5p* in glioblastoma cell lines should be validated. As *HOTAIRM1* has been shown to sponge *miR-17-5p* [80, 117, 141], the interaction between *TGM2* and *miR-17-5p* should be demonstrated by performing luciferase reporter assays including the 3'-untranslated region (UTR) of *TGM2* with and without mutations in the predicted *miR-17-5p* binding site. Hypothetically, *miR-17-5p* should potentially inhibit the luciferase activity due to targeting *TGM2* via the miRNA-mediated exonucleolytic degradation.

Further investigations may also follow up on the observed association between increased asparaginase sensitivity and high *HOTAIRM1* expression. Since asparaginase has been proposed as an alternative therapy option in glioblastoma [29, 84], *in vitro* asparaginase sensitivity of the other glioblastoma cell lines upon *HOTAIRM1* knockdown should be performed and afterwards *in vivo* studies should be carried out to validate the *in vitro* findings. If the asparaginase treatments are confirmed to be closely linked to *HOTAIRM1* expression level, *HOTAIRM1* expression levels might serve as a potentially predictive biomarker for better response to either asparaginase treatment in tumors with high *HOTAIRM1* expression or to better response to radiotherapy in tumors with low *HOTAIRM1* expression.

8 References

- 1 Akimov SS, Krylov D, Fleischman LF, Belkin AM (2000) Tissue transglutaminase is an integrin-binding adhesion coreceptor for fibronectin. *J Cell Biol* 148: 825-838 Doi 10.1083/jcb.148.4.825
- 2 Aldape K, Zadeh G, Mansouri S, Reifenberger G, von Deimling A (2015) Glioblastoma: pathology, molecular mechanisms and markers. *Acta Neuropathol* 129: 829-848 Doi 10.1007/s00401-015-1432-1
- 3 An Z, Yu JR, Park WY (2017) Rosiglitazone enhances radiosensitivity by inhibiting repair of DNA damage in cervical cancer cells. *Radiat Environ Biophys* 56: 89-98 Doi 10.1007/s00411-016-0679-9
- 4 Anderson NM, Mucka P, Kern JG, Feng H (2018) The emerging role and targetability of the TCA cycle in cancer metabolism. *Protein Cell* 9: 216-237 Doi 10.1007/s13238-017-0451-1
- 5 Arienti C, Tesei A, Carloni S, Ulivi P, Romeo A, Ghigi G, Menghi E, Sarnelli A, Parisi E, Silvestrini Ret al (2013) SLUG silencing increases radiosensitivity of melanoma cells in vitro. *Cell Oncol (Dordr)* 36: 131-139 Doi 10.1007/s13402-012-0120-6
- 6 Askarian-Amiri ME, Leung E, Finlay G, Baguley BC (2016) The Regulatory Role of Long Noncoding RNAs in Cancer Drug Resistance. *Methods Mol Biol* 1395: 207-227 Doi 10.1007/978-1-4939-3347-1_12
- 7 Atamna H (2004) Heme, iron, and the mitochondrial decay of ageing. *Ageing Res Rev* 3: 303-318 Doi 10.1016/j.arr.2004.02.002
- 8 Augoff K, McCue B, Plow EF, Sossey-Alaoui K (2012) miR-31 and its host gene lncRNA LOC554202 are regulated by promoter hypermethylation in triple-negative breast cancer. *Mol Cancer* 11: 5 Doi 10.1186/1476-4598-11-5
- 9 Ayers D, Vandesompele J (2017) Influence of microRNAs and Long Non-Coding RNAs in Cancer Chemoresistance. *Genes (Basel)* 8: Doi 10.3390/genes8030095
- 10 Baylin SB, Esteller M, Rountree MR, Bachman KE, Schuebel K, Herman JG (2001) Aberrant patterns of DNA methylation, chromatin formation and gene expression in cancer. *Hum Mol Genet* 10: 687-692 Doi 10.1093/hmg/10.7.687
- 11 Benetatos L, Vartholomatos G, Hatzimichael E (2011) MEG3 imprinted gene contribution in tumorigenesis. *Int J Cancer* 129: 773-779 Doi 10.1002/ijc.26052
- 12 Bergamini CM, Griffin M, Pansini FS (2005) Transglutaminase and vascular biology: physiopathologic implications and perspectives for therapeutic interventions. *Curr Med Chem* 12: 2357-2372
- 13 Bezzi M, Guarnerio J, Pandolfi PP (2017) A circular twist on microRNA regulation. *Cell Res* 27: 1401-1402 Doi 10.1038/cr.2017.136
- 14 Bhan A, Mandal SS (2015) lncRNA HOTAIR: A master regulator of chromatin dynamics and cancer. *Biochim Biophys Acta* 1856: 151-164 Doi 10.1016/j.bbcan.2015.07.001
- 15 Bhat AH, Dar KB, Anees S, Zargar MA, Masood A, Sofi MA, Ganie SA (2015) Oxidative stress, mitochondrial dysfunction and neurodegenerative diseases; a mechanistic insight. *Biomed Pharmacother* 74: 101-110 Doi 10.1016/j.biopha.2015.07.025
- 16 Bi Y, Li H, Yi D, Bai Y, Zhong S, Liu Q, Chen Y, Zhao G (2019) Corrigendum to "beta-catenin contributes to cordycepin-induced MGMT inhibition and reduction of temozolomide resistance in glioma cells by increasing intracellular reactive oxygen species". [Cancer Lett. 435 (2018) 66-79]. *Cancer Lett* 461: 157-158 Doi 10.1016/j.canlet.2019.06.006
- 17 Brat DJ, Castellano-Sanchez AA, Hunter SB, Pecot M, Cohen C, Hammond EH, Devi SN, Kaur B, Van Meir EG (2004) Pseudopalisades in glioblastoma are hypoxic, express extracellular matrix proteases, and are formed by an actively migrating cell population. *Cancer Res* 64: 920-927

- 18 Broome JD (1963) Evidence that the L-asparaginase of guinea pig serum is responsible for its antilymphoma effects. I. Properties of the L-asparaginase of guinea pig serum in relation to those of the antilymphoma substance. *J Exp Med* 118: 99-120 Doi 10.1084/jem.118.1.99
- 19 Buttgereit F, Brand MD (1995) A hierarchy of ATP-consuming processes in mammalian cells. *Biochem J* 312 (Pt 1): 163-167 Doi 10.1042/bj3120163
- 20 Cabili MN, Trapnell C, Goff L, Koziol M, Tazon-Vega B, Regev A, Rinn JL (2011) Integrative annotation of human large intergenic noncoding RNAs reveals global properties and specific subclasses. *Genes Dev* 25: 1915-1927 Doi 10.1101/gad.17446611
- 21 Cairncross JG, Ueki K, Zlatescu MC, Lisle DK, Finkelstein DM, Hammond RR, Silver JS, Stark PC, Macdonald DR, Ino Y et al (1998) Specific genetic predictors of chemotherapeutic response and survival in patients with anaplastic oligodendrogliomas. *J Natl Cancer Inst* 90: 1473-1479 Doi 10.1093/jnci/90.19.1473
- 22 Camacho CV, Choudhari R, Gadad SS (2018) Long noncoding RNAs and cancer, an overview. *Steroids* 133: 93-95 Doi 10.1016/j.steroids.2017.12.012
- 23 Cancer Genome Atlas Research N (2008) Comprehensive genomic characterization defines human glioblastoma genes and core pathways. *Nature* 455: 1061-1068 Doi 10.1038/nature07385
- 24 Chakravarthi BV, Nepal S, Varambally S (2016) Genomic and Epigenomic Alterations in Cancer. *Am J Pathol* 186: 1724-1735 Doi 10.1016/j.ajpath.2016.02.023
- 25 Chaudhry MA, Sachdeva H, Omaruddin RA (2010) Radiation-induced micro-RNA modulation in glioblastoma cells differing in DNA-repair pathways. *DNA Cell Biol* 29: 553-561 Doi 10.1089/dna.2009.0978
- 26 Chen G, Wang Z, Wang D, Qiu C, Liu M, Chen X, Zhang Q, Yan G, Cui Q (2013) LncRNADisease: a database for long-non-coding RNA-associated diseases. *Nucleic Acids Res* 41: D983-986 Doi 10.1093/nar/gks1099
- 27 Chen HH, Zong J, Wang SJ (2019) LncRNA GAPLINC promotes the growth and metastasis of glioblastoma by sponging miR-331-3p. *Eur Rev Med Pharmacol Sci* 23: 262-270 Doi 10.26355/eurev_201901_16772
- 28 Chen LL (2016) The biogenesis and emerging roles of circular RNAs. *Nat Rev Mol Cell Biol* 17: 205-211 Doi 10.1038/nrm.2015.32
- 29 Chen Q, Ye L, Fan J, Zhang X, Wang H, Liao S, Song P, Wang Z, Wang S, Li Y et al (2017) Autophagy suppression potentiates the anti-glioblastoma effect of asparaginase in vitro and in vivo. *Oncotarget* 8: 91052-91066 Doi 10.18632/oncotarget.19409
- 30 Chen Y, Wu JJ, Lin XB, Bao Y, Chen ZH, Zhang CR, Cai Z, Zhou JY, Ding MH, Wu XJ et al (2015) Differential lncRNA expression profiles in recurrent gliomas compared with primary gliomas identified by microarray analysis. *Int J Clin Exp Med* 8: 5033-5043
- 31 Chen YG, Satpathy AT, Chang HY (2017) Gene regulation in the immune system by long noncoding RNAs. *Nat Immunol* 18: 962-972 Doi 10.1038/ni.3771
- 32 Cheng CT, Qi Y, Wang YC, Chi KK, Chung Y, Ouyang C, Chen YR, Oh ME, Sheng X, Tang Y et al (2018) Arginine starvation kills tumor cells through aspartate exhaustion and mitochondrial dysfunction. *Commun Biol* 1: 178 Doi 10.1038/s42003-018-0178-4
- 33 Chistiakov DA, Shkurat TP, Melnichenko AA, Grechko AV, Orekhov AN (2018) The role of mitochondrial dysfunction in cardiovascular disease: a brief review. *Ann Med* 50: 121-127 Doi 10.1080/07853890.2017.1417631
- 34 Cipolla GA, de Oliveira JC, Salviano-Silva A, Lobo-Alves SC, Lemos DS, Oliveira LC, Jucoski TS, Mathias C, Pedrosa GA, Zambalde EP et al (2018) Long Non-Coding RNAs in Multifactorial Diseases: Another Layer of Complexity. *Noncoding RNA* 4: Doi 10.3390/ncrna4020013

- 35 Clamp M, Fry B, Kamal M, Xie X, Cuff J, Lin MF, Kellis M, Lindblad-Toh K, Lander ES (2007) Distinguishing protein-coding and noncoding genes in the human genome. *Proc Natl Acad Sci U S A* 104: 19428-19433 Doi 10.1073/pnas.0709013104
- 36 Costello JF, Plass C, Arap W, Chapman VM, Held WA, Berger MS, Su Huang HJ, Cavenee WK (1997) Cyclin-dependent kinase 6 (CDK6) amplification in human gliomas identified using two-dimensional separation of genomic DNA. *Cancer Res* 57: 1250-1254
- 37 Cui X, Niu W, Kong L, He M, Jiang K, Chen S, Zhong A, Zhang Q, Li W, Lu J et al (2017) Long noncoding RNA as an indicator differentiating schizophrenia from major depressive disorder and generalized anxiety disorder in nonpsychiatric hospital. *Biomark Med* 11: 221-228 Doi 10.2217/bmm-2016-0317
- 38 Davies PJ, Murtaugh MP, Moore WT, Jr., Johnson GS, Lucas D (1985) Retinoic acid-induced expression of tissue transglutaminase in human promyelocytic leukemia (HL-60) cells. *J Biol Chem* 260: 5166-5174
- 39 DeBerardinis RJ, Chandel NS (2016) Fundamentals of cancer metabolism. *Sci Adv* 2: e1600200 Doi 10.1126/sciadv.1600200
- 40 Devaux Y, Zangrando J, Schroen B, Creemers EE, Pedrazzini T, Chang CP, Dorn GW, 2nd, Thum T, Heymans S, Cardiolinc n (2015) Long noncoding RNAs in cardiac development and ageing. *Nat Rev Cardiol* 12: 415-425 Doi 10.1038/nrcardio.2015.55
- 41 Dhir A, Dhir S, Proudfoot NJ, Jopling CL (2015) Microprocessor mediates transcriptional termination of long noncoding RNA transcripts hosting microRNAs. *Nat Struct Mol Biol* 22: 319-327 Doi 10.1038/nsmb.2982
- 42 Di Ruscio A, Ebralidze AK, Benoukraf T, Amabile G, Goff LA, Terragni J, Figueroa ME, De Figueiredo Pontes LL, Alberich-Jorda M, Zhang P et al (2013) DNMT1-interacting RNAs block gene-specific DNA methylation. *Nature* 503: 371-376 Doi 10.1038/nature12598
- 43 Diaz-Beya M, Brunet S, Nomdedeu J, Pratcorona M, Cordeiro A, Gallardo D, Escoda L, Tormo M, Heras I, Ribera J Met al (2015) The lincRNA HOTAIRM1, located in the HOXA genomic region, is expressed in acute myeloid leukemia, impacts prognosis in patients in the intermediate-risk cytogenetic category, and is associated with a distinctive microRNA signature. *Oncotarget* 6: 31613-31627 Doi 10.18632/oncotarget.5148
- 44 Diserens AC, de Tribolet N, Martin-Achard A, Gaide AC, Schnegg JF, Carrel S (1981) Characterization of an established human malignant glioma cell line: LN-18. *Acta Neuropathol* 53: 21-28
- 45 Djebali S, Davis CA, Merkel A, Dobin A, Lassmann T, Mortazavi A, Tanzer A, Lagarde J, Lin W, Schlesinger F et al (2012) Landscape of transcription in human cells. *Nature* 489: 101-108 Doi 10.1038/nature11233
- 46 Erdmann VA, Szymanski M, Hochberg A, de Groot N, Barciszewski J (1999) Collection of mRNA-like non-coding RNAs. *Nucleic Acids Res* 27: 192-195 Doi 10.1093/nar/27.1.192
- 47 Ernster L, Schatz G (1981) Mitochondria: a historical review. *J Cell Biol* 91: 227s-255s Doi 10.1083/jcb.91.3.227s
- 48 Faghihi MA, Zhang M, Huang J, Modarresi F, Van der Brug MP, Nalls MA, Cookson MR, St-Laurent G, 3rd, Wahlestedt C (2010) Evidence for natural antisense transcript-mediated inhibition of microRNA function. *Genome Biol* 11: R56 Doi 10.1186/gb-2010-11-5-r56
- 49 Fan J, Xing Y, Wen X, Jia R, Ni H, He J, Ding X, Pan H, Qian G, Ge S et al (2015) Erratum to: Long non-coding RNA ROR decoys gene-specific histone methylation to promote tumorigenesis. *Genome Biol* 16: 275 Doi 10.1186/s13059-015-0852-5

- 50 Fang J, Qiao F, Tu J, Xu J, Ding F, Liu Y, Akuo BA, Hu J, Shao S (2017) High expression of long non-coding RNA NEAT1 indicates poor prognosis of human cancer. *Oncotarget* 8: 45918-45927 Doi 10.18632/oncotarget.17439
- 51 Fernandes JCR, Acuna SM, Aoki JI, Floeter-Winter LM, Muxel SM (2019) Long Non-Coding RNAs in the Regulation of Gene Expression: Physiology and Disease. *Noncoding RNA* 5: Doi 10.3390/ncrna5010017
- 52 Flockhart RJ, Webster DE, Qu K, Mascarenhas N, Kovalski J, Kretz M, Khavari PA (2012) BRAFV600E remodels the melanocyte transcriptome and induces BANCER to regulate melanoma cell migration. *Genome Res* 22: 1006-1014 Doi 10.1101/gr.140061.112
- 53 Frederick L, Wang XY, Eley G, James CD (2000) Diversity and frequency of epidermal growth factor receptor mutations in human glioblastomas. *Cancer Res* 60: 1383-1387
- 54 Fung MKL, Chan GC (2017) Drug-induced amino acid deprivation as strategy for cancer therapy. *J Hematol Oncol* 10: 144 Doi 10.1186/s13045-017-0509-9
- 55 Furio-Tari P, Tarazona S, Gabaldon T, Enright AJ, Conesa A (2016) spongeScan: A web for detecting microRNA binding elements in lncRNA sequences. *Nucleic Acids Res* 44: W176-180 Doi 10.1093/nar/gkw443
- 56 Gezer U, Ozgur E, Cetinkaya M, Isin M, Dalay N (2014) Long non-coding RNAs with low expression levels in cells are enriched in secreted exosomes. *Cell Biol Int* 38: 1076-1079 Doi 10.1002/cbin.10301
- 57 Ghezzi D, Zeviani M (2012) Assembly factors of human mitochondrial respiratory chain complexes: physiology and pathophysiology. *Adv Exp Med Biol* 748: 65-106 Doi 10.1007/978-1-4614-3573-0_4
- 58 Gorovets D, Kannan K, Shen R, Kastenhuber ER, Islamdoust N, Campos C, Pentsova E, Heguy A, Jhanwar SC, Mellinshoff IK et al (2012) IDH mutation and neuroglial developmental features define clinically distinct subclasses of lower grade diffuse astrocytic glioma. *Clin Cancer Res* 18: 2490-2501 Doi 10.1158/1078-0432.CCR-11-2977
- 59 Gravendeel LA, Kouwenhoven MC, Gevaert O, de Rooi JJ, Stubbs AP, Duijm JE, Daemen A, Bleeker FE, Bralten LB, Kloosterhof NK et al (2009) Intrinsic gene expression profiles of gliomas are a better predictor of survival than histology. *Cancer Res* 69: 9065-9072 Doi 10.1158/0008-5472.CAN-09-2307
- 60 Guda P, Guda C, Subramaniam S (2007) Reconstruction of pathways associated with amino acid metabolism in human mitochondria. *Genomics Proteomics Bioinformatics* 5: 166-176 Doi 10.1016/S1672-0229(08)60004-2
- 61 Gupta RA, Shah N, Wang KC, Kim J, Horlings HM, Wong DJ, Tsai MC, Hung T, Argani P, Rinn JL et al (2010) Long non-coding RNA HOTAIR reprograms chromatin state to promote cancer metastasis. *Nature* 464: 1071-1076 Doi 10.1038/nature08975
- 62 Gutmann DH, Rasmussen SA, Wolkenstein P, MacCollin MM, Guha A, Inskip PD, North KN, Poyhonen M, Birch PH, Friedman JM (2002) Gliomas presenting after age 10 in individuals with neurofibromatosis type 1 (NF1). *Neurology* 59: 759-761 Doi 10.1212/wnl.59.5.759
- 63 Haemmig S, Simion V, Yang D, Deng Y, Feinberg MW (2017) Long noncoding RNAs in cardiovascular disease, diagnosis, and therapy. *Curr Opin Cardiol* 32: 776-783 Doi 10.1097/HCO.0000000000000454
- 64 Han L, Zhang K, Shi Z, Zhang J, Zhu J, Zhu S, Zhang A, Jia Z, Wang G, Yu S et al (2012) LncRNA profile of glioblastoma reveals the potential role of lncRNAs in contributing to glioblastoma pathogenesis. *Int J Oncol* 40: 2004-2012 Doi 10.3892/ijo.2012.1413
- 65 Hansen TB, Jensen TI, Clausen BH, Bramsen JB, Finsen B, Damgaard CK, Kjems J (2013) Natural RNA circles function as efficient microRNA sponges. *Nature* 495: 384-388 Doi 10.1038/nature11993
- 66 Hauptman N, Glavac D (2013) Long non-coding RNA in cancer. *Int J Mol Sci* 14: 4655-4669 Doi 10.3390/ijms14034655

- 67 Hawkins PG, Morris KV (2010) Transcriptional regulation of Oct4 by a long non-coding RNA antisense to Oct4-pseudogene 5. *Transcription* 1: 165-175 Doi 10.4161/trns.1.3.13332
- 68 Heery R, Finn SP, Cuffe S, Gray SG (2017) Long Non-Coding RNAs: Key Regulators of Epithelial-Mesenchymal Transition, Tumour Drug Resistance and Cancer Stem Cells. *Cancers (Basel)* 9: Doi 10.3390/cancers9040038
- 69 Hegi ME, Diserens AC, Gorlia T, Hamou MF, de Tribolet N, Weller M, Kros JM, Hainfellner JA, Mason W, Mariani Let al (2005) MGMT gene silencing and benefit from temozolomide in glioblastoma. *N Engl J Med* 352: 997-1003 Doi 10.1056/NEJMoa043331
- 70 Hewson C, Capraro D, Burdach J, Whitaker N, Morris KV (2016) Extracellular vesicle associated long non-coding RNAs functionally enhance cell viability. *Noncoding RNA Res* 1: 3-11 Doi 10.1016/j.ncrna.2016.06.001
- 71 Hidaka H, Seki N, Yoshino H, Yamasaki T, Yamada Y, Nohata N, Fuse M, Nakagawa M, Enokida H (2012) Tumor suppressive microRNA-1285 regulates novel molecular targets: aberrant expression and functional significance in renal cell carcinoma. *Oncotarget* 3: 44-57 Doi 10.18632/oncotarget.417
- 72 Hollensworth SB, Shen C, Sim JE, Spitz DR, Wilson GL, LeDoux SP (2000) Glial cell type-specific responses to menadione-induced oxidative stress. *Free Radic Biol Med* 28: 1161-1174
- 73 Huarte M (2015) The emerging role of lncRNAs in cancer. *Nat Med* 21: 1253-1261 Doi 10.1038/nm.3981
- 74 Huse JT, Brennan C, Hambardzumyan D, Wee B, Pena J, Rouhanifard SH, Sohn-Lee C, le Sage C, Agami R, Tuschl Tet al (2009) The PTEN-regulating microRNA miR-26a is amplified in high-grade glioma and facilitates gliomagenesis in vivo. *Genes Dev* 23: 1327-1337 Doi 10.1101/gad.1777409
- 75 Hutchinson JN, Ensminger AW, Clemson CM, Lynch CR, Lawrence JB, Chess A (2007) A screen for nuclear transcripts identifies two linked noncoding RNAs associated with SC35 splicing domains. *BMC Genomics* 8: 39 Doi 10.1186/1471-2164-8-39
- 76 Ida CM, Lambert SR, Rodriguez FJ, Voss JS, Mc Cann BE, Seys AR, Halling KC, Collins VP, Giannini C (2012) BRAF alterations are frequent in cerebellar low-grade astrocytomas with diffuse growth pattern. *J Neuropathol Exp Neurol* 71: 631-639 Doi 10.1097/NEN.0b013e31825c448a
- 77 Ideraabdullah FY, Vigneau S, Bartolomei MS (2008) Genomic imprinting mechanisms in mammals. *Mutat Res* 647: 77-85 Doi 10.1016/j.mrfmmm.2008.08.008
- 78 Inamura K (2017) Major Tumor Suppressor and Oncogenic Non-Coding RNAs: Clinical Relevance in Lung Cancer. *Cells* 6: Doi 10.3390/cells6020012
- 79 Jen J, Tang YA, Lu YH, Lin CC, Lai WW, Wang YC (2017) Oct4 transcriptionally regulates the expression of long non-coding RNAs NEAT1 and MALAT1 to promote lung cancer progression. *Mol Cancer* 16: 104 Doi 10.1186/s12943-017-0674-z
- 80 Ji F, Wuerkenbieke D, He Y, Ding Y, Du R (2018) Long Noncoding RNA HOTAIR: An Oncogene in Human Cervical Cancer Interacting With MicroRNA-17-5p. *Oncol Res* 26: 353-361 Doi 10.3727/096504017X15002869385155
- 81 Jiang X, Wang X (2004) Cytochrome C-mediated apoptosis. *Annu Rev Biochem* 73: 87-106 Doi 10.1146/annurev.biochem.73.011303.073706
- 82 Jiang X, Zhang F (2017) Long noncoding RNA: a new contributor and potential therapeutic target in fibrosis. *Epigenomics* 9: 1233-1241 Doi 10.2217/epi-2017-0020
- 83 Johnson R, Richter N, Jauch R, Gaughwin PM, Zuccato C, Cattaneo E, Stanton LW (2010) Human accelerated region 1 noncoding RNA is repressed by REST in Huntington's disease. *Physiol Genomics* 41: 269-274 Doi 10.1152/physiolgenomics.00019.2010

- 84 Karpel-Massler G, Ramani D, Shu C, Halatsch ME, Westhoff MA, Bruce JN, Canoll P, Siegelin MD (2016) Metabolic reprogramming of glioblastoma cells by L-asparaginase sensitizes for apoptosis in vitro and in vivo. *Oncotarget* 7: 33512-33528 Doi 10.18632/oncotarget.9257
- 85 Kawaji H, Severin J, Lizio M, Forrest AR, van Nimwegen E, Rehli M, Schroder K, Irvine K, Suzuki H, Carninci Pet al (2011) Update of the FANTOM web resource: from mammalian transcriptional landscape to its dynamic regulation. *Nucleic Acids Res* 39: D856-860 Doi 10.1093/nar/gkq1112
- 86 Khalil AM, Guttman M, Huarte M, Garber M, Raj A, Rivea Morales D, Thomas K, Presser A, Bernstein BE, van Oudenaarden Aet al (2009) Many human large intergenic noncoding RNAs associate with chromatin-modifying complexes and affect gene expression. *Proc Natl Acad Sci U S A* 106: 11667-11672 Doi 10.1073/pnas.0904715106
- 87 Kidd JG (1953) Regression of transplanted lymphomas induced in vivo by means of normal guinea pig serum. I. Course of transplanted cancers of various kinds in mice and rats given guinea pig serum, horse serum, or rabbit serum. *J Exp Med* 98: 565-582 Doi 10.1084/jem.98.6.565
- 88 Kim DK, Zhang L, Dzau VJ, Pratt RE (1994) H19, a developmentally regulated gene, is reexpressed in rat vascular smooth muscle cells after injury. *J Clin Invest* 93: 355-360 Doi 10.1172/JCI116967
- 89 Kim H, Huang W, Jiang X, Pennicooke B, Park PJ, Johnson MD (2010) Integrative genome analysis reveals an oncomir/oncogene cluster regulating glioblastoma survivorship. *Proc Natl Acad Sci U S A* 107: 2183-2188 Doi 10.1073/pnas.0909896107
- 90 Kong L, Zhang Y, Ye ZQ, Liu XQ, Zhao SQ, Wei L, Gao G (2007) CPC: assess the protein-coding potential of transcripts using sequence features and support vector machine. *Nucleic Acids Res* 35: W345-349 Doi 10.1093/nar/gkm391
- 91 Kretz M, Webster DE, Flockhart RJ, Lee CS, Zehnder A, Lopez-Pajares V, Qu K, Zheng GX, Chow J, Kim GEet al (2012) Suppression of progenitor differentiation requires the long noncoding RNA ANCR. *Genes Dev* 26: 338-343 Doi 10.1101/gad.182121.111
- 92 Kroemer G, Galluzzi L, Brenner C (2007) Mitochondrial membrane permeabilization in cell death. *Physiol Rev* 87: 99-163 Doi 10.1152/physrev.00013.2006
- 93 Kumar A, Xu J, Brady S, Gao H, Yu D, Reuben J, Mehta K (2010) Tissue transglutaminase promotes drug resistance and invasion by inducing mesenchymal transition in mammary epithelial cells. *PLoS One* 5: e13390 Doi 10.1371/journal.pone.0013390
- 94 Kumarswamy R, Bauters C, Volkmann I, Maury F, Fetisch J, Holzmann A, Lemesle G, de Groote P, Pinet F, Thum T (2014) Circulating long noncoding RNA, LIPCAR, predicts survival in patients with heart failure. *Circ Res* 114: 1569-1575 Doi 10.1161/CIRCRESAHA.114.303915
- 95 Kung JT, Colognori D, Lee JT (2013) Long noncoding RNAs: past, present, and future. *Genetics* 193: 651-669 Doi 10.1534/genetics.112.146704
- 96 Lai TS, Hausladen A, Slaughter TF, Eu JP, Stamler JS, Greenberg CS (2001) Calcium regulates S-nitrosylation, denitrosylation, and activity of tissue transglutaminase. *Biochemistry* 40: 4904-4910
- 97 Lai TS, Lin CJ, Wu YT, Wu CJ (2017) Tissue transglutaminase (TG2) and mitochondrial function and dysfunction. *Front Biosci (Landmark Ed)* 22: 1114-1137
- 98 Lasda E, Parker R (2014) Circular RNAs: diversity of form and function. *RNA* 20: 1829-1842 Doi 10.1261/rna.047126.114
- 99 Lee C, Kikyo N (2012) Strategies to identify long noncoding RNAs involved in gene regulation. *Cell Biosci* 2: 37 Doi 10.1186/2045-3701-2-37
- 100 Lee JC, Vivanco I, Beroukhir R, Huang JH, Feng WL, DeBiasi RM, Yoshimoto K, King JC, Nghiemphu P, Yuza Yet al (2006) Epidermal growth factor receptor

- activation in glioblastoma through novel missense mutations in the extracellular domain. *PLoS Med* 3: e485 Doi 10.1371/journal.pmed.0030485
- 101 Leicht DT, Kausar T, Wang Z, Ferrer-Torres D, Wang TD, Thomas DG, Lin J, Chang AC, Lin L, Beer DG (2014) TGM2: a cell surface marker in esophageal adenocarcinomas. *J Thorac Oncol* 9: 872-881 Doi 10.1097/JTO.0000000000000229
 - 102 Li C, Cai J, Ge F, Wang G (2018) TGM2 knockdown reverses cisplatin chemoresistance in osteosarcoma. *Int J Mol Med* 42: 1799-1808 Doi 10.3892/ijmm.2018.3753
 - 103 Li J, Ji X, Wang H (2018) Targeting Long Noncoding RNA HMMR-AS1 Suppresses and Radiosensitizes Glioblastoma. *Neoplasia* 20: 456-466 Doi 10.1016/j.neo.2018.02.010
 - 104 Li Q, Dong C, Cui J, Wang Y, Hong X (2018) Over-expressed lncRNA HOTAIRM1 promotes tumor growth and invasion through up-regulating HOXA1 and sequestering G9a/EZH2/Dnmts away from the HOXA1 gene in glioblastoma multiforme. *J Exp Clin Cancer Res* 37: 265 Doi 10.1186/s13046-018-0941-x
 - 105 Li W, Zhang Z, Liu X, Cheng X, Zhang Y, Han X, Zhang Y, Liu S, Yang J, Xu Bet al (2017) The FOXN3-NEAT1-SIN3A repressor complex promotes progression of hormonally responsive breast cancer. *J Clin Invest* 127: 3421-3440 Doi 10.1172/JCI94233
 - 106 Li X, Wang S, Li Z, Long X, Guo Z, Zhang G, Zu J, Chen Y, Wen L (2017) The lncRNA NEAT1 facilitates cell growth and invasion via the miR-211/HMGA2 axis in breast cancer. *Int J Biol Macromol* 105: 346-353 Doi 10.1016/j.ijbiomac.2017.07.053
 - 107 Li Z, Huang C, Bao C, Chen L, Lin M, Wang X, Zhong G, Yu B, Hu W, Dai Let al (2017) Corrigendum: Exon-intron circular RNAs regulate transcription in the nucleus. *Nat Struct Mol Biol* 24: 194 Doi 10.1038/nsmb0217-194a
 - 108 Li Z, Xu X, Bai L, Chen W, Lin Y (2011) Epidermal growth factor receptor-mediated tissue transglutaminase overexpression couples acquired tumor necrosis factor-related apoptosis-inducing ligand resistance and migration through c-FLIP and MMP-9 proteins in lung cancer cells. *J Biol Chem* 286: 21164-21172 Doi 10.1074/jbc.M110.207571
 - 109 Liang Q, Li X, Guan G, Xu X, Chen C, Cheng P, Cheng W, Wu A (2019) Long non-coding RNA, HOTAIRM1, promotes glioma malignancy by forming a ceRNA network. *Aging (Albany NY)* 11: Doi 10.18632/aging.102205
 - 110 Liao Q, Liu C, Yuan X, Kang S, Miao R, Xiao H, Zhao G, Luo H, Bu D, Zhao Het al (2011) Large-scale prediction of long non-coding RNA functions in a coding-non-coding gene co-expression network. *Nucleic Acids Res* 39: 3864-3878 Doi 10.1093/nar/gkq1348
 - 111 Liu XY, Gerges N, Korshunov A, Sabha N, Khuong-Quang DA, Fontebasso AM, Fleming A, Hadjadj D, Schwartzentruber J, Majewski Jet al (2012) Frequent ATRX mutations and loss of expression in adult diffuse astrocytic tumors carrying IDH1/IDH2 and TP53 mutations. *Acta Neuropathol* 124: 615-625 Doi 10.1007/s00401-012-1031-3
 - 112 Long Y, Wang X, Youmans DT, Cech TR (2017) How do lncRNAs regulate transcription? *Sci Adv* 3: eaao2110 Doi 10.1126/sciadv.aao2110
 - 113 Lorand L, Graham RM (2003) Transglutaminases: crosslinking enzymes with pleiotropic functions. *Nat Rev Mol Cell Biol* 4: 140-156 Doi 10.1038/nrm1014
 - 114 Louis DN (1994) The p53 gene and protein in human brain tumors. *J Neuropathol Exp Neurol* 53: 11-21 Doi 10.1097/00005072-199401000-00002
 - 115 Louis DN, Ohgaki H, Wiestler OD, Cavenee WK, Burger PC, Jouvet A, Scheithauer BW, Kleihues P (2007) The 2007 WHO classification of tumours of the central nervous system. *Acta Neuropathol* 114: 97-109 Doi 10.1007/s00401-007-0243-4

- 116 Louis DN, Perry A, Reifenberger G, von Deimling A, Figarella-Branger D, Cavenee WK, Ohgaki H, Wiestler OD, Kleihues P, Ellison DW (2016) The 2016 World Health Organization Classification of Tumors of the Central Nervous System: a summary. *Acta Neuropathol* 131: 803-820 Doi 10.1007/s00401-016-1545-1
- 117 Lu R, Zhao G, Yang Y, Jiang Z, Cai J, Zhang Z, Hu H (2019) Long noncoding RNA HOTAIRM1 inhibits cell progression by regulating miR-17-5p/ PTEN axis in gastric cancer. *J Cell Biochem* 120: 4952-4965 Doi 10.1002/jcb.27770
- 118 Luo Y, He Y, Ye X, Song J, Wang Q, Li Y, Xie X (2019) High Expression of Long Noncoding RNA HOTAIRM1 is Associated with the Proliferation and Migration in Pancreatic Ductal Adenocarcinoma. *Pathol Oncol Res*: Doi 10.1007/s12253-018-00570-4
- 119 Magistri M, Velmeshev D, Makhmutova M, Faghihi MA (2015) Transcriptomics Profiling of Alzheimer's Disease Reveal Neurovascular Defects, Altered Amyloid-beta Homeostasis, and Dereglated Expression of Long Noncoding RNAs. *J Alzheimers Dis* 48: 647-665 Doi 10.3233/JAD-150398
- 120 Mazor G, Levin L, Picard D, Ahmadov U, Carén H, Borkhardt A, Reifenberger G, Lepruvier G, Remke M, Rotblat B (2019) The lncRNA TP73-AS1 is linked to aggressiveness in glioblastoma and promotes temozolomide resistance in glioblastoma cancer stem cells. *Cell Death & Disease* 10: 246 Doi 10.1038/s41419-019-1477-5
- 121 McBride SM, Perez DA, Polley MY, Vandenberg SR, Smith JS, Zheng S, Lamborn KR, Wiencke JK, Chang SM, Prados MD et al (2010) Activation of PI3K/mTOR pathway occurs in most adult low-grade gliomas and predicts patient survival. *J Neurooncol* 97: 33-40 Doi 10.1007/s11060-009-0004-4
- 122 Michelhaugh SK, Lipovich L, Blythe J, Jia H, Kapatos G, Bannon MJ (2011) Mining Affymetrix microarray data for long non-coding RNAs: altered expression in the nucleus accumbens of heroin abusers. *J Neurochem* 116: 459-466 Doi 10.1111/j.1471-4159.2010.07126.x
- 123 Mikkelsen TS, Ku M, Jaffe DB, Issac B, Lieberman E, Giannoukos G, Alvarez P, Brockman W, Kim TK, Koche RP et al (2007) Genome-wide maps of chromatin state in pluripotent and lineage-committed cells. *Nature* 448: 553-560 Doi 10.1038/nature06008
- 124 Murat A, Migliavacca E, Gorlia T, Lambiv WL, Shay T, Hamou MF, de Tribolet N, Regli L, Wick W, Kouwenhoven MC et al (2008) Stem cell-related "self-renewal" signature and high epidermal growth factor receptor expression associated with resistance to concomitant chemoradiotherapy in glioblastoma. *J Clin Oncol* 26: 3015-3024 Doi 10.1200/JCO.2007.15.7164
- 125 Nakaoka H, Perez DM, Baek KJ, Das T, Husain A, Misono K, Im MJ, Graham RM (1994) Gh: a GTP-binding protein with transglutaminase activity and receptor signaling function. *Science* 264: 1593-1596
- 126 Network TC (2013) Corrigendum: Comprehensive genomic characterization defines human glioblastoma genes and core pathways. *Nature* 494: 506 Doi 10.1038/nature11903
- 127 Ng HH, Bird A (1999) DNA methylation and chromatin modification. *Curr Opin Genet Dev* 9: 158-163
- 128 Ni Y, Huang H, Chen Y, Cao M, Zhou H, Zhang Y (2017) Investigation of Long Non-coding RNA Expression Profiles in the Substantia Nigra of Parkinson's Disease. *Cell Mol Neurobiol* 37: 329-338 Doi 10.1007/s10571-016-0373-0
- 129 Oancea-Castillo LR, Klein C, Abdollahi A, Weber KJ, Regnier-Vigouroux A, Dokic I (2017) Comparative analysis of the effects of a sphingosine kinase inhibitor to temozolomide and radiation treatment on glioblastoma cell lines. *Cancer Biol Ther* 18: 400-406 Doi 10.1080/15384047.2017.1323583
- 130 Ohgaki H, Kleihues P (2013) The definition of primary and secondary glioblastoma. *Clin Cancer Res* 19: 764-772 Doi 10.1158/1078-0432.CCR-12-3002

- 131 Ostrom QT, Gittleman H, Liao P, Vecchione-Koval T, Wolinsky Y, Kruchko C, Barnholtz-Sloan JS (2017) CBTRUS Statistical Report: Primary brain and other central nervous system tumors diagnosed in the United States in 2010-2014. *Neuro Oncol* 19: v1-v88 Doi 10.1093/neuonc/nox158
- 132 Ozawa T, Brennan CW, Wang L, Squatrito M, Sasayama T, Nakada M, Huse JT, Pedraza A, Utsuki S, Yasui Yet al (2010) PDGFRA gene rearrangements are frequent genetic events in PDGFRA-amplified glioblastomas. *Genes Dev* 24: 2205-2218 Doi 10.1101/gad.1972310
- 133 Pang KC, Frith MC, Mattick JS (2006) Rapid evolution of noncoding RNAs: lack of conservation does not mean lack of function. *Trends Genet* 22: 1-5 Doi 10.1016/j.tig.2005.10.003
- 134 Parsons DW, Jones S, Zhang X, Lin JC, Leary RJ, Angenendt P, Mankoo P, Carter H, Siu IM, Gallia GLet al (2008) An integrated genomic analysis of human glioblastoma multiforme. *Science* 321: 1807-1812 Doi 10.1126/science.1164382
- 135 Paugh BS, Qu C, Jones C, Liu Z, Adamowicz-Brice M, Zhang J, Bax DA, Coyle B, Barrow J, Hargrave Det al (2010) Integrated molecular genetic profiling of pediatric high-grade gliomas reveals key differences with the adult disease. *J Clin Oncol* 28: 3061-3068 Doi 10.1200/JCO.2009.26.7252
- 136 Paul VD, Lill R (2015) Biogenesis of cytosolic and nuclear iron-sulfur proteins and their role in genome stability. *Biochim Biophys Acta* 1853: 1528-1539 Doi 10.1016/j.bbamcr.2014.12.018
- 137 Ponten J, Macintyre EH (1968) Long term culture of normal and neoplastic human glia. *Acta Pathol Microbiol Scand* 74: 465-486
- 138 Poschmann G, Seyfarth K, Besong Agbo D, Klafki HW, Rozman J, Wurst W, Wiltfang J, Meyer HE, Klingenspor M, Stuhler K (2014) High-fat diet induced isoform changes of the Parkinson's disease protein DJ-1. *J Proteome Res* 13: 2339-2351 Doi 10.1021/pr401157k
- 139 Reifenberger G, Weber RG, Riehmer V, Kaulich K, Willscher E, Wirth H, Gietzelt J, Hentschel B, Westphal M, Simon Met al (2014) Molecular characterization of long-term survivors of glioblastoma using genome- and transcriptome-wide profiling. *Int J Cancer* 135: 1822-1831 Doi 10.1002/ijc.28836
- 140 Reifenberger G, Wirsching HG, Knobbe-Thomsen CB, Weller M (2017) Advances in the molecular genetics of gliomas - implications for classification and therapy. *Nat Rev Clin Oncol* 14: 434-452 Doi 10.1038/nrclinonc.2016.204
- 141 Ren T, Hou J, Liu C, Shan F, Xiong X, Qin A, Chen J, Ren W (2019) The long non-coding RNA HOTAIRM1 suppresses cell progression via sponging endogenous miR-17-5p/ B-cell translocation gene 3 (BTG3) axis in 5-fluorouracil resistant colorectal cancer cells. *Biomed Pharmacother* 117: 109171 Doi 10.1016/j.biopha.2019.109171
- 142 Rinn JL, Chang HY (2012) Genome regulation by long noncoding RNAs. *Annu Rev Biochem* 81: 145-166 Doi 10.1146/annurev-biochem-051410-092902
- 143 Rinn JL, Kertesz M, Wang JK, Squazzo SL, Xu X, Brugmann SA, Goodnough LH, Helms JA, Farnham PJ, Segal Eet al (2007) Functional demarcation of active and silent chromatin domains in human HOX loci by noncoding RNAs. *Cell* 129: 1311-1323 Doi 10.1016/j.cell.2007.05.022
- 144 Risueno A, Fontanillo C, Dinger ME, De Las Rivas J (2010) GATEExplorer: genomic and transcriptomic explorer; mapping expression probes to gene loci, transcripts, exons and ncRNAs. *BMC Bioinformatics* 11: 221 Doi 10.1186/1471-2105-11-221
- 145 Rodolfo C, Mormone E, Matarrese P, Ciccocanti F, Farrace MG, Garofano E, Piredda L, Fimia GM, Malorni W, Piacentini M (2004) Tissue transglutaminase is a multifunctional BH3-only protein. *J Biol Chem* 279: 54783-54792 Doi 10.1074/jbc.M410938200

- 146 Rolfe DF, Brown GC (1997) Cellular energy utilization and molecular origin of standard metabolic rate in mammals. *Physiol Rev* 77: 731-758 Doi 10.1152/physrev.1997.77.3.731
- 147 Rosenblum ML, Dougherty DV, Reese C, Wilson CB (1981) Potentials and possible pitfalls of human stem cell analysis. *Cancer Chemother Pharmacol* 6: 227-235
- 148 Rossier MF (2006) T channels and steroid biosynthesis: in search of a link with mitochondria. *Cell Calcium* 40: 155-164 Doi 10.1016/j.ceca.2006.04.020
- 149 Sahu A, Singhal U, Chinnaiyan AM (2015) Long noncoding RNAs in cancer: from function to translation. *Trends Cancer* 1: 93-109 Doi 10.1016/j.trecan.2015.08.010
- 150 Sakamoto K, Crowley JJ (2018) A comprehensive review of the genetic and biological evidence supports a role for MicroRNA-137 in the etiology of schizophrenia. *Am J Med Genet B Neuropsychiatr Genet* 177: 242-256 Doi 10.1002/ajmg.b.32554
- 151 Sarfi M, Abbastabar M, Khalili E (2019) Long noncoding RNAs biomarker-based cancer assessment. *J Cell Physiol*: Doi 10.1002/jcp.28417
- 152 Seystahl K, Wick W, Weller M (2016) Therapeutic options in recurrent glioblastoma--An update. *Crit Rev Oncol Hematol* 99: 389-408 Doi 10.1016/j.critrevonc.2016.01.018
- 153 Shadel GS (2005) Mitochondrial DNA, aconitase 'wraps' it up. *Trends Biochem Sci* 30: 294-296 Doi 10.1016/j.tibs.2005.04.007
- 154 Shah AH, Graham R, Bregy A, Thambuswamy M, Komotar RJ (2014) Recognizing and correcting failures in glioblastoma treatment. *Cancer Invest* 32: 299-302 Doi 10.3109/07357907.2014.909827
- 155 Song L, Zhang S, Duan C, Ma S, Hussain S, Wei L, Chu M (2019) Genome-wide identification of lncRNAs as novel prognosis biomarkers of glioma. *J Cell Biochem*: Doi 10.1002/jcb.29259
- 156 Stein GH (1979) T98G: an anchorage-independent human tumor cell line that exhibits stationary phase G1 arrest in vitro. *J Cell Physiol* 99: 43-54 Doi 10.1002/jcp.1040990107
- 157 Stupp R, Mason WP, van den Bent MJ, Weller M, Fisher B, Taphoorn MJ, Belanger K, Brandes AA, Marosi C, Bogdahn U et al (2005) Radiotherapy plus concomitant and adjuvant temozolomide for glioblastoma. *N Engl J Med* 352: 987-996 Doi 10.1056/NEJMoa043330
- 158 Sturm D, Witt H, Hovestadt V, Khuong-Quang DA, Jones DT, Konermann C, Pfaff E, Tonjes M, Sill M, Bender S et al (2012) Hotspot mutations in H3F3A and IDH1 define distinct epigenetic and biological subgroups of glioblastoma. *Cancer Cell* 22: 425-437 Doi 10.1016/j.ccr.2012.08.024
- 159 Su X, Malouf GG, Chen Y, Zhang J, Yao H, Valero V, Weinstein JN, Spano JP, Meric-Bernstam F, Khayat D et al (2014) Comprehensive analysis of long non-coding RNAs in human breast cancer clinical subtypes. *Oncotarget* 5: 9864-9876 Doi 10.18632/oncotarget.2454
- 160 Szymanska B, Wilczynska-Kalak U, Kang MH, Liem NL, Carol H, Boehm I, Groepper D, Reynolds CP, Stewart CF, Lock RB (2012) Pharmacokinetic modeling of an induction regimen for in vivo combined testing of novel drugs against pediatric acute lymphoblastic leukemia xenografts. *PLoS One* 7: e33894 Doi 10.1371/journal.pone.0033894
- 161 Tait SW, Green DR (2010) Mitochondria and cell death: outer membrane permeabilization and beyond. *Nat Rev Mol Cell Biol* 11: 621-632 Doi 10.1038/nrm2952
- 162 Tang Y, Cheung BB, Atmadibrata B, Marshall GM, Dinger ME, Liu PY, Liu T (2017) The regulatory role of long noncoding RNAs in cancer. *Cancer Lett* 391: 12-19 Doi 10.1016/j.canlet.2017.01.010

- 163 Topisirovic I, Sonenberg N (2011) mRNA translation and energy metabolism in cancer: the role of the MAPK and mTORC1 pathways. *Cold Spring Harb Symp Quant Biol* 76: 355-367 Doi 10.1101/sqb.2011.76.010785
- 164 Ueki K, Ono Y, Henson JW, Efird JT, von Deimling A, Louis DN (1996) CDKN2/p16 or RB alterations occur in the majority of glioblastomas and are inversely correlated. *Cancer Res* 56: 150-153
- 165 van den Bent M, Gan HK, Lassman AB, Kumthekar P, Merrell R, Butowski N, Lwin Z, Mikkelsen T, Nabors LB, Papadopoulos KP et al (2017) Efficacy of depatuxizumab mafodotin (ABT-414) monotherapy in patients with EGFR-amplified, recurrent glioblastoma: results from a multi-center, international study. *Cancer Chemother Pharmacol* 80: 1209-1217 Doi 10.1007/s00280-017-3451-1
- 166 Vital AL, Tabernero MD, Castrillo A, Rebelo O, Tao H, Gomes F, Nieto AB, Resende Oliveira C, Lopes MC, Orfao A (2010) Gene expression profiles of human glioblastomas are associated with both tumor cytogenetics and histopathology. *Neuro Oncol* 12: 991-1003 Doi 10.1093/neuonc/noq050
- 167 Wan L, Kong J, Tang J, Wu Y, Xu E, Lai M, Zhang H (2016) HOTAIRM1 as a potential biomarker for diagnosis of colorectal cancer functions the role in the tumour suppressor. *J Cell Mol Med* 20: 2036-2044 Doi 10.1111/jcmm.12892
- 168 Wanders RJ, Ruiter JP, L IJ, Waterham HR, Houten SM (2010) The enzymology of mitochondrial fatty acid beta-oxidation and its application to follow-up analysis of positive neonatal screening results. *J Inherit Metab Dis* 33: 479-494 Doi 10.1007/s10545-010-9104-8
- 169 Wang Y, Wang Y, Li J, Zhang Y, Yin H, Han B (2015) CRNDE, a long-noncoding RNA, promotes glioma cell growth and invasion through mTOR signaling. *Cancer Lett* 367: 122-128 Doi 10.1016/j.canlet.2015.03.027
- 170 Wang Z, Zou Q, Song M, Chen J (2017) NEAT1 promotes cell proliferation and invasion in hepatocellular carcinoma by negative regulating miR-613 expression. *Biomed Pharmacother* 94: 612-618 Doi 10.1016/j.biopha.2017.07.111
- 171 Watanabe T, Yokoo H, Yokoo M, Yonekawa Y, Kleihues P, Ohgaki H (2001) Concurrent inactivation of RB1 and TP53 pathways in anaplastic oligodendrogliomas. *J Neuropathol Exp Neurol* 60: 1181-1189 Doi 10.1093/jnen/60.12.1181
- 172 Wei YH, Lu CY, Wei CY, Ma YS, Lee HC (2001) Oxidative stress in human aging and mitochondrial disease-consequences of defective mitochondrial respiration and impaired antioxidant enzyme system. *Chin J Physiol* 44: 1-11
- 173 Weller M, Tabatabai G, Kastner B, Felsberg J, Steinbach JP, Wick A, Schnell O, Hau P, Herrlinger U, Sabel MC et al (2015) MGMT Promoter Methylation Is a Strong Prognostic Biomarker for Benefit from Dose-Intensified Temozolomide Rechallenge in Progressive Glioblastoma: The DIRECTOR Trial. *Clin Cancer Res* 21: 2057-2064 Doi 10.1158/1078-0432.CCR-14-2737
- 174 Weller M, van den Bent M, Hopkins K, Tonn JC, Stupp R, Falini A, Cohen-Jonathan-Moyal E, Frappaz D, Henriksson R, Balana C et al (2014) EANO guideline for the diagnosis and treatment of anaplastic gliomas and glioblastoma. *Lancet Oncol* 15: e395-403 Doi 10.1016/S1470-2045(14)70011-7
- 175 Weller M, Wick W, Aldape K, Brada M, Berger M, Pfister SM, Nishikawa R, Rosenthal M, Wen PY, Stupp R et al (2015) Glioma. *Nat Rev Dis Primers* 1: 15017 Doi 10.1038/nrdp.2015.17
- 176 Wick W, Meisner C, Hentschel B, Platten M, Schilling A, Wiestler B, Sabel MC, Koeppen S, Ketter R, Weiler M et al (2013) Prognostic or predictive value of MGMT promoter methylation in gliomas depends on IDH1 mutation. *Neurology* 81: 1515-1522 Doi 10.1212/WNL.0b013e3182a95680
- 177 Wick W, Weller M, van den Bent M, Sanson M, Weiler M, von Deimling A, Plass C, Hegi M, Platten M, Reifenberger G (2014) MGMT testing--the challenges for

- biomarker-based glioma treatment. *Nat Rev Neurol* 10: 372-385 Doi 10.1038/nrneurol.2014.100
- 178 Wiencke JK, Zheng S, Jelluma N, Tihan T, Vandenberg S, Tamguney T, Baumber R, Parsons R, Lamborn KR, Berger MSet al (2007) Methylation of the PTEN promoter defines low-grade gliomas and secondary glioblastoma. *Neuro Oncol* 9: 271-279 Doi 10.1215/15228517-2007-003
- 179 Wilkinson B, Campbell DB (2013) Contribution of long noncoding RNAs to autism spectrum disorder risk. *Int Rev Neurobiol* 113: 35-59 Doi 10.1016/B978-0-12-418700-9.00002-2
- 180 Wong AJ, Ruppert JM, Bigner SH, Grzeschik CH, Humphrey PA, Bigner DS, Vogelstein B (1992) Structural alterations of the epidermal growth factor receptor gene in human gliomas. *Proc Natl Acad Sci U S A* 89: 2965-2969 Doi 10.1073/pnas.89.7.2965
- 181 Wu H, Yang L, Chen LL (2017) The Diversity of Long Noncoding RNAs and Their Generation. *Trends Genet* 33: 540-552 Doi 10.1016/j.tig.2017.05.004
- 182 Wu X, Cao X, Chen F (2017) WITHDRAWN: LncRNA-HOTAIR Activates Tumor Cell Proliferation and Migration by Suppressing MiR-326 in Cervical Cancer. *Oncol Res*: Doi 10.3727/096504017X15037515496840
- 183 Xiao Y, Yan X, Yang Y, Ma X (2019) Downregulation of long noncoding RNA HOTAIRM1 variant 1 contributes to osteoarthritis via regulating miR-125b/BMPR2 axis and activating JNK/MAPK/ERK pathway. *Biomed Pharmacother* 109: 1569-1577 Doi 10.1016/j.biopha.2018.10.181
- 184 Xu CH, Xiao LM, Liu Y, Chen LK, Zheng SY, Zeng EM, Li DH (2019) The lncRNA HOXA11-AS promotes glioma cell growth and metastasis by targeting miR-130a-5p/HMGB2. *Eur Rev Med Pharmacol Sci* 23: 241-252 Doi 10.26355/eurev_201901_16770
- 185 Xu L, Begum S, Hearn JD, Hynes RO (2006) GPR56, an atypical G protein-coupled receptor, binds tissue transglutaminase, TG2, and inhibits melanoma tumor growth and metastasis. *Proc Natl Acad Sci U S A* 103: 9023-9028 Doi 10.1073/pnas.0602681103
- 186 Xu N, Liu B, Lian C, Doycheva DM, Fu Z, Liu Y, Zhou J, He Z, Yang Z, Huang Qet al (2018) Long noncoding RNA AC003092.1 promotes temozolomide chemosensitivity through miR-195/TFPI-2 signaling modulation in glioblastoma. *Cell Death Dis* 9: 1139 Doi 10.1038/s41419-018-1183-8
- 187 Yager JD, Chen JQ (2007) Mitochondrial estrogen receptors--new insights into specific functions. *Trends Endocrinol Metab* 18: 89-91 Doi 10.1016/j.tem.2007.02.006
- 188 Yan H, Parsons DW, Jin G, McLendon R, Rasheed BA, Yuan W, Kos I, Batinic-Haberle I, Jones S, Riggins GJet al (2009) IDH1 and IDH2 mutations in gliomas. *N Engl J Med* 360: 765-773 Doi 10.1056/NEJMoA0808710
- 189 Yan Y, Zhang B, Liu N, Qi C, Xiao Y, Tian X, Li T, Liu B (2016) Circulating Long Noncoding RNA UCA1 as a Novel Biomarker of Acute Myocardial Infarction. *Biomed Res Int* 2016: 8079372 Doi 10.1155/2016/8079372
- 190 Yang L (2015) Splicing noncoding RNAs from the inside out. *Wiley Interdiscip Rev RNA* 6: 651-660 Doi 10.1002/wrna.1307
- 191 Yao Y, Ma J, Xue Y, Wang P, Li Z, Liu J, Chen L, Xi Z, Teng H, Wang Zet al (2015) Knockdown of long non-coding RNA XIST exerts tumor-suppressive functions in human glioblastoma stem cells by up-regulating miR-152. *Cancer Lett* 359: 75-86 Doi 10.1016/j.canlet.2014.12.051
- 192 Ye L, Yu G, Wang C, Du B, Sun D, Liu J, Qi T, Yu X, Wei W, Cheng J et al (2015) MicroRNA128a, BMI1 polycomb ring finger oncogene, and reactive oxygen species inhibit the growth of U87 MG glioblastoma cells following exposure to Xray radiation. *Mol Med Rep* 12: 6247-6254 Doi 10.3892/mmr.2015.4175
- 193 Yin J, Oh YT, Kim JY, Kim SS, Choi E, Kim TH, Hong JH, Chang N, Cho HJ, Sa JKet al (2017) Transglutaminase 2 Inhibition Reverses Mesenchymal

- Transdifferentiation of Glioma Stem Cells by Regulating C/EBPbeta Signaling. *Cancer Res* 77: 4973-4984 Doi 10.1158/0008-5472.CAN-17-0388
- 194 Yoon JH, Abdelmohsen K, Gorospe M (2014) Functional interactions among microRNAs and long noncoding RNAs. *Semin Cell Dev Biol* 34: 9-14 Doi 10.1016/j.semcdb.2014.05.015
- 195 Zhang C, Li JY, Tian FZ, Zhao G, Hu H, Ma YF, Yang YL (2018) Long Noncoding RNA NEAT1 Promotes Growth and Metastasis of Cholangiocarcinoma Cells. *Oncol Res* 26: 879-888 Doi 10.3727/096504017X15024935181289
- 196 Zhang X, Lian Z, Padden C, Gerstein MB, Rozowsky J, Snyder M, Gingeras TR, Kapranov P, Weissman SM, Newburger PE (2009) A myelopoiesis-associated regulatory intergenic noncoding RNA transcript within the human HOXA cluster. *Blood* 113: 2526-2534 Doi 10.1182/blood-2008-06-162164
- 197 Zhang X, Sun S, Pu JK, Tsang AC, Lee D, Man VO, Lui WM, Wong ST, Leung GK (2012) Long non-coding RNA expression profiles predict clinical phenotypes in glioma. *Neurobiol Dis* 48: 1-8 Doi 10.1016/j.nbd.2012.06.004
- 198 Zhang Y, Mi L, Xuan Y, Gao C, Wang YH, Ming HX, Liu J (2018) LncRNA HOTAIRM1 inhibits the progression of hepatocellular carcinoma by inhibiting the Wnt signaling pathway. *Eur Rev Med Pharmacol Sci* 22: 4861-4868 Doi 10.26355/eurev_201808_15622
- 199 Zheng M, Liu X, Zhou Q, Liu G (2018) HOTAIRM1 competed endogenously with miR-148a to regulate DLGAP1 in head and neck tumor cells. *Cancer Med*: Doi 10.1002/cam4.1523
- 200 Zhong Y, Du Y, Yang X, Mo Y, Fan C, Xiong F, Ren D, Ye X, Li C, Wang Yet al (2018) Circular RNAs function as ceRNAs to regulate and control human cancer progression. *Mol Cancer* 17: 79 Doi 10.1186/s12943-018-0827-8
- 201 Zhou X, Zhang W, Jin M, Chen J, Xu W, Kong X (2017) lncRNA MIAT functions as a competing endogenous RNA to upregulate DAPK2 by sponging miR-22-3p in diabetic cardiomyopathy. *Cell Death Dis* 8: e2929 Doi 10.1038/cddis.2017.321
- 202 Zhou Y, Gong B, Jiang ZL, Zhong S, Liu XC, Dong K, Wu HS, Yang HJ, Zhu SK (2016) Microarray expression profile analysis of long non-coding RNAs in pancreatic ductal adenocarcinoma. *Int J Oncol* 48: 670-680 Doi 10.3892/ijo.2015.3292
- 203 Ziats MN, Rennert OM (2013) Aberrant expression of long noncoding RNAs in autistic brain. *J Mol Neurosci* 49: 589-593 Doi 10.1007/s12031-012-9880-8

9 Acknowledgement

First of all, I would like to thank Prof. Dr. Guido Reifengerger and Dr. Marc Remke for giving me the opportunity to complete my PhD thesis with their guidance and for this interesting project. I would like to thank them for correcting my thesis and offering me the chance to work on this and other projects with outstanding collaborators. Furthermore, I would like to thank Prof. Dr. Andreas Reichert for evaluating my thesis as a second referee and for his great input during my Thesis Advisory Committee (TAC) meetings. Moreover, I would like to thank my other TAC member Prof. Dr. Björn Scheffler for his great input and helpful critics.

I want to thank Daniel Picard and Dr. Jasmin Bartl for all the support and their guidance during my PhD thesis and during writing my thesis. I very much appreciate the fact that I could always discuss the projects especially with Daniel and that he always seemed to have an idea when something did not work immediately. Thank you guys for your help and for proofreading this thesis, it is highly appreciated.

Moreover, I want to thank Prof. Dr. Arndt Borkhardt and Dr. Ute Fischer for giving me the opportunity to work in the KMT lab. I would like to thank the numerous collaborators I had: Prof. Dr. Michael Weller, Dr. Patrick Roth and Dr. Manuela Silginer for supporting the *in vivo* experiments; Prof. Dr. Jens Siveke and Dr. Marija Trajkovic-Arsic and their group for supporting the Seahorse assays; Dr. Felix Distelmaier and Marlen Melcher for supporting the reactive oxygen species staining.

Special thanks to Dr. Nan Qin for all her help with cloning and stable cell line generation experiments and all the discussions about our projects. Thank you Frauke Meyer and Sarah Göbbels for all your technical support. Thank you Lena Blümel and Christina Mölders for your support in western blotting analysis. Thank you Viktoria Marquardt for being my “doctor mama” with your instructions as a senior PhD student. I also want to thank all present and past members of the Remke lab. You made the lab a very friendly place to work at. Thank you Daniel, Jasmin, Nan, Lena, Viktoria, David, Mara, Kubra, Christian, Mascha, Christina, Eva, Stefan and Daniel Nigel Rickert for generating a nice atmosphere in the lab, for the laughs, for fruitful discussions, and for just being my friends.

Last but not least, I would like to thank my family: My idol, my grandfather Yusif Ahmadow who believed in me and supported my education till his last breath; my parents and siblings, who have always supported me and without them this would have never been possible; and my dear friends, who encouraged and supported me throughout my study with patience. Thank you for everything!

10 Appendix

10.1 Abbreviations

Table 10.1: List of abbreviations.

Abbreviation	Full name
2HG	2-hydroxyglutarate
AGO	Argonaute
AP-1/2	Activator protein-1/2
ASNS	Asparagine synthesis
<i>asOct4-pg5</i>	<i>antisense organic cation/carnitine transporter 4 – pseudogene 5</i>
ASPG	Asparaginase
ATCC	American Type Culture Collection
ATRX	ATRX chromatin remodeler
<i>BACE1</i>	<i>beta-secretase-1</i>
BACE1-AS	Beta-secretase-1-antisense
<i>BACE1-AS</i>	<i>beta-secretase-1-antisense</i>
BRAF	B-Raf proto-oncogene, serine/threonine kinase
BSA	Bovine serum albumin
BSD	Blasticidin
CCLC	Cancer Cell Line Encyclopedia
CDKN2A	Cyclin dependent kinase inhibitor 2A
ceRNA	Endogenous competitors RNA
ceRNA	endogenous competitors RNA
CFA	Colony formation assay
<i>circEIF3J</i>	<i>circRNA eukaryotic translation initiation factor 3 subunit</i>
<i>circPAIP2</i>	<i>circRNA poly(A) binding protein interacting protein 2 (circPAIP2)</i>
circRNA	Circular RNA
CNS	Central nervous system
Cntrl	Control
CPC	Coding Potential Calculator
<i>CRNDE</i>	<i>colorectal neoplasia differentially expressed</i>
Cyt C	Cytochrome C
DAPI	4',6-diamidino-2-phenylindole
Dimethylsulfoxide	DMSO
DMEM	Dulbecco's Modified Eagle Medium
<i>ecCEBPA</i>	<i>extra coding CCAAT enhancer binding protein alpha</i>
EGF	Epidermal growth factor
EGFR	Epidermal growth factor receptor
elncRNA	Enhancer long noncoding RNA
ETC	Electron-transport chain
EV	Extracellular vesicle
FBS	Fetal bovine serum
FCCP	Carbonyl cyanide-4-phenylhydrazone
FDR	False discovery rate
Fe-S	Iron-sulfur
GSEA	Gene Set Enrichment Analysis
Gy	gray
H&E	Hematoxylin and eosin
<i>H19</i>	<i>H19 imprinted maternally expressed transcript</i>
H3	Histone 3
HD	Huntington's disease
HET	Dihydroethidium
HIF	Hypoxia-inducible factor

<i>HOTAIR</i>	<i>HOX transcript antisense RNA</i>
HOTAIRM1	HOXA transcript antisense RNA myeloid-specific 1
<i>HOXA11-AS</i>	<i>HOXA11 antisense RNA</i>
HRP	Horseradish peroxidase
IDH	Isocitrate dehydrogenase
IDT	Integrated DNA Technologies
IMM	Inner membrane
IR	irradiation
JCRB	Japanese Collection of Research Bioresources Cell Bank
KD	Knockdown
lincRNA	Long intergenic noncoding RNA
lncRNA	Long non-coding RNAs
<i>lncRNA-ROR</i>	<i>long non-coding RNA-regulator of reprogramming</i>
<i>MALAT1</i>	<i>metastasis associated lung adenocarcinoma transcript 1</i>
MAPK	Mitogen-activated protein kinase
MEF	Mouse embryonic fibroblast
<i>MEG3</i>	<i>maternally expressed 3</i>
MGMT	O-6-methylguanine-DNA methyltransferase
miRISC	miRNA-induced silencing complex
miRNA	Micro RNA
mRNA	Messenger RNA
MS	Mass spectrometry
mtDNA	Mitochondrial DNA
NAC	N-acetyl cysteine
NADH	Nicotinamide adenine dinucleotide
NADPH	Nicotinamide adenine dinucleotide phosphate
ncRNA	Noncoding RNA
<i>NEAT1</i>	<i>nuclear paraspeckle assembly transcript 1</i>
NES	Normalized expression score
NF1	Neurofibromin 1
NOM	Nominal
NOS	Not otherwise specified
NSCLC	non-small cell lung cancer
OCR	Oxygen consumption rate
OMM	Outer membranes
OxPhos	Oxidative phosphorylation
PBS	Phosphate-buffered saline
PDGFRA	Platelet-derived growth factor receptor alpha
PDI	Protein disulfide isomerase
PEI	Polyethylenimine
PGC1 α	PPARG coactivator 1a
<i>PGK1</i>	<i>phosphoglycerate kinase 1</i>
PKM2	Pyruvate kinase M2
poly-A	Polyadenylated
PPARG	Peroxisome proliferator-activated receptor-g
PTEN	Phosphatase and tensin homolog
PVDF	Polyvinylidene difluoride
RA	Retinoic acid
Rb	Retinoblastoma
RB1	RB transcriptional corepressor 1
RNA Pol II	RNA polymerase II
RNA-seq	RNA sequencing
ROS	Reactive oxygen species
rRNA	Ribosomal RNA
RT	Room temperature
RTK	Receptor tyrosine kinases

RT-qPCR	Real-time q-PCR
SEM	Standard error of the mean
shControl	Non-target short hairpin RNA
shHOTAIRM1	shRNA targeting HOTAIRM1
siControl	Non-target siRNA
siHOTAIRM1	siRNA targeting HOTAIRM1
siTGM2	siRNA targeting TGM2
TBS	Tris-buffered saline
TCA	Tricarboxylic acid cycle
TCGA	The Cancer Genome Atlas
TERT	Telomerase reverse transcriptase
TF	Transcription factors
TGM2	Transglutaminase 2
TMRM	Tetramethylrhodamine
TMZ	Temozolomide
<i>TP53</i>	Tumor protein p53
tRNA	Transfer RNA
TSS	Transcriptional start site
UI	international unit
WHO	World Health Organization
<i>XIST</i>	X inactivation-specific transcription
α -KG	α -ketoglutarate

10.2 Nomenclature

Nomenclature	
human gene	all uppercase, italic (e.g. <i>HOTAIRM1</i>)
human protein	all uppercase (e.g. TGM2)

10.3 Figure Directory

Figure 1.1:	Classification of RNAs.....	13
Figure 1.2:	The diversity of long non-coding RNAs (lncRNAs) in the mammalian genome.....	14
Figure 1.3:	Long non-coding RNAs (lncRNAs) in gene expression regulation.....	16
Figure 1.4:	Interaction between microRNAs and long non-coding RNAs (lncRNAs).	18
Figure 1.5:	High <i>HOXA transcript antisense RNA myeloid-specific 1 (HOTAIRM1)</i> expression is associated with poorer prognosis in glioblastoma.....	20
Figure 1.6:	High <i>HOXA transcript antisense RNA myeloid-specific 1 (HOTAIRM1)</i> expression is independent of <i>IDH</i> status and is associated with trisomy 7 in glioblastoma.	21
Figure 5.1:	Expression of <i>HOXA transcript antisense RNA, myeloid-specific 1 (HOTAIRM1)</i> in non-neoplastic (“healthy”) brain tissues, primary glioblastoma tissues and various cell lines.....	35
Figure 5.2:	Relative expression of <i>HOXA transcript antisense RNA, myeloid-specific 1 (HOTAIRM1)</i> in glioblastoma cell lines.....	36
Figure 5.3:	SiRNA-mediated <i>HOXA transcript antisense RNA, myeloid-specific 1 (HOTAIRM1)</i> knockdown decreases oncogenic potential in established glioblastoma cell lines.	37
Figure 5.4:	<i>HOXA transcript antisense RNA, myeloid-specific 1 (HOTAIRM1)</i> expression is affected by selection antibiotic.	38
Figure 5.5:	Stable <i>HOXA transcript antisense RNA, myeloid-specific 1 (HOTAIRM1)</i> knockdown decreases oncogenic potential in established glioblastoma cell lines.	39
Figure 5.6:	RNA sequencing results upon siRNA-mediated <i>HOXA transcript antisense RNA, myeloid-specific 1 (HOTAIRM1)</i> knockdown in U251MG, LN229 and T98G glioblastoma cell lines.	40
Figure 5.7:	Proteomics results obtained upon siRNA-mediated <i>HOXA transcript antisense RNA, myeloid-specific 1 (HOTAIRM1)</i> knockdown in U251MG, LN229 and T98G cell lines.....	42
Figure 5.8:	Integrative proteogenomics analysis results.	44
Figure 5.9:	Proteomics result upon <i>HOXA transcript antisense RNA, myeloid-specific 1 (HOTAIRM1)</i> stable knockdown in LN229 glioblastoma cells.....	47
Figure 5.10:	Tricarboxylic acid cycle (TCA) metabolomics assay.	50
Figure 5.11:	Seahorse Mito Stress assay for stably transfected <i>HOXA transcript antisense RNA, myeloid-specific 1 (HOTAIRM1)</i> knockdown and control U251MG cells..	52
Figure 5.12:	Reactive oxygen species (ROS) staining.	53
Figure 5.13:	Antioxidant N-acetyl cysteine (NAC) treatment in stable LN229 and LN18 cells.	54
Figure 5.14:	<i>HOXA transcript antisense RNA, myeloid-specific 1 (HOTAIRM1)</i> knockdown sensitizes glioblastoma cells to radiation <i>in vitro</i>	55
Figure 5.15:	Survival curves and tumor growth in mice carrying orthotopic LN229 xenografts with and without radiation..	56
Figure 5.16:	Asparaginase dose kinetics in stable transfected <i>HOXA transcript antisense RNA, myeloid-specific 1 (HOTAIRM1)</i> knockdown and control LN229 cells.	57
Figure 5.17:	<i>Transglutaminase 2 (TGM2)</i> is downregulated upon <i>HOXA transcript antisense RNA, myeloid-specific 1 (HOTAIRM1)</i> knockdown in glioblastoma cells..	60

Figure 5.18:	SiRNA-mediated <i>transglutaminase 2</i> (<i>TGM2</i>) knockdown decreases oncogenic potential in established glioblastoma cell lines.	61
--------------	--	----

10.4 Table Directory

Table 1.1:	Key characteristics of IDH-wildtype and IDH-mutant glioblastomas.	12
Table 3.1:	List of media and cell culture reagents.	23
Table 3.2:	List of kits, chemicals, reagents and others.	23
Table 3.3:	List of antibodies.	25
Table 3.4:	List of buffers.	25
Table 3.5:	List of TagMan and siTOOLS probes.	26
Table 3.6:	List of shRNA sequence, plasmids and primers for GoTaq® real-time PCR.	26
Table 3.7:	List of software.	26
Table 3.8:	List of hardware.	27
Table 5.1:	GeneSet Enrichment Analysis (GSEA) based on RNA sequencing upon <i>HOXA transcript antisense RNA, myeloid-specific 1 (HOTAIRM1)</i> siRNA-mediated knockdown in glioblastoma cells.	41
Table 5.2:	GeneSet Enrichment Analysis (GSEA) based on RNA sequencing upon <i>HOXA transcript antisense RNA, myeloid-specific 1 (HOTAIRM1)</i> siRNA-mediated knockdown in glioblastoma cells.	41
Table 5.3:	GeneSet Enrichment Analysis (GSEA) results using proteomic data upon <i>HOXA transcript antisense RNA, myeloid-specific 1 (HOTAIRM1)</i> siRNA-mediated knockdown.	43
Table 5.4:	GeneSet Enrichment Analysis (GSEA) using proteomic data upon <i>HOXA transcript antisense RNA, myeloid-specific 1 (HOTAIRM1)</i> siRNA-mediated knockdown.	43
Table 5.5:	GeneSet Enrichment Analysis (GSEA) of integrated proteogenomic datasets obtained upon <i>HOXA transcript antisense RNA, myeloid-specific 1 (HOTAIRM1)</i> siRNA-mediated knockdown in glioma cells.	45
Table 5.6:	GeneSet Enrichment Analysis (GSEA) results after proteomics upon <i>HOXA transcript antisense RNA, myeloid-specific 1 (HOTAIRM1)</i> stable knockdown in LN229 glioblastoma cells.	47
Table 5.7:	GeneSet Enrichment Analysis (GSEA) results after proteomics upon <i>HOXA transcript antisense RNA, myeloid-specific 1 (HOTAIRM1)</i> stable knockdown in LN229 glioblastoma cells.	48
Table 5.8:	List of top significantly upregulated proteins following <i>HOXA transcript antisense RNA, myeloid-specific 1 (HOTAIRM1)</i> stable knockdown in LN229 glioblastoma cells.	57
Table 5.9:	List of top significantly downregulated proteins following <i>HOXA transcript antisense RNA, myeloid-specific 1 (HOTAIRM1)</i> stable knockdown in LN229 glioblastoma cells.	58
Table 5.10:	List of microRNAs predicted to bind to <i>HOXA transcript antisense RNA, myeloid-specific 1 (HOTAIRM1)</i> and the mRNAs of one or more of the 12 downregulated proteins identified upon <i>HOTAIRM1</i> knockdown in LN229 cells.	59
Table 10.1:	List of abbreviations.	83

Curriculum Vitae

Personal data

Name: Ulvi Ahmadov

Address: Kruppstr. 103, 40227 Düsseldorf, Germany

Email: ulviahmedov@gmail.com

Phone: +49 157 50644438

Date and place of birth: March 31, 1991 in Nakhchivan, Azerbaijan

Nationality: Azerbaijani

Education

10/2016 - present	<p>PhD thesis</p> <p>Department of Pediatric Oncology, Hematology and Clinical Immunology, University Hospital Düsseldorf, Düsseldorf, Germany; Division of Pediatric Neuro-Oncogenomics, German Cancer Research Center (DKFZ), Heidelberg, Germany, and German Consortium for Translational Cancer Research (DKTK), partner site Essen/Düsseldorf, Düsseldorf, Germany.</p> <p>PhD thesis title: The long non-coding RNA <i>HOTAIRM1</i> promotes tumor aggressiveness and radiotherapy resistance in glioblastoma</p> <p>Supervisors: Dr. Marc Remke / Prof. Dr. Guido Reifenberger</p>
2013 – 2016	<p>Master of Science</p> <p>Department of Molecular Biology and Genetics, Izmir Institute of Technology (IzTech), Izmir, Turkey.</p> <p>M.Sc. thesis title: Identification of long non-coding RNAs that regulate apoptosis in human</p> <p>Supervisor: Assoc. Prof. Bünyamin Akgül</p>
2008 – 2013	<p>Bachelor of Science</p> <p>Department of Molecular Biology and Genetics, Izmir Institute of Technology (IzTech), Izmir, Turkey.</p>
2011 – 2012	<p>Erasmus Exchange Program</p> <p>University of Gothenburg (GU), Gothenburg, Sweden</p>

Publications

Marquardt V., Theruvath J., Pauck D., Picard D., Qin N., Blümel L., Maue M., Bartl J., Ahmadov U. et al., *HDAC and NFκB antagonists synergistically inhibit growth and metastatic dissemination of MYC-driven medulloblastoma*. Cancer Res (in revision)

Varon M., Levy T., Mazor G., Ben David H., Marciano R., Kerlin Y., Prasad M., Elkabets M., Pauck D., Ahmadov U. et al., *The long non-coding RNA TP73-AS1 promotes tumorigenicity of medulloblastoma cells*. Int J Cancer. 2019 May 13. doi: 10.1002/ijc.32400

Mazor G., Levin L., Picard D., Ahmadov U. et al., *The lncRNA TP73-AS1 is linked to aggressiveness in glioblastoma and promotes temozolomide resistance in glioblastoma cancer stem cells*. Cell Death Dis 2019. **10**(3):246

Affirmation

Hereby, I declare on oath that I composed this dissertation independently by myself. I used only the references and resources indicated in this thesis. With the exception of such quotations, the work presented in this thesis is my own. I have accredited all the sources of help. This PhD thesis was never submitted or presented in a similar form to any other institution or examination board. I have not undertaken a doctoral examination without success so far.

Düsseldorf, October 2019

Ulvi Ahmadov